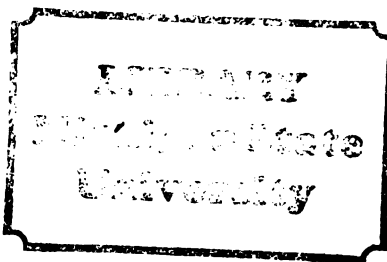


THESIS



3 1293 10437 2234



This is to certify that the

thesis entitled

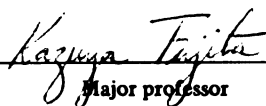
THE EFFECTS OF SUBDUCTING SLABS ON
SEISMIC AMPLITUDES AND TRAVEL-TIMES FROM
FOREARC AND OUTER RISE EARTHQUAKES

presented by

William John Rogers, Jr.

has been accepted towards fulfillment
of the requirements for

M.S. degree in Geology


Major professor

Date 4 May, 1982



RETURNING MATERIALS:
Place in book drop to
remove this checkout from
your record. FINES will
be charged if book is
returned after the date
stamped below.

2-07-2000

~~10-24-2000~~

2-07-2000

THE EFFECTS OF SUBDUCTING SLABS ON
SEISMIC AMPLITUDES AND TRAVEL-TIMES FROM
FOREARC AND OUTER RISE EARTHQUAKES

By

William John Rogers, Jr.

A THESIS

Submitted to

Michigan State University

in partial fulfillment of the requirements

for the degree of

MASTER OF SCIENCE

Department of Geology

1982

ABSTRACT

THE EFFECTS OF SUBDUCTING SLABS ON
SEISMIC AMPLITUDES AND TRAVEL-TIMES FROM
FOREARC AND OUTER RISE EARTHQUAKES

By

William John Rogers, Jr.

6117561

The assumption that subducting slabs are too far from earthquakes occurring in the forearc and outer rise to cause teleseismic mislocations is investigated for the Aleutians using seismic ray tracing. Results indicate that effects should be seen for earthquakes as far out as the outer rise, but these effects become lower in intensity and affect only a small area. Thus, teleseismic hypocentral locations are probably relatively accurate seaward of the trench. Theoretical slab effects include a low seismic amplitude zone with a high amplitude band at its edge. Observed amplitude data agrees fairly well with theoretical calculations and indicates the model is generally correct. The subducting slab also distorts focal mechanism solutions. Short period waveforms for an earthquake are consistent between stations, and focal depths determined using depth phases for forearc and outer rise earthquakes are generally shallower than ISC determinations.

In memory of
Dr. William J. Rogers, Ed.D

ACKNOWLEDGMENTS

I would like to thank my committee chairman and advisor, Kazuya Fujita, who did everything which could be expected to see this study through, and more. He also taught me that foreign foodstuffs can be delicious even if you can't pronounce them. I would like to thank the other members of my committee, F. William Cambray, Masaharu Kato, and James W. Trow, for their help, criticism, and encouragement. Thanks to the faculty and staff at both Northwestern University and Michigan State University for their understanding and cooperation. Mom paid for part of this; so did the Department of Geology of Michigan State University, and I am grateful to both parties.

This research was supported in part by National Science Foundation grant EAR 80-25267 and by Petroleum Research Fund grant G12366.

TABLE OF CONTENTS

Chapter 1: Introduction	1
1.1 The nature of forearc and outer rise earthquakes	5
1.2 Rheology of the lithosphere	7
1.3 Regional stress in the lithosphere	15
1.4 Effects of subducting slabs on earthquake location	16
 Chapter 2: Real and Theoretical Slab Effects	 26
2.1 Ray tracing and model slabs	26
2.2 Ray tracing results	29
2.3 Amplitude effects	47
2.4 Waveform effects	60
2.5 Effects on focal mechanism plotting	71
2.6 The practical limits of slab mislocation effects in the Aleutians.....	71
 Conclusions	 77
 Bibliography	 79
 Appendix I: Program "Raytrak"	 84
 Appendix II: Using "Raytrak"	 107

FIGURES

1.	Index map of study area	3
2.	Adak local seismological network	4
3.	Sample Raytrak plot output	23
4.	Thermal model of slab	25
5.	Seismic velocity model of slab	25
6.	Ray tracing results	31
7.	Ray path sketch	45
8.	Relative amplitude vs. zero residual line	55
9.	ISC earthquake depths vs. depth phase earthquake depth determinations.	61
10.	"Escalating" waveform arrivals at several seismological observatories ..	63
11.	"Clean" waveform arrivals at several seismological observatories ..	65
12.	Ray emergence points corrected for slab ray path distortion effects vs. the same emergence points uncorrected.....	70
13.	Stations detecting the earthquake of February 27, 1970, showing which ones would have shown slab effects for different values of δ	70
14.	Stations detecting the earthquake of May 30, 1967, showing which ones would have shown slab effects for different values of δ	72
15.	Percentages of stations affected for different values of δ ..	76

TABLES

1.	Earthquakes used in this study	50
2.	WWSSN stations in networks-locations in degrees/minuities/seconds/	51

CHAPTER 1

INTRODUCTION

Precise earthquake location is vital to many fields of geophysical study. Often the seismicity of a certain area and its associated effects are the main or only information available for investigation of the local tectonic processes. This is especially true of tectonically active offshore areas such as island arc and trench systems. The distribution of observed seismicity was originally the main argument for explaining these island arc-trench systems as the sites and surface expression of subducting lithosphere (Isacks et al., 1968). As the precision of hypocentral locations increased, the extreme thinness of Benioff-Wadati zones became apparent (Isacks and Barazangi, 1977). More recently, further refinement in earthquake location procedures has allowed the discovery of double seismic zones in subducted slabs (Umino and Hasegawa, 1975; Barazangi and Isacks, 1979; Fujita and Kanamori, 1981).

This thesis investigates the accuracy of the conventional earthquake hypocentral location method as applied to earthquakes in the forearc and outer rise regions of a subduction zone. It has been generally assumed that these earthquakes are well located by teleseismic means, and that no correction for the effects of the subducting slab on signals from these earthquakes needs to be made (Sleep, 1973). An attempt will be made to decide whether this assumption is correct. It is hoped that it will be possible to improve the accuracy of location of these forearc and outer rise earthquakes. This would improve our knowledge of the subduction process, the state of stress at

FIGURE 1.

INDEX MAP OF STUDY AREA.

Circles indicate ISC epicenters for earthquakes considered in detail in this thesis.

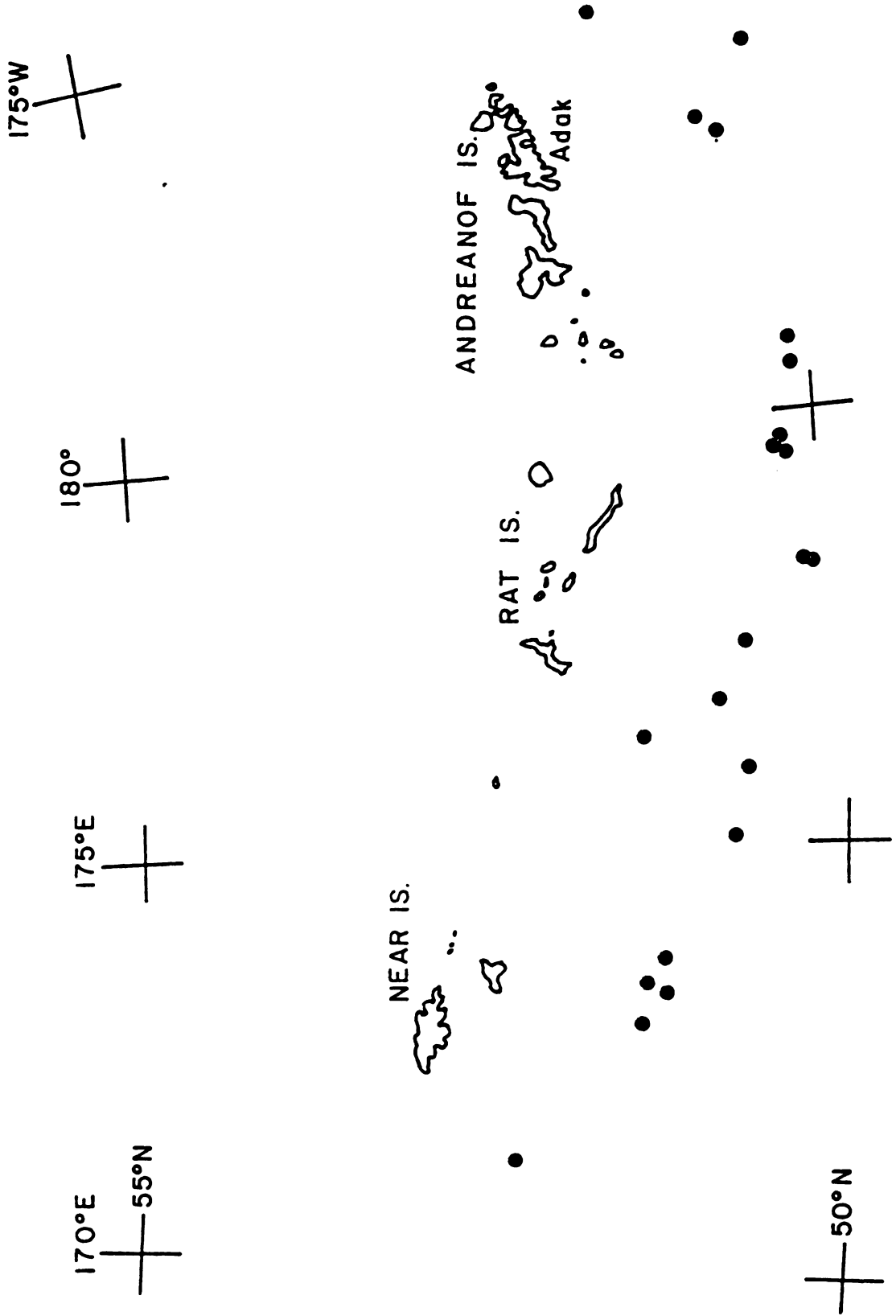


FIGURE 1

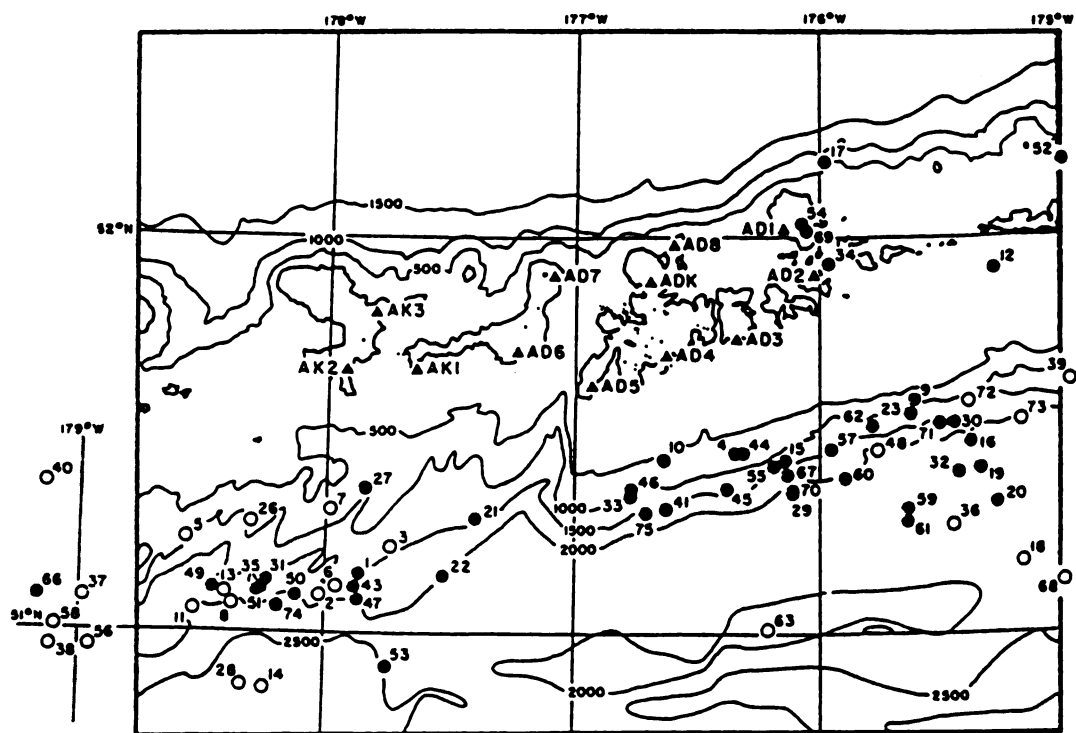


FIGURE 2

ADAK LOCAL SEISMOLOGICAL NETWORK

Triangles indicate instrument locations for this network.

convergent plate boundaries, the structure of the subducting slab, and the rheology of the lithosphere.

The earthquakes studied in this thesis occurred in the central and western Aleutian Islands, Alaska (Figure 1). Studies of this area are made easier by the nuclear tests which were carried out on Amchitka Island. In addition, seismicity and crustal structure are well calibrated at the eastern end of the study area, in the region covered by the Adak local microearthquake network (Figure 2).

Portions of this thesis have been presented as Fujita et al.(1980).

1.1 The Nature of Forearc and Outer Rise Earthquakes

Most of the earthquakes in a subduction zone occur in the shallow thrust region. These are the most powerful earthquakes as well as the most frequent. They are not the only earthquakes present in subduction zones, however. Earthquakes also occur downdip of the shallow thrust region within the subducting slab. These concern this study only in as much as it is by their presence that the length of the slab is generally estimated. The other region of seismicity in the subduction zone is the forearc and outer rise.

Earthquakes can occur anywhere in the forearc or outer rise areas, but tend to be concentrated near the trench axis (Forsyth, 1980). These earthquakes tend to have normal fault mechanisms, indicating their being caused by tensional forces. Therefore, it has long been assumed that these earthquakes are caused by the bending of the lithosphere before subduction (Stauder, 1968a, 1968b). There was some thought that a portion of these earthquakes might be in the accretionary prism, associated with the extreme deformation this feature is

subjected to, but there seems to be no evidence which conclusively indicates any earthquakes occurring in the accretionary prism at all (Chen et al., 1981). Because of this information, it appears that the earthquakes in the forearc and outer rise are caused by the bending in the slab as Stauder (1968a, 1968b) stated. This occurs because when the plate is bent, having a finite thickness rather than an infinitesimal one, only the "neutral plane" approximately midway between the top and bottom of the slab bends without being otherwise stressed. Since the slab is bent downward, the part of the slab above the neutral plane is put in tension with the amount of stress depending linearly on the distance above the neutral plane. The part of the slab below the neutral plane is in compression, and again the amount of compression depends linearly on the distance from the neutral plane (Johnson, 1970). The exact position of the neutral plane depends on the regional stresses, if any. A regional compressional or tensional stress will displace the neutral plane upward or downward, respectively (Johnson, 1970). The position of the neutral plane should also depend on the properties of the material being bent. If these properties are not uniform, some displacement of the neutral plane from the ideal position should be seen.

It seems that far more tensional earthquakes than compressional ones are recorded from the forearc and outer rise. If the plate being bent is of uniform properties there should be equal numbers of compressional earthquakes at the bottom of the slab. Several possible reasons for this disparity exist:

[1] There are equal numbers of compressional earthquakes, but for some unknown reason they are not detected. In the absence of an explanation of why this should be so, it seems unlikely.

[2] The lower parts of the lithosphere are hotter than the upper (Toksöz et al., 1973) and may distort plastically without breaking sharply to cause earthquakes.

[3] A combination of the above may occur.

1.2 Rheology of the Lithosphere

Better location of forearc and outer rise earthquakes would help determine the rheology of the lithosphere. Even basic questions about this, such as the thickness of the lithosphere and the definition of what the lithosphere is are more difficult to answer adequately than might at first appear.

The lithosphere is generally defined as the crust of the Earth and that part of the mantle above the low (seismic) velocity asthenosphere. The thickness of the lithosphere is thought to be about 100 km. The exact thickness of the lithosphere varies greatly from place to place. The lithosphere thickens as a function of cooling and therefore of age (Caldwell and Turcotte, 1979; Baer, 1981). An extreme example of the range in thickness occurs in marginal seas such as the Japan Sea, where the lithosphere has a thickness of about 30 km while the nearby Pacific Ocean lithosphere has a thickness of about 75 km (Segawa and Tomoda, 1976).

The problem with this is the question of what method to use for determining the thickness of the lithosphere. One way is to use seismic methods (e.g. Jin and Herrin, 1980). These use observations of seismic

waves to determine where the lithosphere ends. However, it is not certain that materials which behave elastically over very short seismic time spans will also behave elastically over years or millions of years.

There are also thermal methods. The thermal method involves assuming conditions at the midocean ridge axis, cooling rates of the lithosphere, and from these calculating the changes in lithospheric thermal structure with time. In the absence of conclusive data about the composition and temperature-pressure conditions of the lithosphere below relatively modest depths, it is unfortunately impossible to decide whether a given temperature is in itself an absolute indicator of rheological behavior.

Another problem is that of time scales. It is believed that rocks behave differently over different time spans. While the behavior of rocks at high temperatures and pressures can be tested in the laboratory (although not to the extent of duplicating conditions very deep in the Earth) it is impossible to experimentally check the behavior of rocks on the time scale of millions or even hundreds of years. Liu (1980) points out that a common assumption of lithospheric models based on elastic thin plate theory is that the upper part of the mantle behaves elastically over long periods of time while the lower part does so only over very short periods, behaving viscously over longer periods of time. Watts et al. (1980), using thin elastic plate theory, claim that observations indicate that the mechanical thickness of the lithosphere is only one half to one third its "seismic" or "thermal" thickness. Such assumptions are needed to fit observed data, which require a perfectly elastic plate of around 20-30 km thickness and relatively high strength, while seismic studies and thermal

models indicate lithospheric thickness to be much greater.

The mechanical thickness of the lithosphere can also be estimated by observing its behavior under certain loads and bending moments. These include the behavior of the lithosphere at subduction zones, its subsequent straightening, and its deformation under point loads such as seamounts (e.g. Bodine et al., 1981; Forsyth, 1980; Caldwell et al., 1976; Hanks, 1979). These studies have the advantage of avoiding the problems of time dependent behavior of rocks to some extent, since the rocks studied have been under stress for very long periods of time, being real world examples and not laboratory samples. Results of this type of study, however, are very model dependent. Estimates of the mechanical thickness of the lithosphere depend largely on the assumed overall rheology of the lithosphere. Since the results of these studies are model dependent there has been a large degree of success among various authors in fitting the observed behavior of the lithosphere to wildly different rheological models, achieved by altering the properties of the lithospheric materials to fit the data without ever altering the assumed model.

Many different models for the rheology of the lithosphere have been proposed. These include a simple thin elastic plate, an elastic plate under regional compression, an elastic-perfectly plastic plate with or without regional compression, an elastic-perfectly plastic plate with variable strength in different layers, and an all-viscous model (Forsyth, 1980) as well as more complex models such as that of Beaumont (1979) which combine several distinct depth-dependent rheologies.

The distribution of forearc and outer rise earthquakes is already

well enough known to disqualify some rheological models. For example, consider the thin elastic plate model (e.g. Caldwell et al., 1977). This is the simplest rheological model for the lithosphere generally proposed. It can explain the geometry of the outer rise fairly well, and can do so without requiring large amounts of regional compression in the oceanic crust; it can explain the geometry of all subduction zones if it is assumed that those with shorter than normal wavelengths are under regional tensile stresses of about 10 kilobars and bending plate stresses of about 15 kilobars (Forsyth, 1980). Forsyth (1980) claims that it is somewhat unreasonable to assume that the lithosphere can handle such stresses. Many authors claim that the lithosphere either can not or does not support such stresses. For example, Watts et al. (1980) claim that the lithosphere can withstand a much more modest 1 kilobar stress over long periods of time. Kirby (1980) believes on the basis of laboratory experiments that the ultimate compressive strength of the lithosphere in its strongest layer is about 8 kilobars; since this is only for the strongest layer, the overall average strength of the lithosphere would be much less. Lambeck (1980) believes on the basis of observation of the crust's configuration under loads and considerations of isostasy that the average crustal stress is about 500 bars and the maximum stress differences between maximum and minimum on a given piece of the lithosphere is about 1-1.5 kilobars. Solomon et al. (1980) state that average differential stress in the lithosphere is only about 200-300 bars. Liu (1980) believes the lithosphere to be even weaker, being able only to support differential stresses of around 50 bars. Because of these considerations, it seems unlikely that the lithosphere behaves in a perfectly elastic manner.

None of this, however, is able to completely disprove the contention that the lithosphere behaves as a thin elastic plate. The most convincing argument against thin elastic plate theory comes from consideration of the distribution of earthquakes in the forearc and outer rise. If these earthquakes are caused by the bending of the plate, they should be evenly distributed across the area of bending under thin elastic plate theory. This is because a bending perfectly elastic member will have an even amount of stress everywhere across the area of its bending, and so earthquakes will be equally likely anywhere in that area. The present knowledge of the distribution of forearc and outer rise earthquakes is good enough to show that these earthquakes are concentrated in the forearc region, not distributed evenly across the outer rise, which fact effectively disproves the thin elastic plate theory of lithospheric behavior (Forsyth, 1980).

Viscous models of the lithosphere have also been proposed. These models can explain the topography of the trench and outer rise under all conditions. They do not require large bending stresses; a stress of less than one kilobar is sufficient. However, these models are not able to explain the fact that the bending lithosphere can hold a fairly high stress without relaxing over a period of millions of years, as in the Puerto Rico trench (Forsyth, 1980) or in the case of the Michigan Basin, where the stresses caused when this feature first appeared have not relaxed significantly in 450 million years (McAdoo et al., 1978). Therefore, it would seem that the lithosphere does not behave in a completely viscous manner over time scales significant in regard to plate tectonics.

The simplest mechanical model for the lithosphere which seems to

fit all the observed data relatively well is the elastic-perfectly plastic model (e.g., McAdoo et al., 1978). This model suggests that the lithosphere behaves elastically up to a critical yield stress. Below this yield stress any deformation undergone by the lithosphere will be recovered after the stress causing the deformation is removed. At the yield stress the material breaks and deforms in a perfectly plastic manner, causing permanent deformation. A model based on a simple single-layer elastic-perfectly plastic model still requires fairly large regional compression to explain all the observed topography of the sea floor (McAdoo et al., 1978). Again, the distribution of forearc and outer rise earthquakes would tell us much about whether this rheological model of the lithosphere is acceptably close to the real behavior of the lithosphere or not. Forsyth (1980) observes that tensional earthquakes in the forearc and outer rise extend to at least a depth of 25 km, even in subduction zones which are assumed to be under strong compression, and that this is deeper than earthquakes could occur under an elastic-perfectly plastic single layer model. Unfortunately, this is cutting the observations very close to their limit of accuracy. In the areas of subducting slabs, errors on the order of 10 km in hypocentral depth are believed to occur using teleseismic hypocentral location procedures (Fujita et al., 1981); if similar errors occur for earthquakes in the forearc and outer rise, Forsyth's objection to the single layer elastic-perfectly plastic model (1981) may not be valid. In order to make such fine distinctions it would be useful to determine whether these hypocentral location methods are really as accurate in the forearc and outer rise as seems to be generally believed.

The rheological model which Forsyth (1980) prefers to the single layer elastic-perfectly plastic model on the basis of this fine distinction of earthquake depths is the elastic-perfectly plastic variable strength model. Under this rheology, the lithosphere behaves as under the simple elastic-perfectly plastic model except that different layers of the lithosphere have different critical yield stresses. This model reduces or eliminates the need for regional compressive stresses (Chapple and Forsyth, 1979) and can explain all the observed topography of the ocean floor at least to the level of accuracy now available; it can also explain the distribution of the earthquakes in the forearc and outer rise (Forsyth, 1980).

These more or less simple rheological models for the lithosphere are useful in predicting the behavior and seismicity of the lithosphere under different conditions. However, it seems unreasonable to assume that any simple model with only one or two discrete layers explains the actual behavior of the lithosphere in every way. Aside from phase boundaries, temperature and pressure which vary continuously with depth should lead to continuously variable physical properties rather than discrete boundaries.

Several authors have proposed quite involved rheological models for the lithosphere. Beaumont (1979) has developed a rheology based on the olivine flow laws observed in the laboratory, extrapolated to higher temperatures and pressures. He assumes that the temperature of the lithosphere is a linear function of depth in any given location. This leads to a rather complex rheological cross section for the lithosphere. In a typical area with lithosphere 100 km thick, the crust might behave plastically via cataclastic flow down to a depth of

12 km, at a temperature of 180° C. Below this, to a depth of about 58 km and a temperature approaching 800° C, the crust behaves in a pseudo-elastic manner. The rheology of this "pseudo-elastic" area is based on diffusional (Newtonian) creep. Given time the lithosphere will creep out from under any stress applied to it, but since the strain rate for this zone is slow it will take a very long time, up to a billion years. Below this level the lithosphere behaves in an increasingly plastic manner until the base of the lithosphere is reached at about 100 km, where the temperature is around 1,300° C.

The time scales involved in Beaumont's (1979) model can be very long. When a load is applied to the lithosphere, plastic yielding in the lower part of the plate reduces the apparent elastic thickness of the lithosphere from its thermal or seismic thickness to at most half this value. This takes place over a period of 10^6 or 10^7 years. In the upper layers of the lithosphere, diffusional creep will reduce the apparent flexural rigidity over time scales as long as 10^9 years. This is long enough so that the oceanic crust will appear to be elastic over plate tectonic time scales. However, continents (which persist longer than oceanic crust) will eventually be allowed to reach a relatively unstressed isostatic equilibrium over most of their area, as is observed (Beaumont, 1979).

Bodine et al. (1981) have proposed a model of the lithosphere with three different rheologies. They use an elastic-plastic rheology based on cataclastic flow to describe the lithosphere at shallow depths. At greater depths the authors propose a temperature activated creep as the factor which governs yield stress. For shear stresses less than

2 kilobars, power law creep dominates and is expressed as

$$\dot{\epsilon} = 70(\sigma_s)^3 \cdot \exp(-Q_p/RT)$$

where $\dot{\epsilon}$ is the strain rate, σ_s is the shear stress, T is the temperature in degrees Kelvin, R is the universal gas constant and Q_p is the activation energy. At shear stresses greater than 2 kilobars, power law creep breaks down and the authors state that the Dorn law works better, expressing the creep as

$$\dot{\epsilon} = 5.7 \cdot 10^{11} \cdot \exp(-Q_d/RT[1 - \sigma_s/8.5 \cdot 10^4]^2)$$

with all notation as before, except for Q_d . Q_d is an activation energy not equal to Q_p , chosen to assure that both laws agree at 2 kilobars.

Whether the rheological model considered is meant to describe the behavior of the lithosphere as a whole or actually to describe the behavior of rocks at all the specific levels within the lithosphere, accurate data about observed lithospheric behavior is necessary. Sufficiently good data might make it possible to decide which simple model works best and whether the more complicated models are generally worth the extra trouble they cause. In any case, more accurate location of earthquakes in general and forearc and outer rise earthquakes in particular will help answer these questions.

1.3 Regional Stresses in the Lithosphere

A question which is closely related to rheology is the question of the regional field of stresses throughout the lithosphere. There are various means of approaching this problem. Lambeck (1980) uses topography and isostatic considerations to estimate the average stress on the lithosphere. This method is unfortunately dependent on the rheology assumed. Another way of approaching the problem is by

investigation of intraplate earthquakes (Richardson et al., 1976,1977; Richardson and Solomon, 1977) on the assumption that these reflect accurately the regional stress field. Unfortunately, earthquakes in midplate or passive margin regions may occur along pre-existing fault systems. These may date from process on midocean ridges; they are not necessarily well aligned with the present day stress field, but represent a direction of weakness along which slip can easily occur. The mechanisms of the resulting earthquakes may relate to the present-day stress field in only a relatively vague manner (Stein, 1978,1979). This is an especially perplexing problem, since a better understanding of the worldwide regional stress fields would probably help not only in determination of lithospheric rheology but might give information on the driving forces of plate tectonics as well (Richardson et al., 1976).

The seismicity of the forearc and outer rise is one of the best sources of data to solve these problems. As was shown in the last section, seismicity is one of the chief sources of data for determining lithospheric rheology. The questions of rheology and regional stress are so closely intertwined that to answer one is a large part of answering the other.

1.4 Effects of Subducting Slabs on Earthquake Location

One of the major sources of error in hypocentral location is the lateral inhomogeneity of the upper mantle seismic velocity in and near subduction zones. The effect of this inhomogeneity has long been detected for earthquakes in the shallow thrust region of various subduction zones (e.g. Davies and McKenzie, 1969; Biswas, 1973; Suyhiro and Sacks, 1979; Fujita et al., 1981). These mislocation effects have also

been observed in connection with nuclear explosions. It was observed that teleseismic location of nuclear tests in the middle of the Pacific, far from subduction zones, are accurate to within 5 km of the actual focus (Sykes, 1966) while similar solutions for tests in the Aleutians tend to be mislocated farther north and deeper than the actual foci, presumably due to the effect of the subducting slab beneath these islands (Sykes, 1966; Herrin and Taggart, 1968; Jacob, 1972). The disagreement between local seismic network hypocentral locations and teleseismic hypocentral solutions for the same events can be on the order of 50 km (Murdock, 1969; Fujita et al., 1981).

The cause of these effects is fairly well known, although their magnitude generally is not. The subducting slab is cooler, denser, and more rigid than the ambient mantle around it. Because of these differences the seismic velocity is assumed to be higher in the slab than near it. Seismic waves passing down the subducting slab travel faster than they would travelling outside the slab (Engdahl et al., 1977). Because most hypocentral location methods assume that the Earth is spherically symmetric, a lateral inhomogeneity such as a subducting slab causes earthquake hypocenters to be determined erroneously. Specifically, the seismic stations downdip of the slab receive signals early, and since the symmetric earth model assumes that a short travel time indicates a short distance, earthquakes occurring in the shallow regions of a subduction zone appear to be further down the slab than they actually are. This results in a mislocation both in epicentral location and depth of focus, often on the order of 50 - 100 km (Fujita et al., 1981). Conversely, earthquakes deep in the subduction zone can

send seismic waves upward along the slab, causing them to be mislocated (Spencer and Engdahl, 1981).

In order to improve the accuracy of hypocentral locations it is necessary to remove this slab effect. An important means of doing this is the use of local seismological networks such as the one in operation on and near Adak Island in the central Aleutians (Figure 2). These local networks are able to detect smaller earthquakes than the teleseismic seismological stations are. More important from the point of view of earthquake location methods, they are presumably largely free of slab effects. Seismic waves travelling from earthquakes in the shallow thrust zone do not travel very far if at all in the subducting slab. This should presumably make hypocentral locations obtained from local networks more accurate than teleseismic solutions for the same event (Fujita et al., 1981). This provides a check on the accuracy of the teleseismic hypocentral locations and a way of determining the slab effects.

Unfortunately, this method may not be accurate for forearc and outer rise earthquakes. These earthquakes are sufficiently far from any land-based local network so that their seismic signals follow deeper paths than those from shallow thrust zone earthquakes on their way to the local network seismological stations. These deeper ray paths may pass through the lower parts of the lithosphere or inhomogeneous upper mantle, with unpredictable effects on travel times and amplitudes. For these reasons, local network hypocentral solutions for forearc and outer rise earthquakes are considered relatively unreliable. This makes it impossible to meaningfully compare the locations obtained from local networks with those from teleseismic ones.

Another problem in attempting to accurately locate forearc and outer rise earthquakes is that their magnitude is small relative to thrust zone earthquakes. Therefore, their initial signal strength is lower. In addition, Sleep (1973) has noted an extensive region of low seismic amplitude arrivals at teleseismic distances downdip of the slab. The seismic waves from forearc earthquakes which pass through the slab generally fall into this "shadow zone" and are therefore further weakened. This lessens the signal to noise ratio. The signals detected at seismological stations in this shadow zone are likely to be emergent, making accurate determination of arrival (and travel) times difficult. This may create a tendency to pick arrival times as being later than they actually are.

It has generally been assumed that the forearc and outer rise are far enough from the subducting slab so that the slab does not affect their signals. This view is strengthened by the fact that little or no systematic bias in travel times has been observed. This may be an illusion, due to the possible tendency to pick arrival times late and/or the difficulty of determining errors in teleseismic hypocentral locations for these earthquakes by comparison with local network solutions. The first would not be a matter of much concern if the tendency to misread arrivals exactly counteracted any slab effect, but this is not to be expected. The error caused by reading earthquakes differently at the seismological stations in the "shadow zone" is probably random, and if it cancels any slab effect it does so only by chance.

One way to examine the effect of the subducting slab on seismic waves from forearc and outer rise earthquakes is through seismic ray

tracing. This is a method of calculating the path followed by a seismic wave passing through various bodies with different seismic velocities. The simplest version of this is Snell's Law, which predicts the change in ray path between two discrete layers. There are various approaches to ray tracing. Sorrels et al. (1971) used Snell's Law by tracing rays through a medium made up of a series of discrete constant-velocity layers separated by planar or spherical interfaces. They used this method to examine the anomalies in teleseismic data for the nuclear test LONGSHOT, set off on Amchitka Island in the Central Aleutians. This method works but can only handle velocity gradients by using large numbers of very thin layers. This leads to some lack of precision and some increase in digital input.

In order to use gradients of seismic velocity rather than sharply bounded layers, it is necessary to use differential equations. The equations developed to predict the path of a ray in an arbitrarily inhomogeneous three-dimensional medium arise from Fermat's principle of stationary time (Jacob, 1970; Julian, 1970) from which, in the simplest case, Snell's Law also arises.

This thesis examines the effects of a subducting slab on seismic signals from forearc and outer rise earthquakes by using the ray-tracing method of Julian (1970). This involves a mathematical solution of Fermat's Principle in a three dimensional arbitrarily inhomogeneous medium. The solution consists of five simultaneous first order differential equations which give the variation with time of ray direction, based on seismic velocity and its spatial derivatives at the point in question. This method will be used only to find the ray path and travel time, hence the travel time residual. It is also possible

to quantitatively determine the effect of geometric spreading of the rays on the seismic amplitude at any point, but this requires consideration of ten additional differential equations and a large amount of additional calculation (Julian, 1970). For this reason, the calculation of seismic amplitudes based on Julian's equations is not attempted here. Instead, amplitudes will be found qualitatively using the observation that areas from which rays are refracted show a relatively low density of emergence points; ray emergence point density is therefore associated with seismic amplitude (Sleep, 1973). If a distribution of rays uniformly spaced in azimuth and take-off angle are traced throughout their paths and the emergence points of these rays at the surface of the Earth are plotted, the ray emergence points should be concentrated in areas of higher seismic amplitude arrivals and thinned out in any "shadow zone" (Sleep, 1973).

Even ignoring the quantitative determination of amplitudes, the ray tracing equations of Julian (1970) require large amounts of calculation. The cost of using this procedure for large numbers of individual earthquakes would be high. However, unless the slab is contorted or torn, its effects are a smooth function of epicentral distance from the center of arc curvature for any given constant focal depth (Fujita et al., 1981). It is therefore only necessary to determine the effects of the subducting slab at various evenly spaced points across a range of distances and to interpolate for slab effects at intermediate points. Once a table of slab effects has been produced in this manner for a sufficiently accurate slab model, it should no longer be necessary to actually trace rays at all in order to obtain the improvement in accuracy ray tracing provides (Fujita et al., 1981).

FIGURE 3.

SAMPLE RAYTRAK PLOT OUTPUT .

Small crosses indicate ray emergence points for rays calculated in previous runs. Large crosses are for the rays most recently calculated.

ANG. DIST. IS 12.60
20 RAYS.

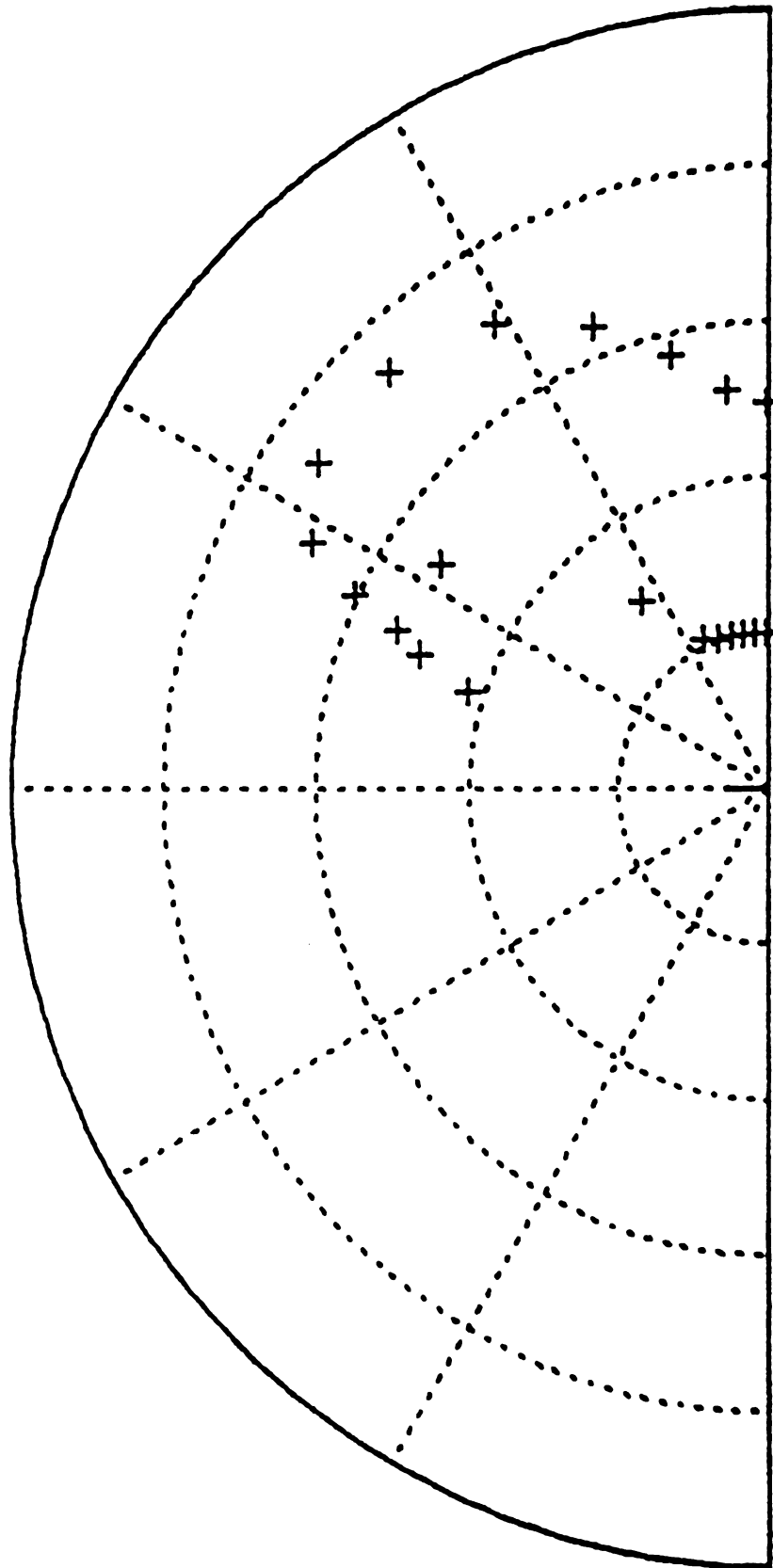


FIGURE 3

FIGURE 4

THERMAL MODEL OF SLAB (from Fujita, Engdahl, and Sleep, 1982)

Triangle at zero depth and distance of 11.4 represents location of volcanic front. Dotted outline is the outline of the subducting slab.

FIGURE 5

SEISMIC VELOCITY MODEL OF SLAB (from Fujita, Engdahl, and Sleep, 1982)

Triangle at zero depth and distance of 11.4 represents location of volcanic front. Dotted outline is the outline of the subducted slab.

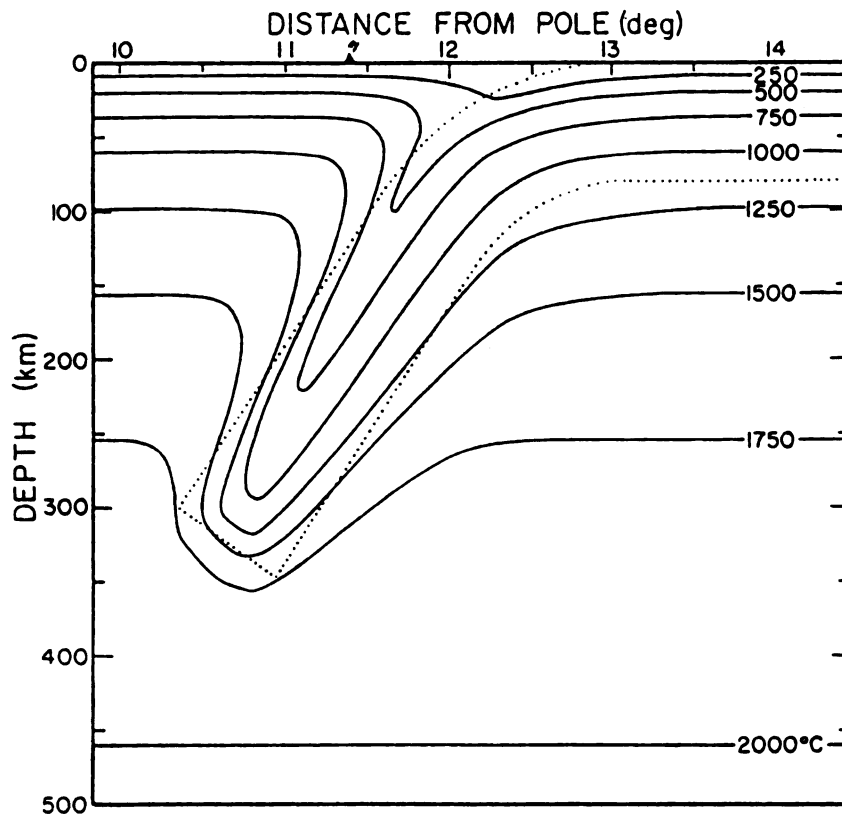


FIGURE 4

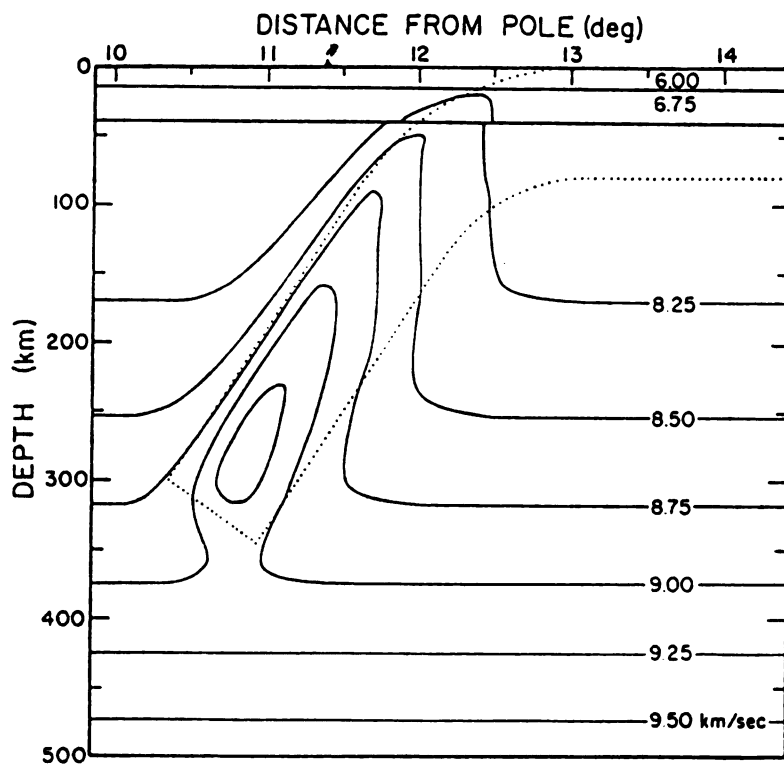


FIGURE 5

CHAPTER 2

REAL AND THEORETICAL SLAB EFFECTS

2.1 Ray Tracing and Model Slabs

The ray tracing for this thesis was done using a computer program first developed by Julian (1970) and modified thrice since (see Appendix 1). This program operates on the "shooting" system, sending rays out from the source at known azimuths and take-off angles to observe the results rather than trying to home in on the ray path between a given source point and receiver point (Julian and Gubbins, 1977). It was modified first by Sleep in 1972, then for interactive use by Fujita in 1978, and most recently by the author for automatic plotting of the ray emergence points using a Tektronix graphics terminal. As modified, the program uses ready-made Tektronix routines to create a polar projection plot showing the distance and azimuth of each ray emergence point from the earthquake epicenter. It shows these points as two sizes of crosses; the rays most recently ordered by the operator as large crosses and any previous rays as small ones. It also produces a simple polar coordinate grid for easy reference. The resulting plot (Figure 3) provides a useful display of what has been done and what remains to be done.

In order to use ray tracing, a seismic velocity model for the subducting slab is needed. This thesis uses a thermal model (Figure 4) of the slab calculated using the methods and parameters of Toksöz et al. (1973). The specific model used for the Aleutian slab in this thesis was developed by Fujita et al. (1981). A dip angle of 57.3° and a convergence rate of 4.5 cm/yr. were assumed. The model slab is 300 KM long and 80 km thick.

Fujita et al (1981) constructed a velocity model based on this thermal model (Figure 5). This was done by assuming that the difference in seismic velocity between the slab and the normal mantle velocity distribution depends linearly on the temperature difference between them. The seismic velocity at any point is given by Sleep (1973) as:

$$V(x,z) = V_o(z) + \partial V / \partial T [T_o(z) - T(x,z)] + \sum \partial V / \partial m [m_o(z) - m(x,z)]$$

where:

V = seismic velocity,

T = calculated temperature,

$_o$ (subscript) indicates an unperturbed quantity,

x = horizontal coordinate,

z = vertical coordinate, and

m = the amount of a given phase present.

However, Fujita et al. (1981) point out that the final term of this equation (which deals with velocity differences due to phase changes between slab and ambient mantle) is small with respect to the others, and is probably too small to be significant considering the data currently available. Because of this, the last term of the equation above is dropped, and it becomes:

$$V(x,z) = V_o(z) + \partial V / \partial T [T_o(z) - T(x,z)]$$

with the notation as before.

The value for the derivative of velocity with respect to temperature is assumed to be constant; the value used for $\partial V / \partial T$ was $-0.009 \text{ km/sec-}^\circ\text{C}$. This is the value used by Fujita et al. (1981). The resulting velocity model of the slab is shown in Figure 5.

There is some question of how long the slab should be, since this depends on at least two poorly known factors. These are the age of the lithosphere (which determines its thickness) and the duration of subduction. In addition, it is not known whether the slab ends where deep seismicity ends, as most authors seem to believe, or if it continues far beyond this point (Sleep, 1973; Jordan, 1977). The slab model used here is 300 km long. This is longer than the slab model used by Sleep (1973) for the Aleutians, in which paper the theoretical subducting slab had little or no effect on seismic signals from the forearc and outer rise. It is far shorter than Sleep's (1973) slab model for the Tonga arc which he felt did not fit the observed data for the Aleutians as well as the shorter slab model. It is somewhat less than the length of slab indicated by a recent velocity inversion study of the Aleutians, where the data seemed to favor a slab of about 300 km in length, with the best single fit to the data occurring for a slab 386 km long (Spencer and Engdahl, 1981). It has been observed that deep seismicity in the Aleutians extends to a depth of somewhat over 250 km (Engdahl, 1977). It would seem that 300 km is a reasonable length for the slab model based on the data currently available.

The slab model used here is 80 km thick. This thickness may be doubtful. The oceanic lithosphere subducting near Adak Island in the central Aleutians is in the neighborhood of 65 million years old (Pitman et al., 1974). Oceanic lithosphere of this age should be around 60 km in thickness (Yoshii et al., 1976) rather than the assumed 80 km.

Assuming that the subducting slab forms a symmetrical arc about its center of curvature, which is a reasonable approximation in most

areas (Fujita et al., 1981), the only geographical variable which bears on whether or not seismic signals from a given earthquake will be affected by the slab is the distance between the earthquake and the slab. This can be given in terms of the distance between the earthquake and the center of arc curvature, defined as a geocentric angle. This was done by Fujita et al. (1981), who designated this distance as δ ; it will be so designated in this thesis. The center of curvature of the arc is taken as 63.314° N, 178.059° W (Engdahl, 1973), and the bottom hinge point of the bent slab is set at $\delta = 12.5$ (Fujita, 1979) for the slab model.

2.2 Ray Tracing Results

Rays were traced through the slab model from a fixed source depth of 25 km and variable distances from the center of arc curvature. In the Aleutians, the trench axis falls at around $\delta = 13.0^{\circ}$; the range of δ covered in this thesis was from $\delta = 12.4^{\circ}$ to $\delta = 14.6^{\circ}$. This covers the forearc, trench, and outer rise. Ray tracing was done across this area at intervals of 0.2° of δ , except for the distance $\delta = 13.1^{\circ}$, which was checked in order to be certain that the spacing used was adequately close for accurate interpolation of intermediate values. It was found that the slab effect varies smoothly both as a function of azimuth and of δ , confirming the identical observation of Fujita et al. (1981). Based on this, it appears that the 0.2° spacing for values of δ is adequately close in this range of δ .

Results of the computer ray tracing are shown in figures 6A-6L. On the right side of each figure is a contoured plot of the theoretical travel time residuals indicated by the computer study. On the left are

FIGURE 6

RAY TRACING RESULTS

Polar distance plots showing slab effects for different values of δ . The radius of each plot is 100° of geocentric angular distance. Left side of each plot is a contour of travel time residual in seconds early, while the right side shows where the emergence points of rays of a given take-off angle (*italic numbers*) and azimuth (straight numbers) would fall. Dark circles are added to these points in order to emphasize areas of amplitude effects except where this would obscure detail.

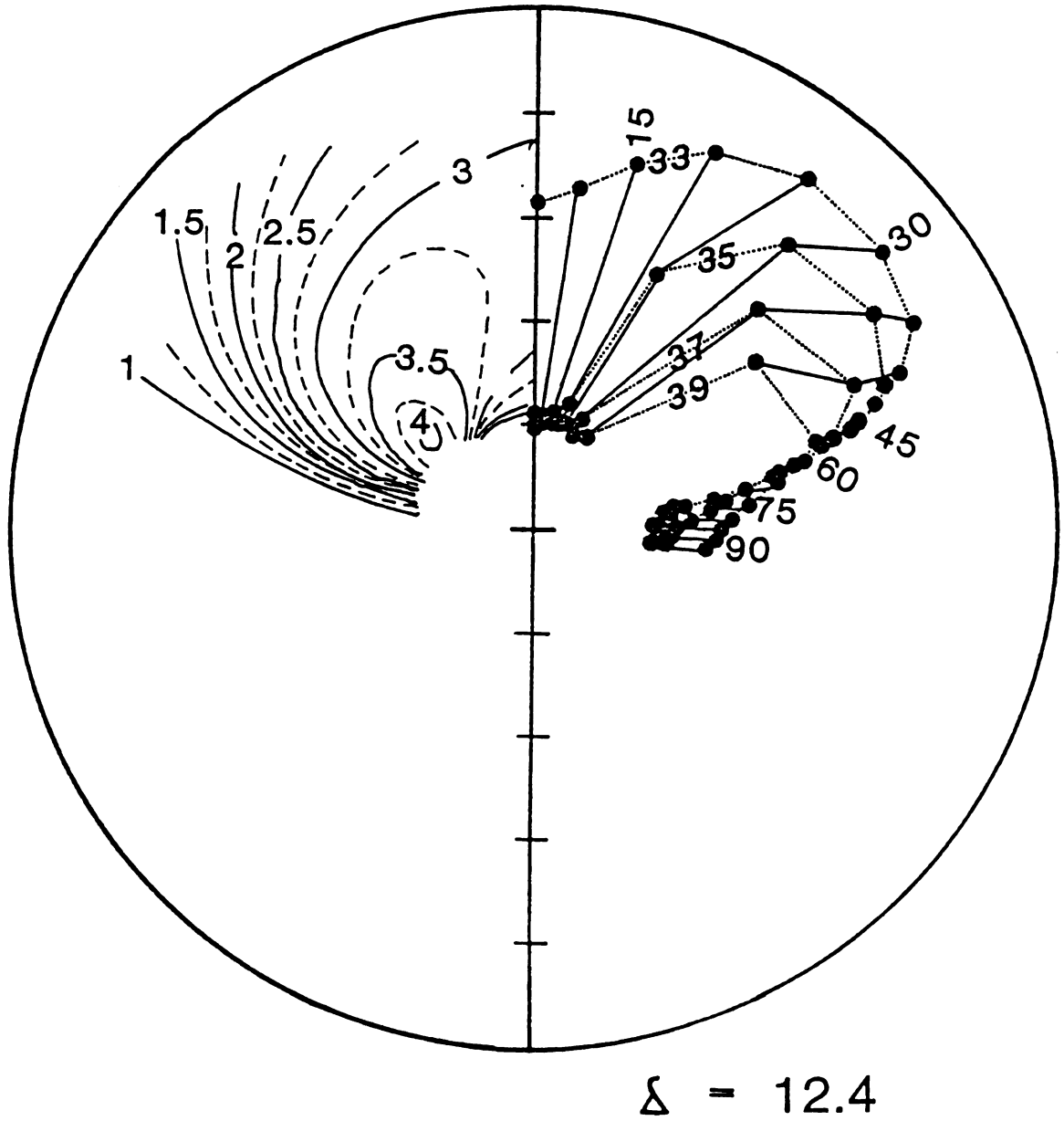


FIGURE 6-A

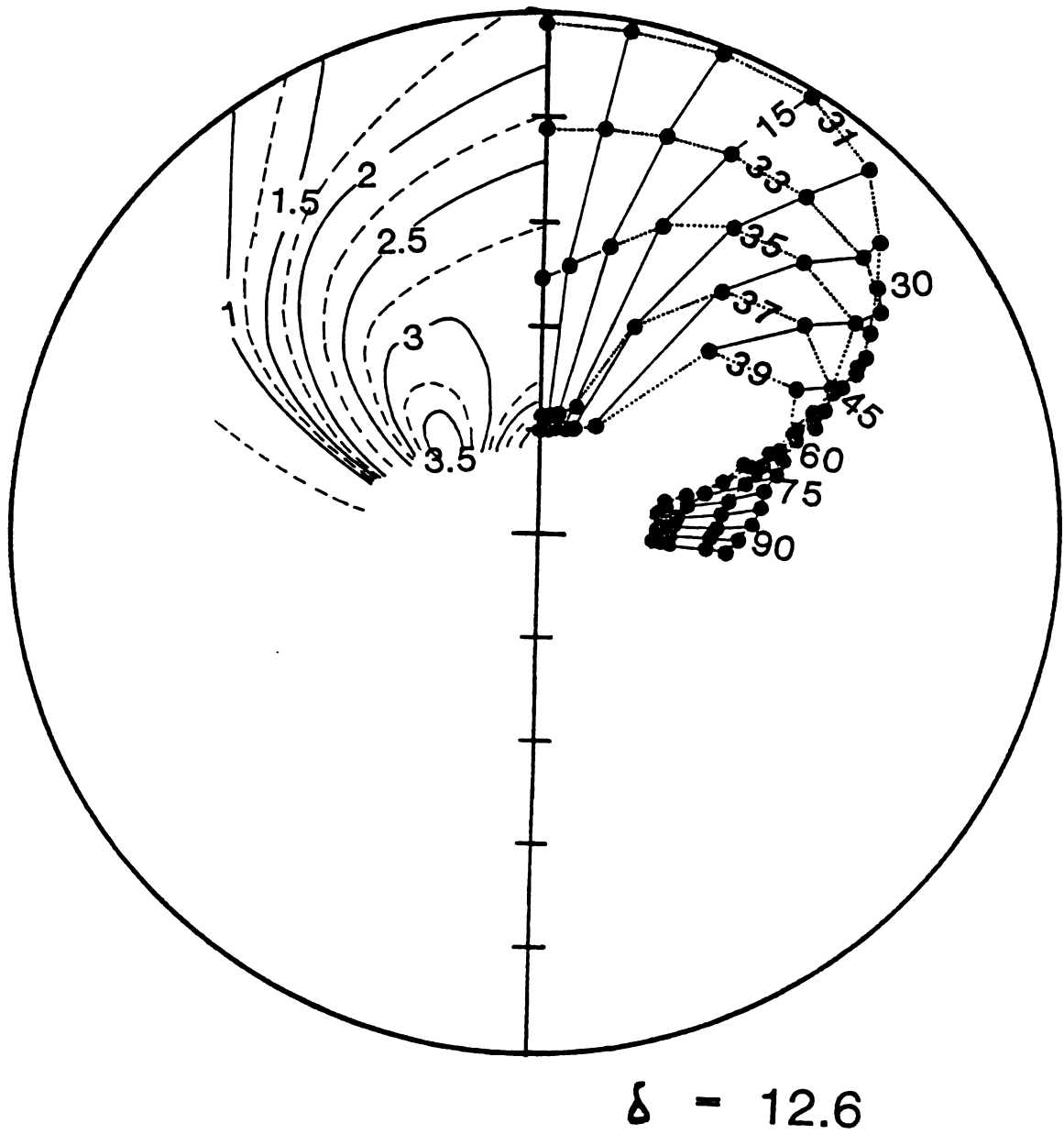


FIGURE 6-B

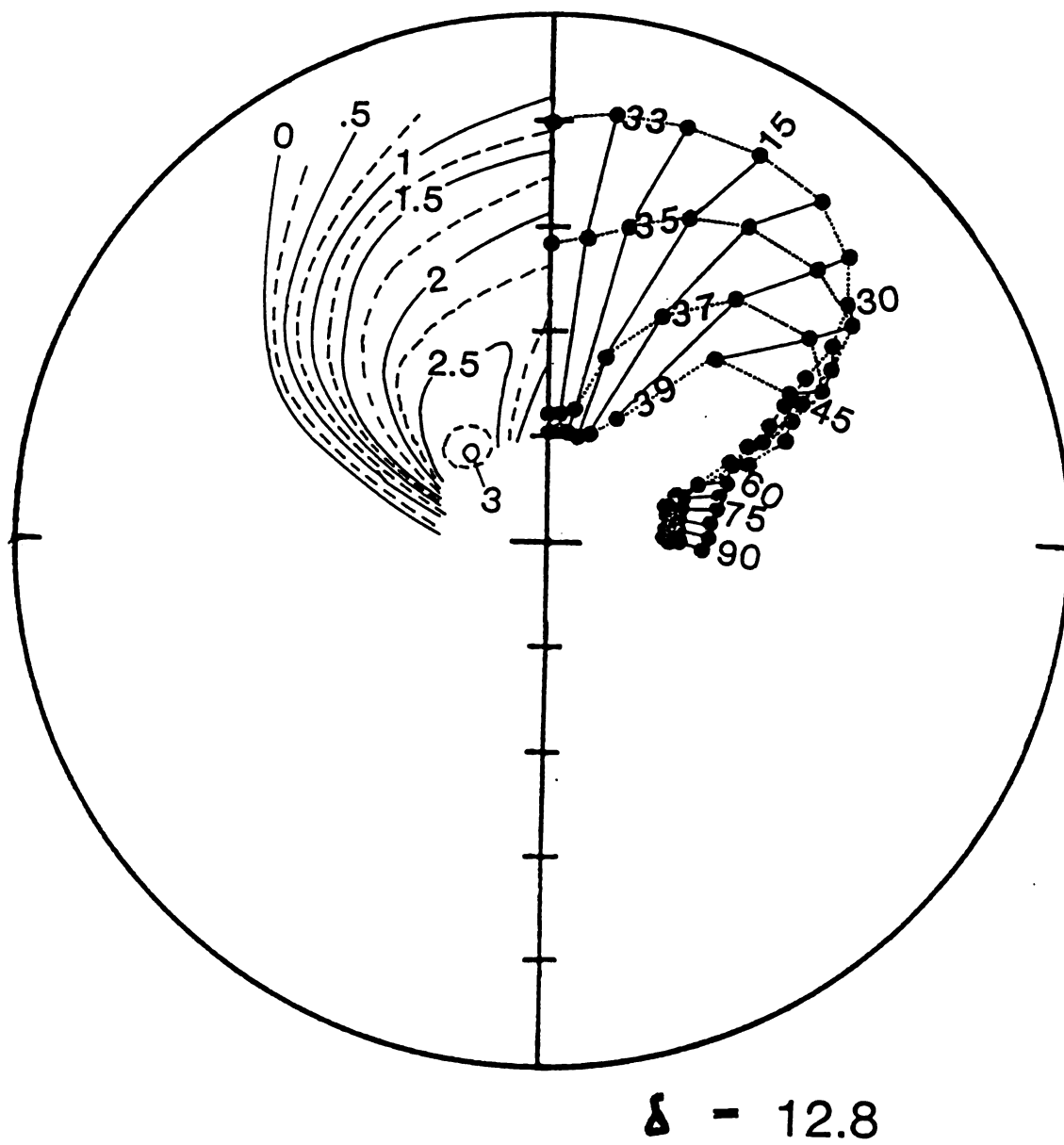


FIGURE 6-C

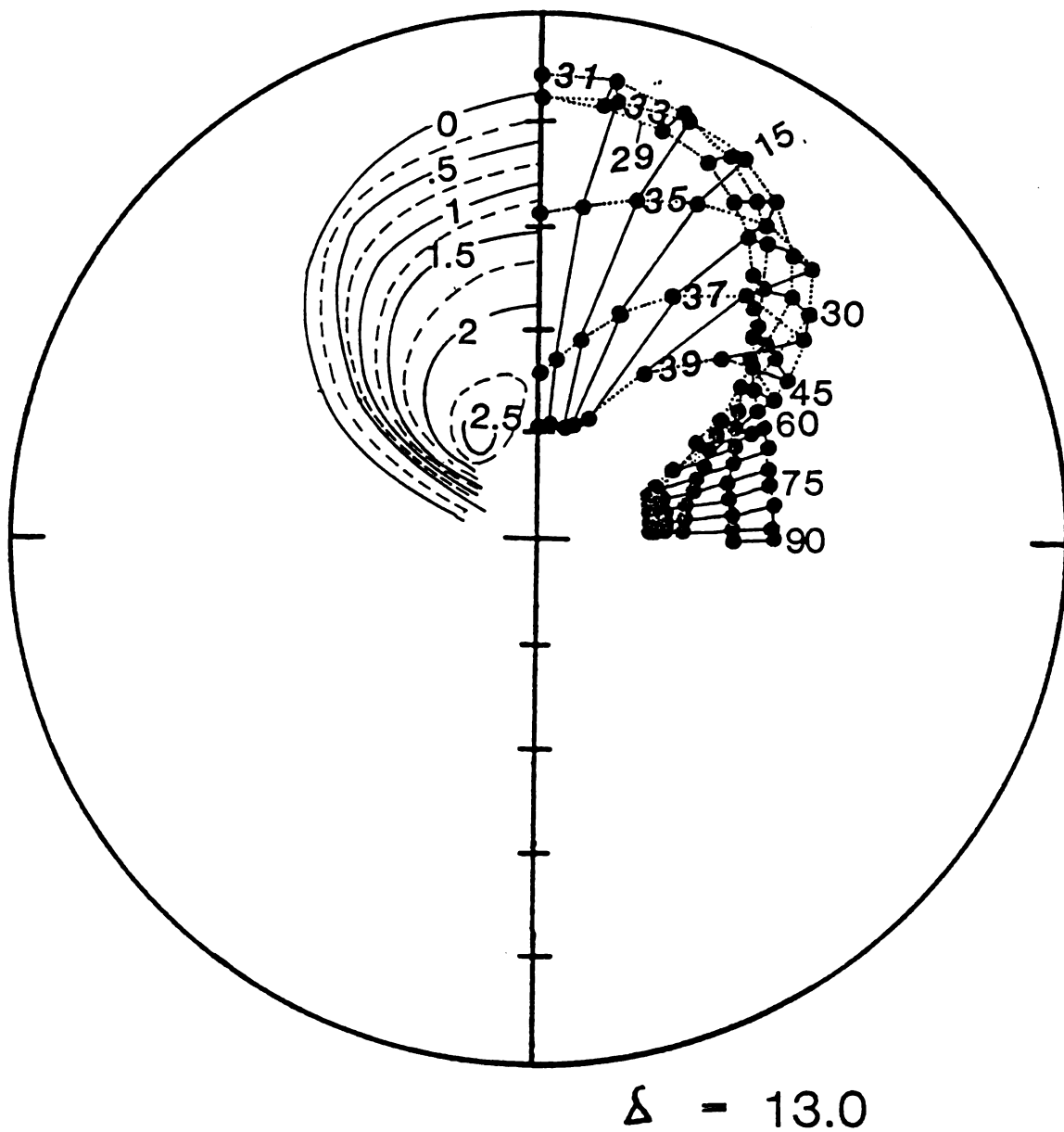


FIGURE 6-D

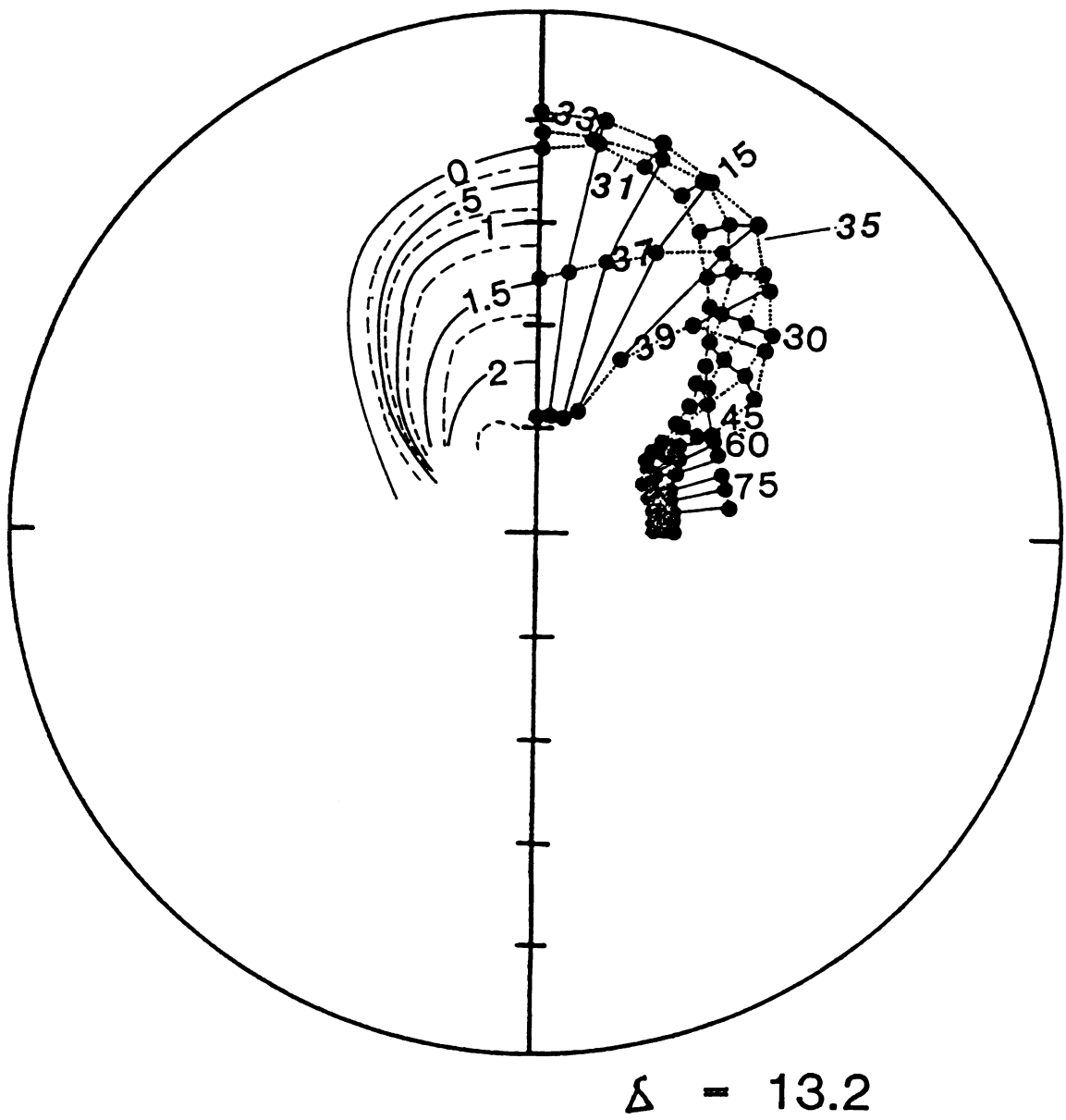


FIGURE 6-E

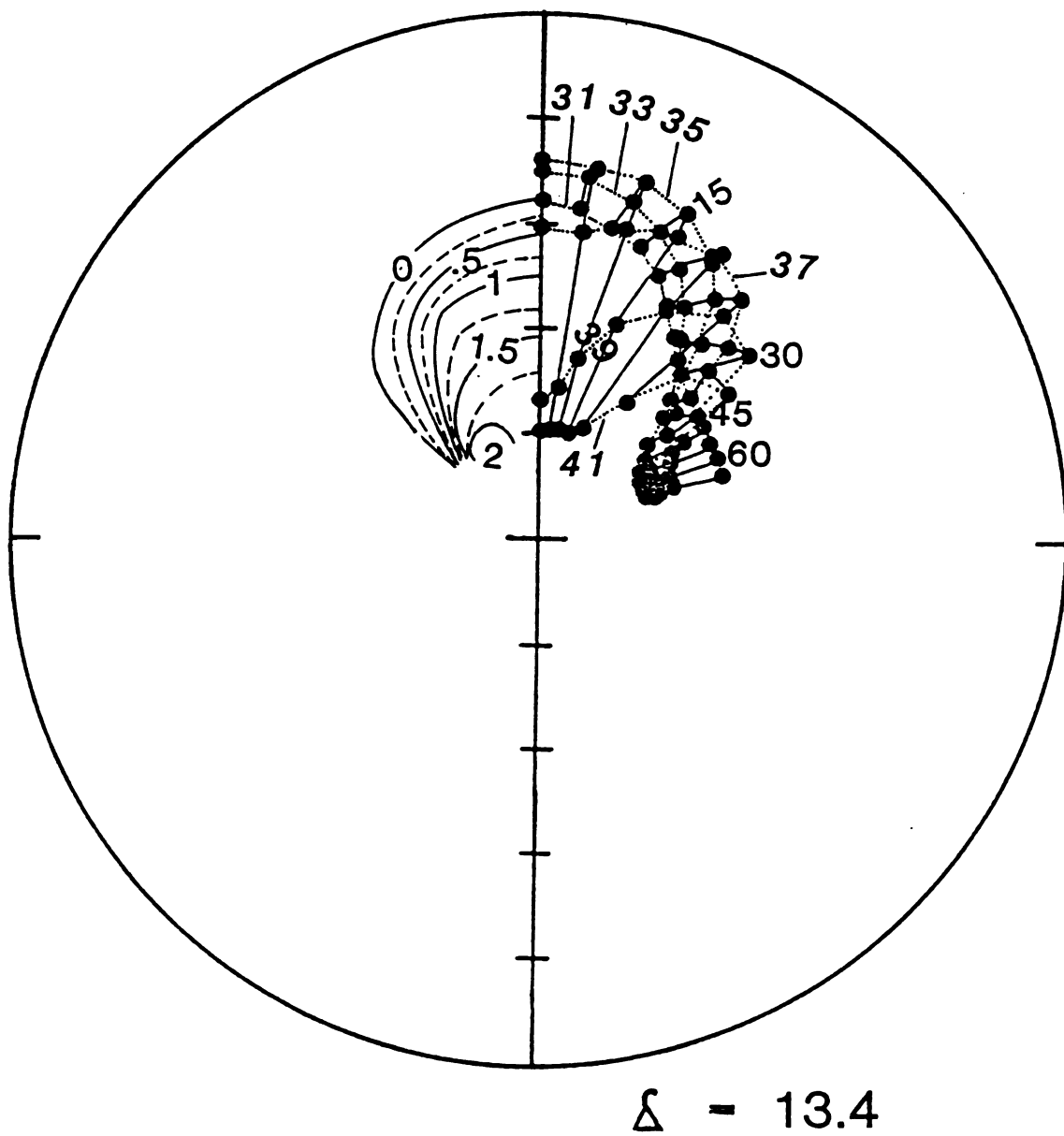
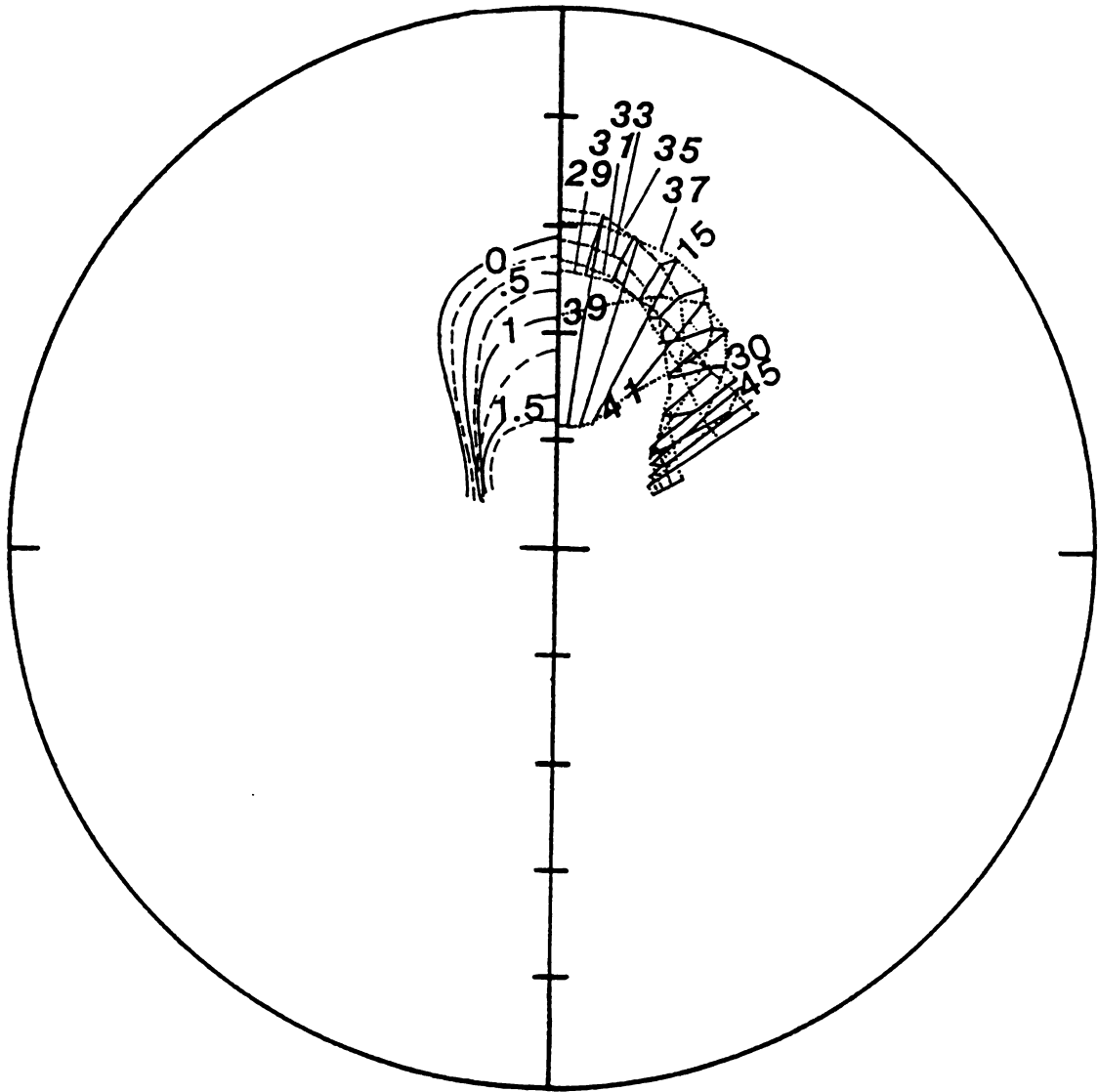


FIGURE 6-F



$\Delta = 13.6$

FIGURE 6-G

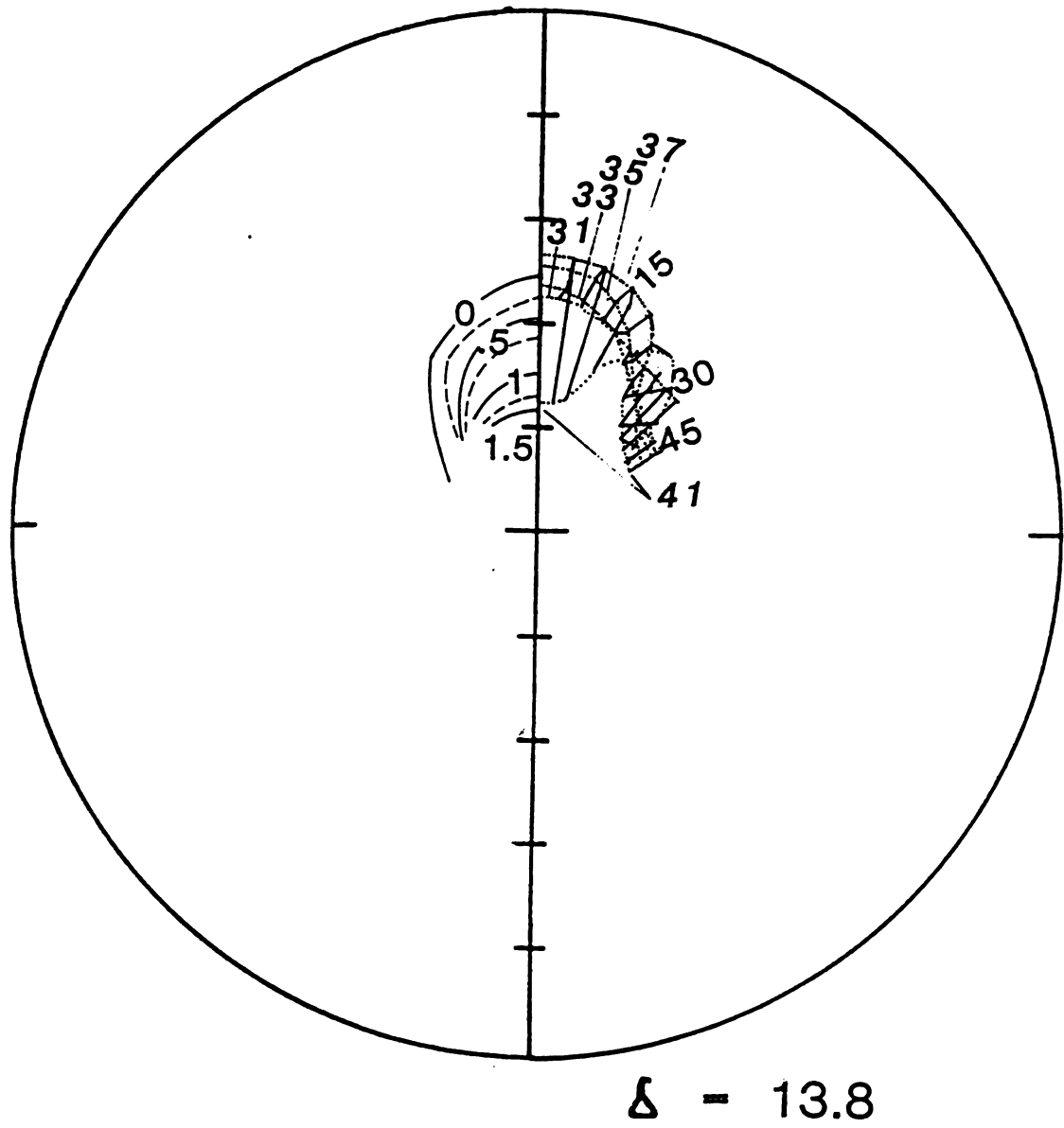


FIGURE 6-H

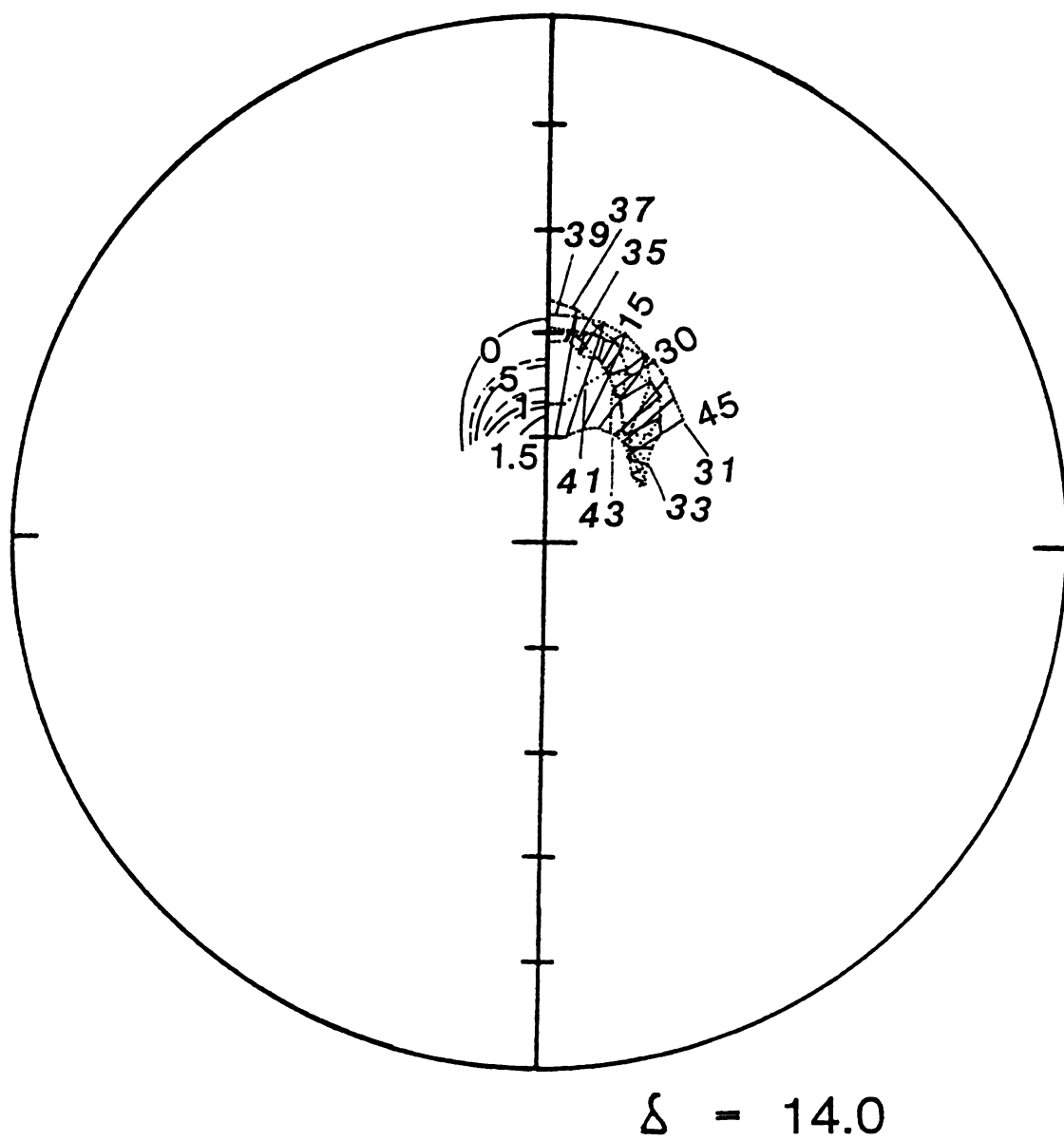
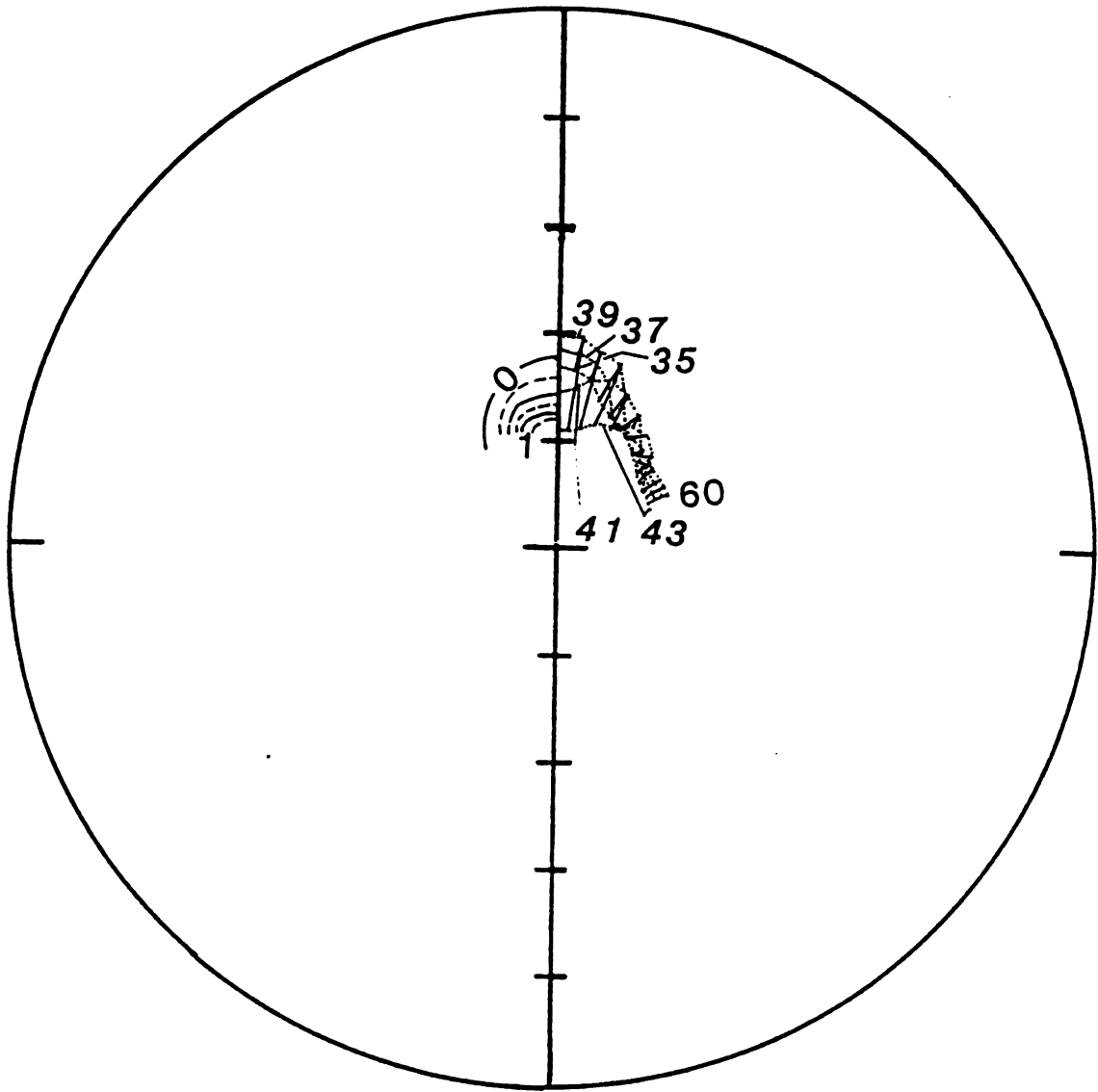
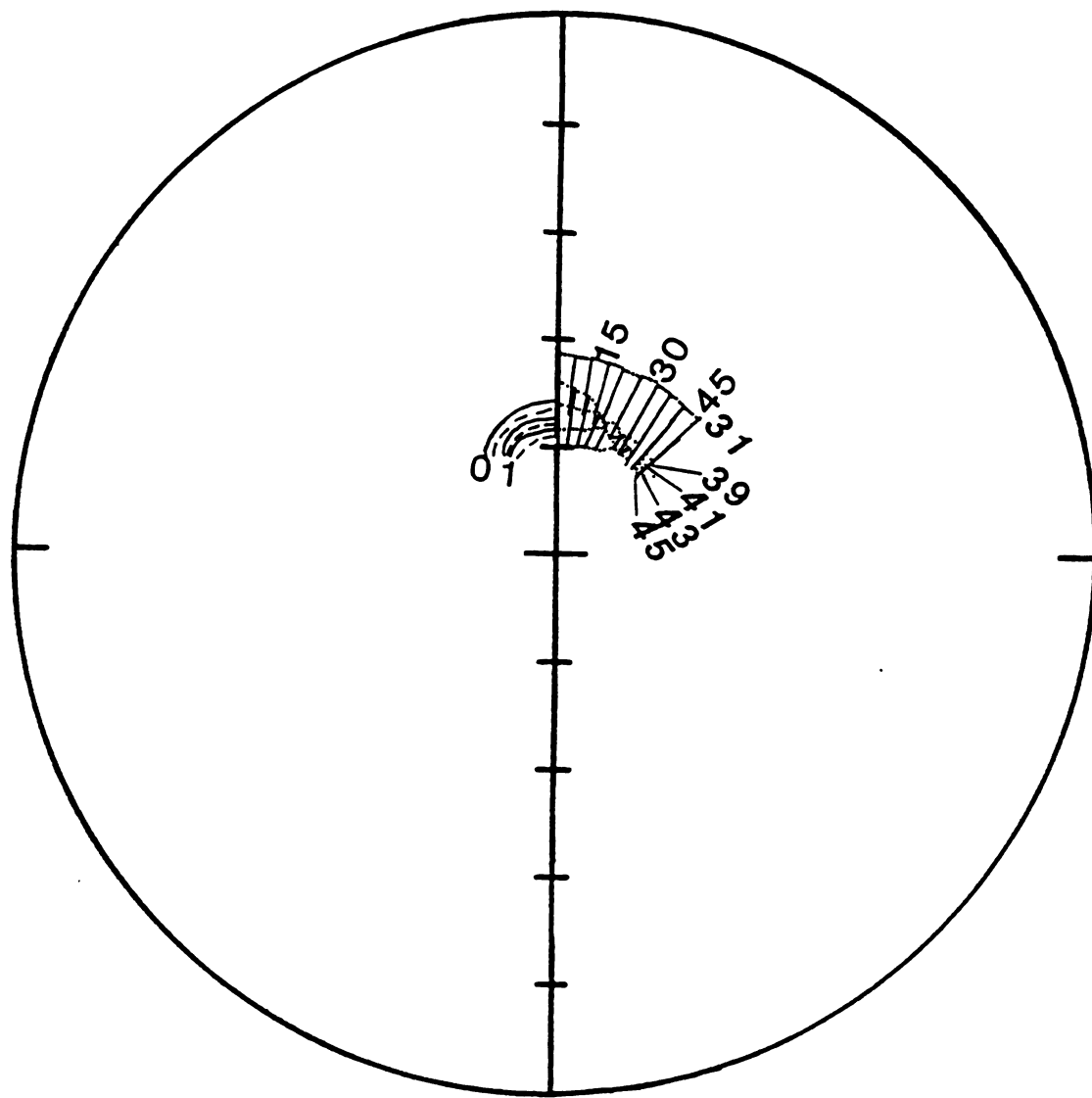


FIGURE 6-I



$\delta = 14.2$

FIGURE 6-J



$\Delta - 14.4$

FIGURE 6-K

shown lines of equal take-off angle. Running across these are another set of lines, generally radial; these are lines of equal take-off azimuth. The azimuth lines are spaced 5° apart, the take-off angle lines are spaced 2° . Radius on these plots marks the epicentral distance (Δ) from the source, in degrees. Zero degrees azimuth points in the downdip direction of the slab, which is by definition toward the center of curvature of the island arc. As it has been assumed that the slab is symmetric about its center of curvature, only half each of the full-circular travel time and ray emergence point plots are shown. The other half could be obtained by reflection across the zero-azimuth line.

Figures 6A-6L, taken individually, show how slab effects vary with azimuth and Δ ; taken as a whole they show how slab effects vary with δ . It can be seen on most of the figures that although a smaller (i.e. near vertical) take-off angle generally causes the ray to emerge farther from the source, this is not always so. Over a narrow range an increase in takeoff angle causes a decrease in Δ . This area marks the edge of the slab effects. Between this narrow band and the seismic source, the rays are going through a relatively great part of the subducted slab. Outside of this band, the rays are either going through a relatively small amount of the subducted slab or are missing it altogether, depending on the location of the earthquake (Figure 7). Rays which pass down the length of the slab are refracted into paths which take them much farther from the source than rays of their take-off angle would normally go. The narrow band between the slab-affected rays and the relatively unaffected rays contains those rays which barely graze the bottom of the slab; in this area the slab effects

FIGURE 7

RAY PATH SKETCH (not to scale)

Dashed lines are a sketch of ray paths from an earthquake close to the subducting slab. Dotted lines are ray paths from an earthquake farther from the slab.

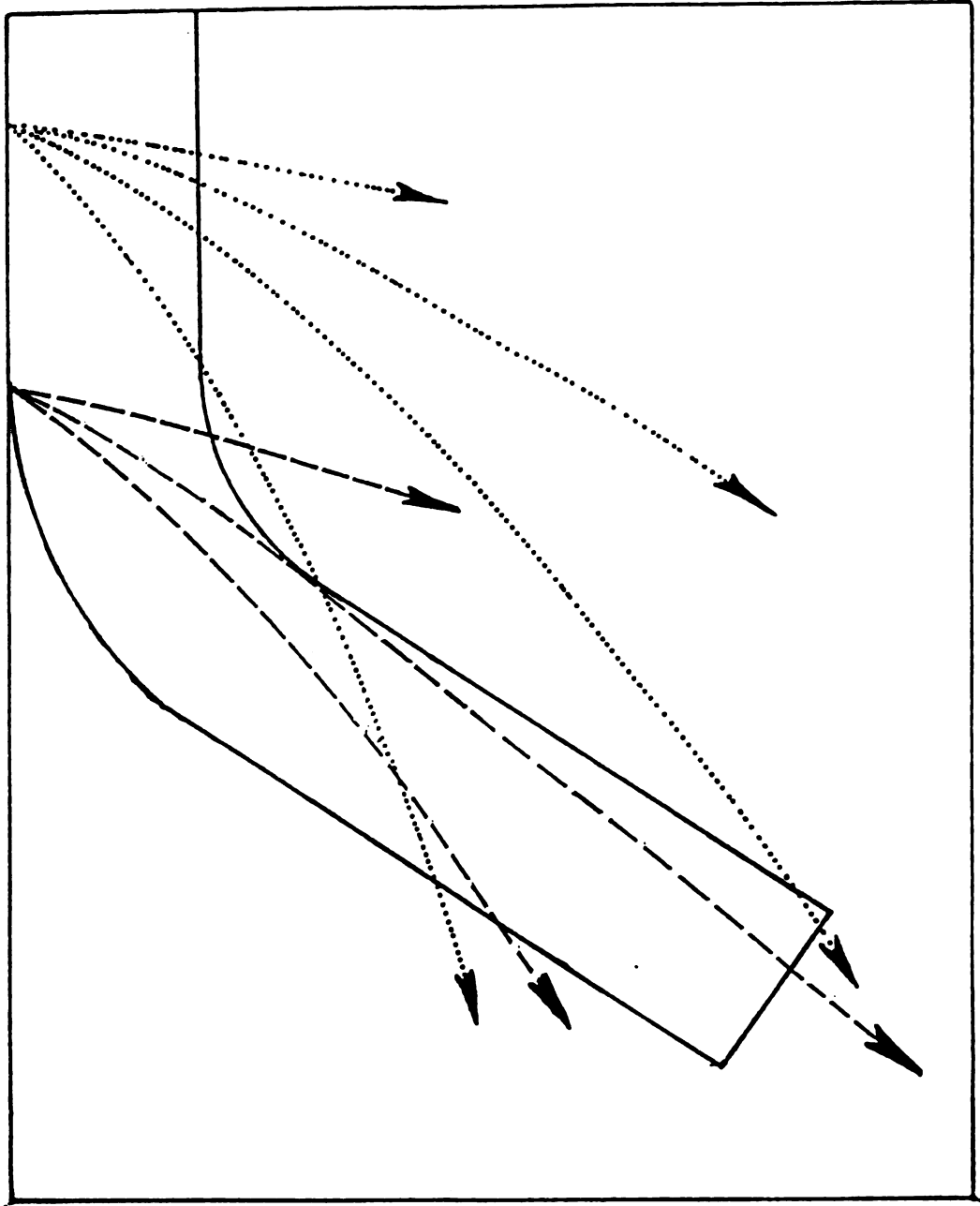


FIGURE 7

rapidly die away, so that for a small range of take-off angle a smaller take-off angle causes the ray to hit less of the slab and emerge closer to the source rather than farther away.

Slab effects also change greatly with δ . The reason for these changes can be seen fairly easily from the geometry of the situation (Figure 7). If an earthquake occurs above the subducting slab, even the rays with shallow take-off angles will strike the slab and be affected by it. They will strike the surface of the slab at a relatively shallow angle, refract into it and continue within the slab for a relatively long time. The effect of the slab on these rays will be correspondingly great. As the seismic source is moved seaward, the situation changes. Increasingly, rays with small take-off angles will miss the slab completely and continue to their destinations unmolested. Rays at some intermediate take-off angle will strike the underside of the slab and refract down it. Since their angle of incidence at the slab surface will be greater than that for rays from more arcward seismic sources, these rays will follow a path which tends more to cut across the slab than follow it. They will still be refracted further from the source than rays with this take-off angle would normally go, but not as far as the rays from arcward sources with shallow take-off angles would. Because of this, the area in which seismic signals are affected by the slab contracts. In addition, not being so strongly refracted, these rays are not geometrically spread as much, and so the emergence point density within the area of slab effects is greater for seaward sources than for arcward ones. With increasing values of δ this process continues until only signals to seismic stations almost

directly above the slab would be affected by it; at this point the slab effect has become a station effect rather than a source effect.

2.3 Amplitude Effects

The slab can have effects on travel time due to its anomalous seismic velocity. It can also affect seismic amplitude, mainly by geometric spreading of rays. The first of these questions to be considered is that of predicted seismic amplitude. This is shown by the density of ray emergence points at the surface of the Earth. These points, plotted in figures 6A-6L, are the emergence points of rays which were sent out in an evenly spaced distribution of azimuths and take-off angles, so that the ray emergence point density reflects amplitude (Sleep, 1973).

Were there no slab effect, the lines of equal take-off angle would describe concentric circles about the origin. They do not. Although all points considered in this thesis are relatively far from the subducting slab, there are still noticeable slab effects over most of the range in δ considered. At $\delta = 12.4^\circ$, for example, the emergence points for rays sent out at a take-off angle of 33° emerge at values of Δ which vary between 85° and 34° across the range of azimuth (with respect to the arc normal direction) of 0° to 90° . The azimuth of the emergence point can vary from the take-off azimuth by as much as 30° . The low emergence point density caused by this ray path distortion is prominent. This shadow zone, reported by Sleep (1973) for earthquakes closer to the island arc, is still present and even strong at this value of δ ; the associated low amplitude seismic signals should be seen at seismological stations in this shadow zone as well. The ray tracing

studies also show a previously mentioned area of high density of ray emergence points in a narrow band at the edge of this shadow zone. A narrow band of unusually high amplitude seismic signals should be associated with this, provided that rays travelling to this area along different routes arrive in phase. As will be seen later, they should do so.

Depending on the location of the earthquake both along the arc and in δ , this area of high amplitude should be detected at stations in western North America or northern Europe. Due to the narrowness of the high amplitude band, the alignment of earthquake, slab, and seismological station is critical to its detection.

The shadow zone loses intensity as the earthquake location is moved away from the slab. At any value of δ where it was possible to make a comparison, the emergence point density in the shadow zone is less than that at the same value of Δ but outside the shadow zone. At the same time, the emergence point density in the shadow zone is higher than it would be for the shadow zone observed at a lower value of δ . As an illustration of this difference in density, consider the relative ease of directing a ray so that its emergence point falls within a desired 10° by 10° area. At $\delta = 12.4^\circ$ this can be done without having to use increments of take-off angle or azimuth smaller than 0.25° . At $\delta = 13.0^\circ$ a 1.0° increment was adequate for this purpose, while at $\delta = 14.0^\circ$ the necessary increment is never less than 2.0° . As distance from the slab increases, it is becoming progressively easier to obtain rays emerging in the shadow zone. Therefore the ray emergence point density in the shadow zone increases accordingly, and with it the seismic amplitude (Sleep, 1973). In other words, as the distance between

TABLE 1

EARTHQUAKES USED IN THIS STUDY

TABLE 1: EARTHQUAKES USED IN THIS STUDY

Date	Time	Latitude	Longitude	h,ISC,km	h,pwP	Mb	# obs.	net	Mech. correction?
Sept 25,1964	15:42:19	50.27N	176.63E	36	13.5	5.4	131	both	no
Feb 7,1965	02:17:10	51.34N	173.44W	45	----	5.8	191	amp	yes
Mar 30,1965	02:27:03	50.32N	177.93E	20	26.8	6.5	296	both	yes
June 15,1965	04:46:14	50.07N	178.26E	26	17.9	5.3	141	both	no
Oct 1,1965	08:52:02	50.02N	178.28E	5	17.6	6.2	275	both	yes
June 2,1966	03:27:54	50.01N	175.98E	48	17.8	5.7	----	nonstandard	yes
May 30,1967	09:54:38	50.1 N	176.6 W	30	----	5.0	107	loc	yes
Oct 25,1968	11:38:15	50.57N	177.46E	38	17.5	5.0	113	both	no
Apr 4,1969	08:45:19	51.17N	173.67E	35	14.6	5.6	193	amp	yes
Feb 27,1970	07:07:57	50.13N	179.59W	7.2	14.9	6.0	327	both	yes
Mar 19,1970	15:20:54	50.03N	179.61W	8	15.2	5.3	139	loc	no
Mar 19,1970	23:33:29	51.34N	173.75E	8	----	5.8	303	amp	yes
July 24,1970	08:02:26	52.23N	171.34E	46	----	5.0	108	amp	no
Oct 8,1970	13:02:05	50.36N	176.8 W	38	19.5	5.2	143	loc	no
Mar 25,1971	03:31:52	50.52N	176.80W	3	18.0	5.2	184	loc	yes
Dec 26,1971	13:19:03	50.70N	175.05W	42	18.3	5.4	147	loc	yes
Mar 27,1964	16:28:47	50.06N	179.60W	32	16.0	5.6	280	loc	yes
Aug 18,1974	17:16:26	50.45N	175.18E	32	18.6	5.0	118	both	yes
Aug 10,1975	03:12:47	51.18E	174.21E	17	----	5.0	153	loc	yes

times, locations and depths from ISC Bulletin

TABLE 2

WSSN Stations in Networks -- locations in degrees/minutes/seconds

Code	Location	Latitude		Longitude	
Location Network:					
COP	Copenhagen, Denmark	55°41'	N	12°26'	E
CTA	Charters Towers, Queensland, Australia	20 05 18	S	146 15 16	E
DAG	Danmarks Havn, Greenland	76 46 12	N	18 46 12	E
ESK	Eskdalemuir, Scotland, U.K.	55 19 00	N	3 12 08	W
GDH	Godhavn, Greenland	69 15	N	53 32	W
KBS	Kingsbay, Svalbard	78 55 03	N	11 55 26	E
KEV	Kevo, Finland	69 45 19	N	27 00 24	E
KIP	Kipapa, Hawaii, USA	21 25 24	N	158 00 54	W
KON	Kongsberg, Norway	59 38 57	N	9 35 54	E
LAH	Lahore, Pakistan	31 33	N	74 20	E
MAT	Matsushiro, Honshu, Japan	36 32 30	N	138 12 24	E
NIL	Nilore, Pakistan	33 39 00	N	73 15 06	E
NOR	Nord, Greenland	81 36	N	16 41	W
STU	Stuttgart, Germany	48 46 19	N	9 11 42	E
UME	Umea, Sweeden	63 48 54	N	20 14 12	E

Both networks:

ALQ	Albuquerque, New Mexico, USA	34 56 33	N	106 27 27	W
DAL	Dallas, Texas, USA	32 50 46	N	96 47 02	W
FLO	Florissant, Missouri, USA	38 48 06	N	90 22 12	W
LON	Longmire, Washington, USA	46 45 00	N	121 48 36	W

Amplitude Network:

BOZ	Bozeman, Montana, USA	45 36	N	118 38	W
COR	Corvallis, Oregon, USA	44 35 09	N	123 18 12	W
FVM	French Village, Missouri, USA	37 59 02	N	90 25 34	W
GOL	Golden, Colorado, USA	39 42 01	N	105 22 16	W
GSC	Goldstone, California, USA	39 42 01	N	116 48 17	W
JCT	Junction City, Texas, USA	30 28 46	N	99 48 08	W
MNN	Minneapolis, Minnesota, USA	44 54 52	N	93 11 24	W
MSO	Missoula, Montana, USA	46 49 45	N	113 56 26	W
TUC	Tucson, Arizona, USA	32 18 35	N	110 46 56	W

data from ISC Catalog

the earthquake and the slab is increased, the amplitudes in the shadow zone are moving toward their normal no-slab values. In addition to this effect, the more obvious shrinking of the shadow zone with increasing δ can be seen on figures 6A - 6L.

The high amplitude band is relatively thin and well-defined at $\delta = 12.4^\circ$. As δ increases, this band broadens, becoming relatively unfocused. The expected effect of this would be that this high amplitude band would follow the behavior of its low amplitude counterpart. As δ increases, the high amplitude zone indicated by the area of high ray emergence point density should disperse and become less apparent. The shape of the high amplitude zone also changes, contracting toward the seismic source. It should be noticed that while the band of high amplitudes becomes less sharp beyond $\delta = 12.4$, it can not become any sharper as δ decreases beyond this point; the ray emergence points which make up the high amplitude zone are essentially all along a single line already (figure 6A).

Seismic data was checked to see if these theoretical amplitude effects actually existed. WWSSN records for nineteen earthquakes in the central and west-central Aleutians were examined (Table 1). Depending on the location of the earthquake, one or both of two sets of seismic stations were considered (Table 2). These two sets of seismic stations were the "amplitude network" and the "location network". The amplitude network was meant to check for the narrow band of unusually high amplitudes at the edge of the low amplitude "shadow zone" (Sleep, 1973). It consists of WWSSN seismological stations in the western United States, where this band was expected to fall. The location network was meant to circle the source area as well as possible,

in order to collect travel time and waveform data for earthquake relocation and depth phase studies. Due to the Arctic and Pacific Oceans and their geographic relationship to the Aleutians, there are large gaps in the desired circle. This situation is worsened by the fact that what stations there are in the central and western Pacific usually produce illegible records.

Amplitudes were obtained from short period vertical component records. The amplitude data recorded was processed to remove apparent amplitude differences based on station magnification. All amplitudes were normalized to what they should have been if all the seismological stations used a magnification of 100,000x. In addition, the data was corrected to remove the amplitude effects of the focal mechanism when possible, using the formulae for focal mechanism amplitude effects given by Aki and Richards (1980). Some of the focal mechanisms used were taken from Stauder (1968b) and the rest were derived from ISC data. Some focal mechanisms were not well constrained by the data and amplitudes for these earthquakes could not be completely corrected. A focal mechanism amplitude correction requires one to know the position of the ray going to a given station with respect to both focal planes. Some earthquakes studied in this thesis are of relatively low magnitude and the data did not seem sufficient to constrain both focal planes; in this case an estimate based on the one known focal plane was made. In some cases, for various reasons, the focal mechanism for a given earthquake was unobtainable. These cases are indicated in Table 1 and on the relevant figures.

The corrected data was then normalized again, this time relative to the amplitude of the strongest arrival recorded. This was given

FIGURE 8

RELATIVE AMPLITUDE VS. "ZERO RESIDUAL LINE"

Amplitudes are normalized so that the strongest is 10 and the rest are in proportion to this value.

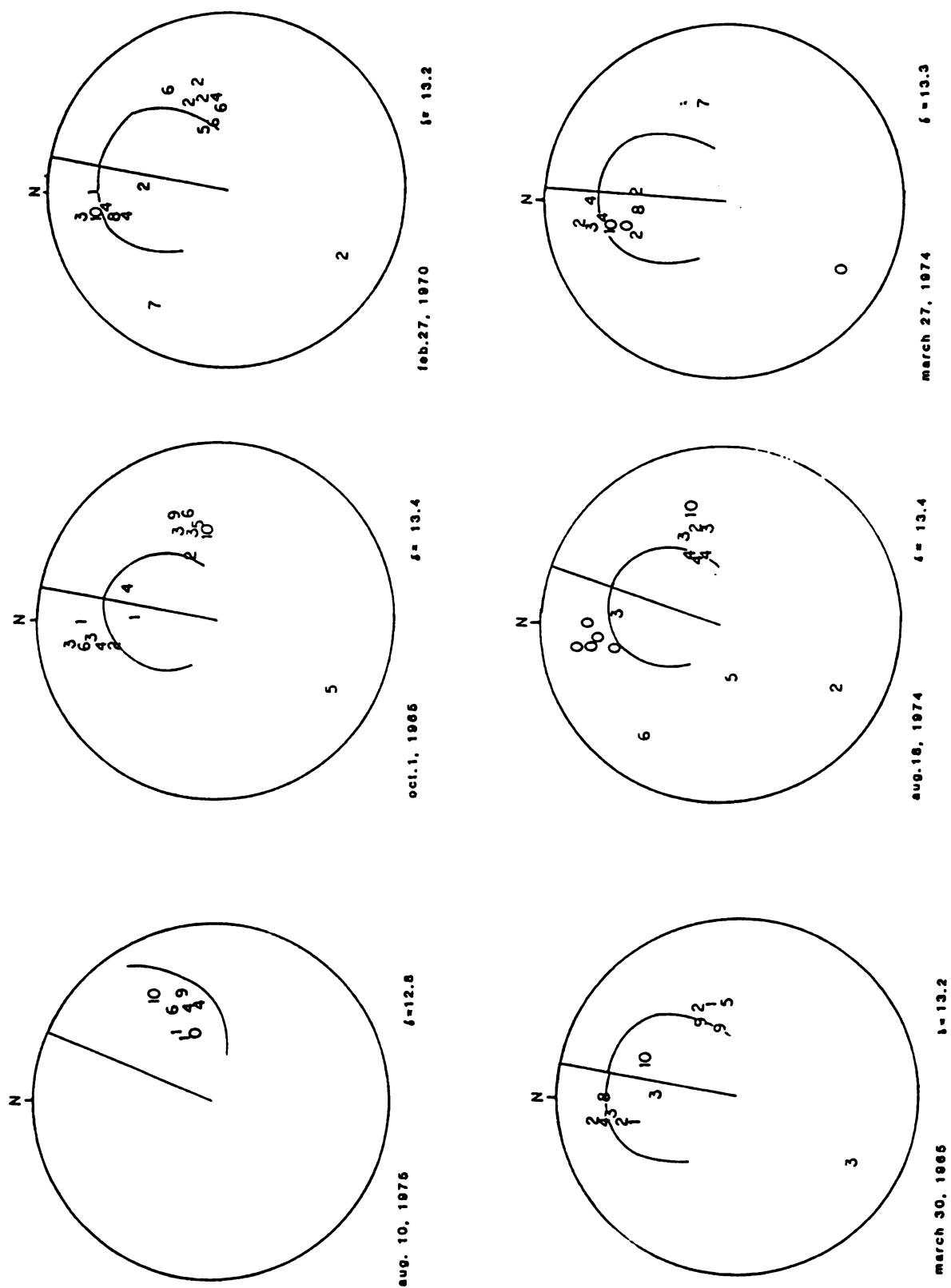


FIGURE 8

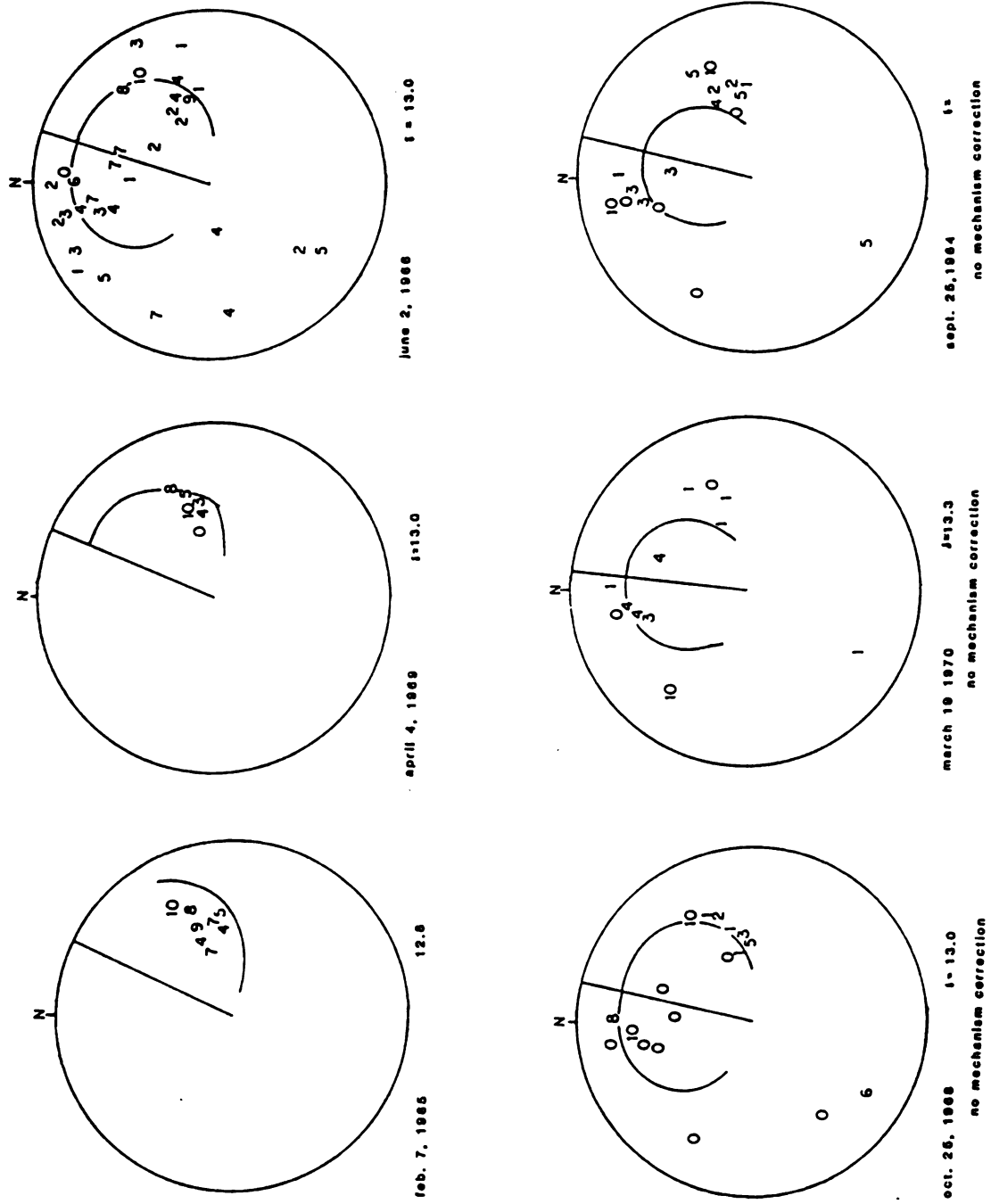
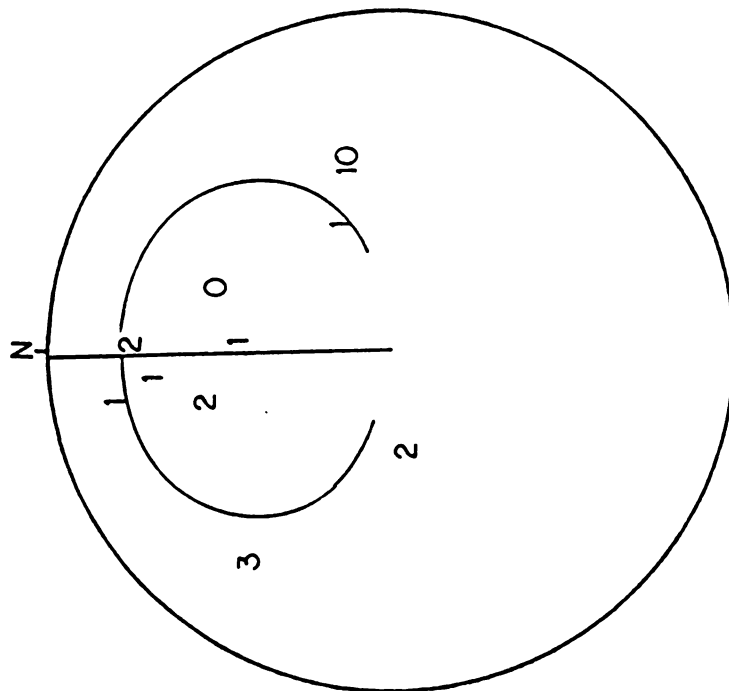
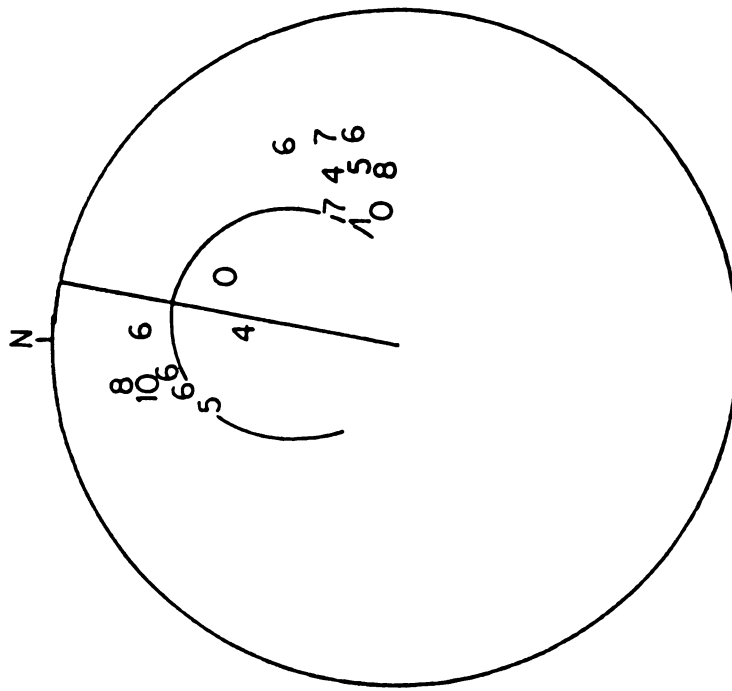


FIGURE 8 (cont.)



oct. 8, 1970 δ 13.0
no mechanism correction



June 15, 1966 δ 13.4
no mechanism correction

FIGURE 8 (cont.)

the arbitrary amplitude value of 10, with weaker signals becoming nines, eights, and so on. All values which were not exactly an integer number of tenths of the strongest amplitude were rounded to the nearest tenth except for those which would have been rounded to zero. These were arbitrarily set as amplitude 1 instead; therefore any station with an amplitude listed as 0 did not receive any noticeable signal at all. These amplitude values were plotted on a polar graph of similar format to that of figure 6, in order to see whether there was a band of high amplitude and if so, how well it corresponded with the theoretical one.

Figure 8 shows the results of this examination. The curved line on each figure indicates the line of zero travel time anomaly for that value of δ nearest the earthquake for which theoretical slab effects were calculated. At this line and slightly to either side of it the slab wave should arrive at the same time as the mantle wave. Being in phase, the two should reinforce each other leading to higher amplitudes; notice that this line coincides fairly well with the zone of high ray emergence point density (Figure 6).

All values of δ for these earthquakes are calculated using ISC hypocentral locations. If these are in error due to a slab mislocation effect, the theoretical high amplitude line should not quite pass through the observed high amplitude area, if any.

At the smaller values of δ represented, the correlation between the "zero line" and the high amplitude area in the observed data is poor. For the earthquake of August 10, 1975 ($\delta = 12.8^\circ$), for example, it looks as if there is a high amplitude band in the data, but it falls inside the "zero line" for this distance. Moving out to about $\delta = 13.0$ the correlation between data and "zero line" becomes

good. For example, consider the earthquakes of June 2, 1966, April 4, 1969, and October 25, 1968. For all of these events the correlation between zero line and high amplitudes is good, although not perfect. This correlation seems to persist out to $\delta = 13.2^\circ$ or so, but beyond this point the correlation between theoretical "zero line" and high amplitude signals becomes very poor.

These results seem to support the idea that at least some forearc and outer rise earthquakes may be mislocated due to slab effects. If earthquakes closer to the slab (the ones placed by the ISC at $\delta = 12.8^\circ$, for example) are mislocated, their actual location would be farther from the slab. Their true "zero lines" would fall inside the zero lines as presently plotted, and in that case the correlation between zero line and high amplitude data would be good. At $\delta = 13.0^\circ$ as indicated by the ISC, the slab mislocation effects have decreased, and therefore the "zero lines" plotted on these figures already correlate with areas of high amplitude.

At higher values of δ , approximately $\delta = 13.4^\circ$ and out, there seems to be much scatter of high amplitude signals away from the zero line. Many high amplitude stations do not fall on or near the line, including some of the highest amplitude ones. This scatter is probably associated with the fading of both the shadow zone and the high amplitude band at its edge. Neither of these are as intense as they were for earthquakes closer to the slab. The amplitude anomalies they cause do not contrast as sharply with the general range of amplitudes as before. The results are therefore more open to distortion by receiver structure or error; also possibly due to maladjustment of the receivers themselves (Stein, personal communication).

2.4 Waveform Effects

It was proposed in Chapter 1 that a possible reason for the fact that slab effects had not been observed for forearc and outer rise earthquakes is that the arrivals from these earthquakes at seismological stations in the shadow zone are systematically picked late. It was thought that this tendency might be defeated by matching waveforms of signals received at different stations and attempting to correlate them. At the same time it was possible to check the accuracy of ISC hypocentral depth determinations by study of depth phases, if any.

Location network stations were used for this (Table 2). As with the amplitude study, short period vertical component records were used when available. Where short period records were unreadable, arrival times could sometimes be obtained from the long period vertical records for the same event. Where practical, amplitude network events were used for this study as well.

Results of the attempt to check the depth of focus using depth phases are given in Table 1. Where depth phases can be read, they seem to indicate that these earthquakes fall in the depth range of 7 to 20 km below mean sea level, assuming that rocks in this area have seismic velocities of around 6 km/sec. In general, focal depths indicated by depth phases were shallower than those indicated in the ISC Bulletin, whenever there was any significant difference between them. Some of the ISC solutions were very shallow, e.g. about 3 - 5 km below msl, and in these cases the depth phases seemed to indicate a deeper source. The average depth as determined by the ISC was 26.3 km. Maximum was 48 km, minimum was 3 km, with a standard deviation of 14.6 km. Taking 6 km/sec as the average seismic velocity between the hypocenter and the

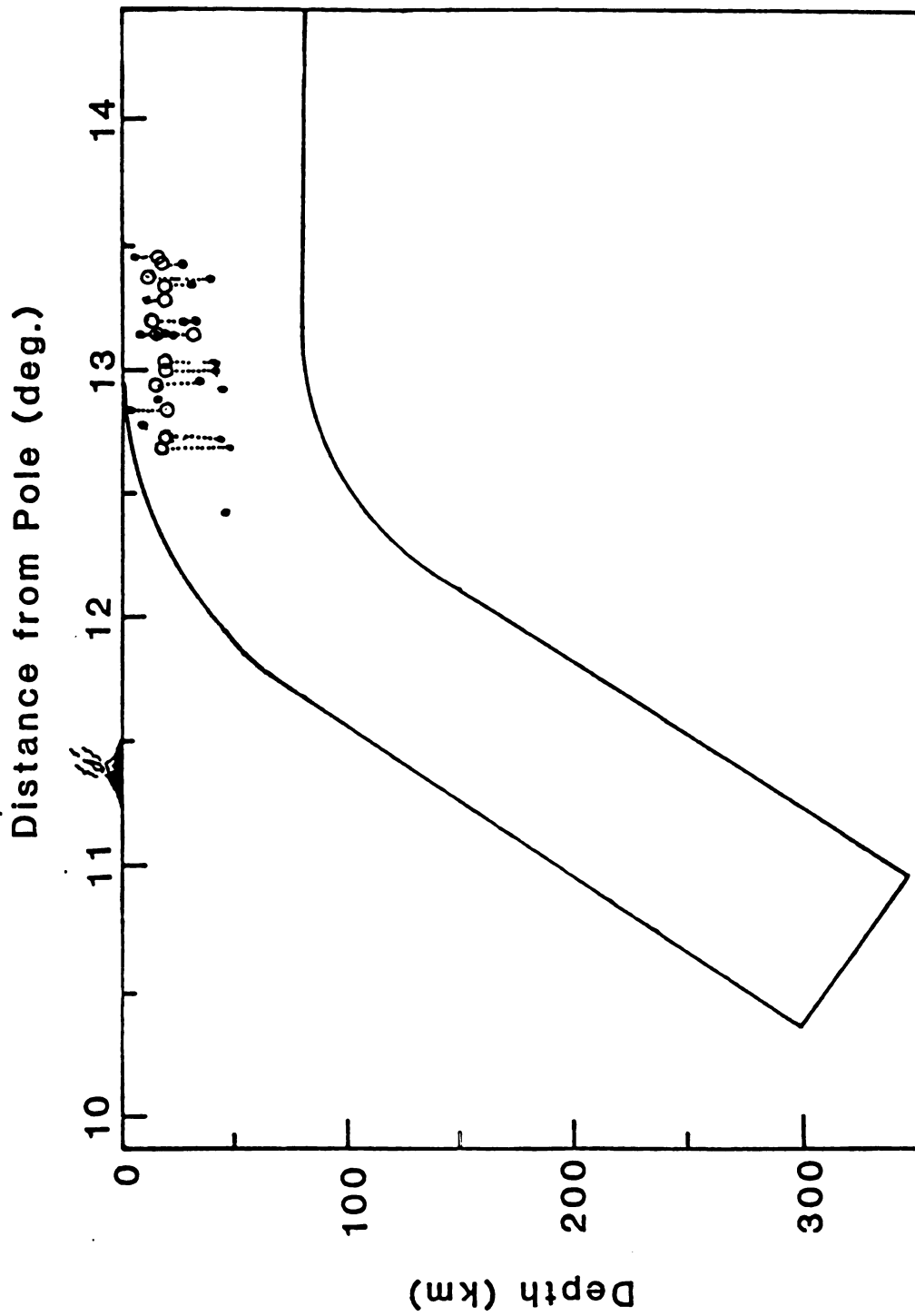
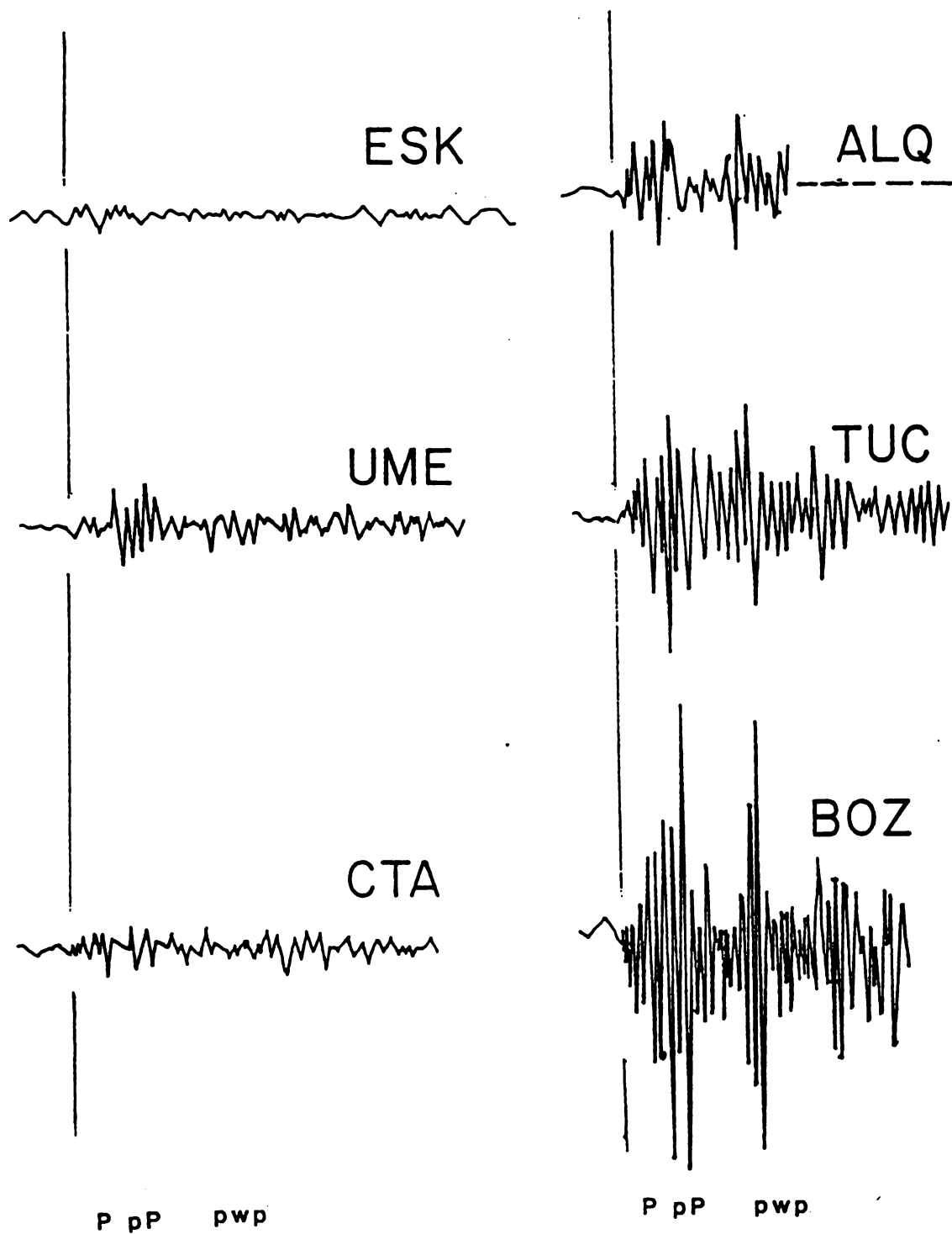


FIGURE 9

ISC EARTHQUAKE DEPTHS VS. DEPTH PHASE EARTHQUAKE DEPTH DETERMINATIONS

FIGURE 10

"ESCALATING" WAVEFORM ARRIVALS AT SEVERAL SEISMIC OBSERVATORIES.

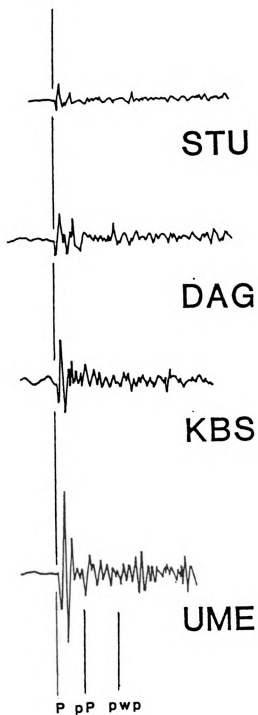


September 25, 1964

FIGURE 10

FIGURE 11

"CLEAN" WAVEFORM ARRIVALS AT SEVERAL SEISMIC OBSERVATORIES.



March 27, 1974

FIGURE 11

sediment-water interface, depth phases give an average hypocentral depth of 17.6 km. Maximum depth using this method was 27 km, minimum was 13.5, with a standard deviation of 3.23 km. If the picks of depth phases were correct, this would seem to indicate that seismicity in the trench and outer rise is at a relatively uniform level. This would also indicate that the depth of earthquakes in the forearc and outer rise is not as great as had been generally believed, removing one objection to the single layer elastic-perfectly plastic rheology as a model for the lithosphere (Forsyth, 1980). A comparison of ISC and pwP depths is shown in Figure 9.

An attempt was made to determine if, as suggested earlier, earthquakes in the forearc and outer rise might be systematically picked late at European seismological observatories due to their low magnitude. The method for doing this was suggested by the observation that seismic signal waveforms on short period seismograms are relatively consistent for a given earthquake no matter where received (Hong and Fujita, 1981). It was hoped that by comparing waveforms of emergent arrivals with the waveform of a clear, impulsive arrival at a different station, it would be possible to more precisely determine when the signal actually arrived at the station with the emergent signal. This was partially successful. The waveform matching method does work. This is because the short period waveform seems to be, aside from some high frequency attenuation, amazingly consistent from station to station (Figures 10 and 11). This similarity seems to continue regardless of geographic location or focal mechanism, and may indicate that most of the short period waveform is determined by source structure and/or the propagation of the fracture along the fault as the earthquake occurs.

However, the utility of this sort of "wave form correction" is limited by the type of waveform involved. The two types of waveform involved can be called "clean" and "escalating" waveforms. Figure 10 is a trace of an escalating waveform, while figure 13 is a clean waveform. In a clean signal the amplitude of the first arrival is almost as large as that of the strongest wave in the wave train. The first arrival may in fact be the largest-amplitude wave itself. In this case a wave form correction is not called for, since if the largest swing of the signal is seen the first swing will almost always be seen as well. This was confirmed by some wave form matching done with this type of signal. On the other hand, the escalating signal calls for a wave form correction in many cases. In this type of arrival, the signal has low amplitude phases just before the first major impulse arrives. It was suggested (Fujita, personal communication) that these "predecessors" might be a wave which travelled in the subducting slab when the main wave was a mantle wave, and this may be so for some stations and some situations. However, for the earthquakes checked here, the relationship between the arrival time of the weak arrival and that of the main signal is constant, regardless of station location or azimuth from the source. It would seem that a slab effect should be highly azimuth dependent. Since this is not, it is probably not a slab effect.

These escalating signal earthquakes may be one of two things. They may be a "slow" earthquake, or they may be a multiple shock event with the first shock being very much smaller than the second. There may be other explanations, but these are the two most obvious.

In these escalating arrivals, the weak wave arrives a second or two before the main signal. It is about a tenth the amplitude of the

main signal, more or less. It is easy to see that with this waveform a low amplitude arrival may lead to the weak wave escaping notice.

"Wave form corrections" were applied to escalating signal earthquakes as needed. A copy was made of a clear example of the short period signal, and its waveform was matched with that of the emergent arrival in question to see where the weak wave would have been if it could be seen. Usually, with this procedure, the weak wave could be found on the "emergent" signal as well as the strong one, but if it was not known to be there it would probably escape notice. These weak waves appeared under emergent conditions as a very small signal or in some cases as a change in the character of the background noise.

It should be noted that the utility of these wave form corrections is severely limited. They are a certain amount of trouble, and should not be used if not really needed. They do not help clarify all earthquakes, only those with escalating arrivals. Finally, only escalating waveform earthquakes within a certain range of magnitudes will benefit from this correction. If the magnitude is too low the weak wave will be seen almost nowhere and if the amplitude is too high it will be seen almost everywhere. In either case the arrival time picks will be consistent and no wave form correction will be needed. A reasonable guess would be that an escalating earthquake of Mb 6.0 or greater would show its weak wave almost everywhere the earthquake was recorded, but this depends strongly on the specific ratio of amplitudes between weak wave and main signal. It is difficult to determine, even as a guess, what the lower limit of the useful range for the wave form correction would be.

FIGURE 12

RAY EMERGENCE POINTS CORRECTED FOR SLAB RAY PATH DISTORTION VS. THE SAME
EMERGENCE POINTS UNCORRECTED.

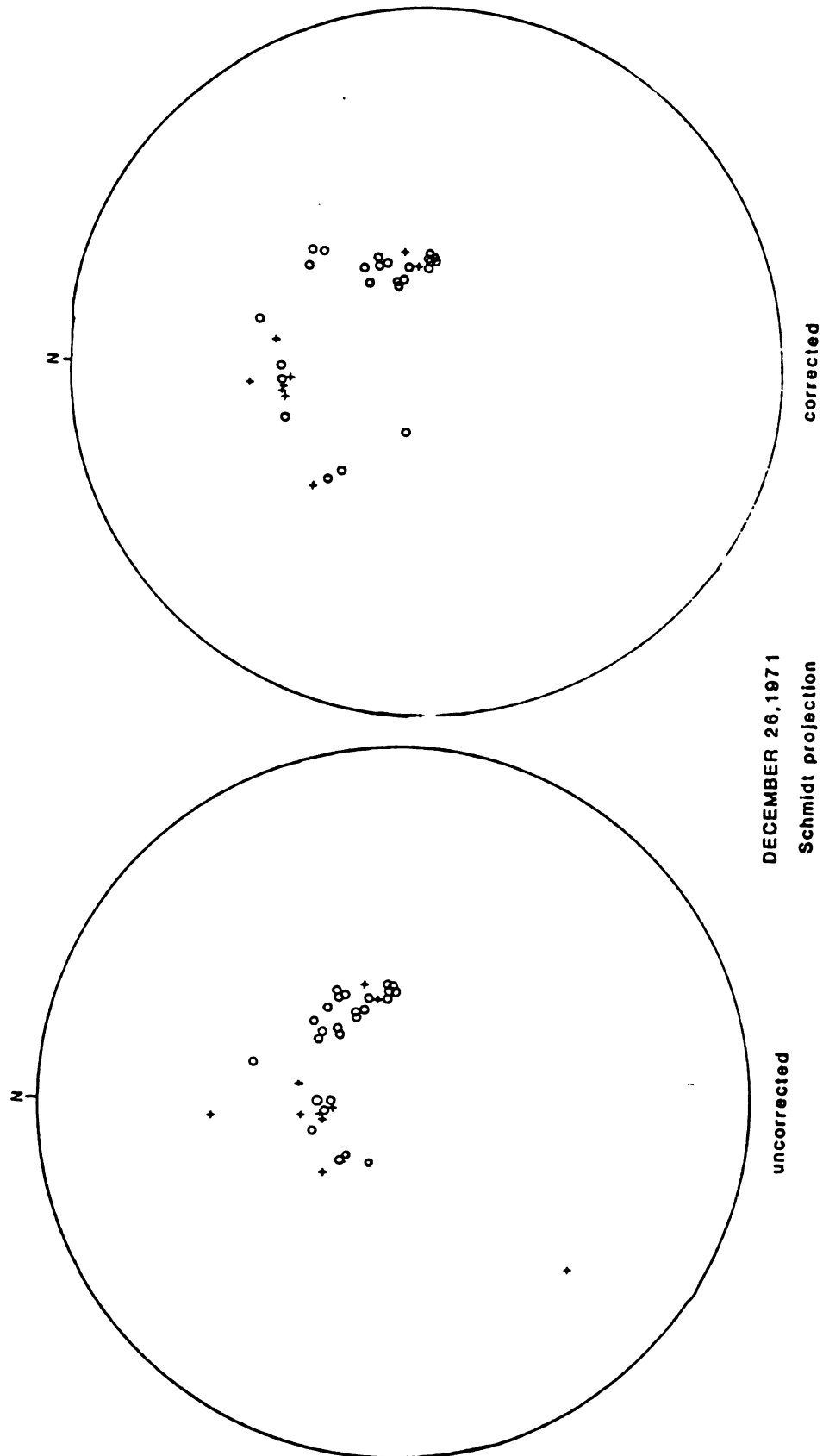


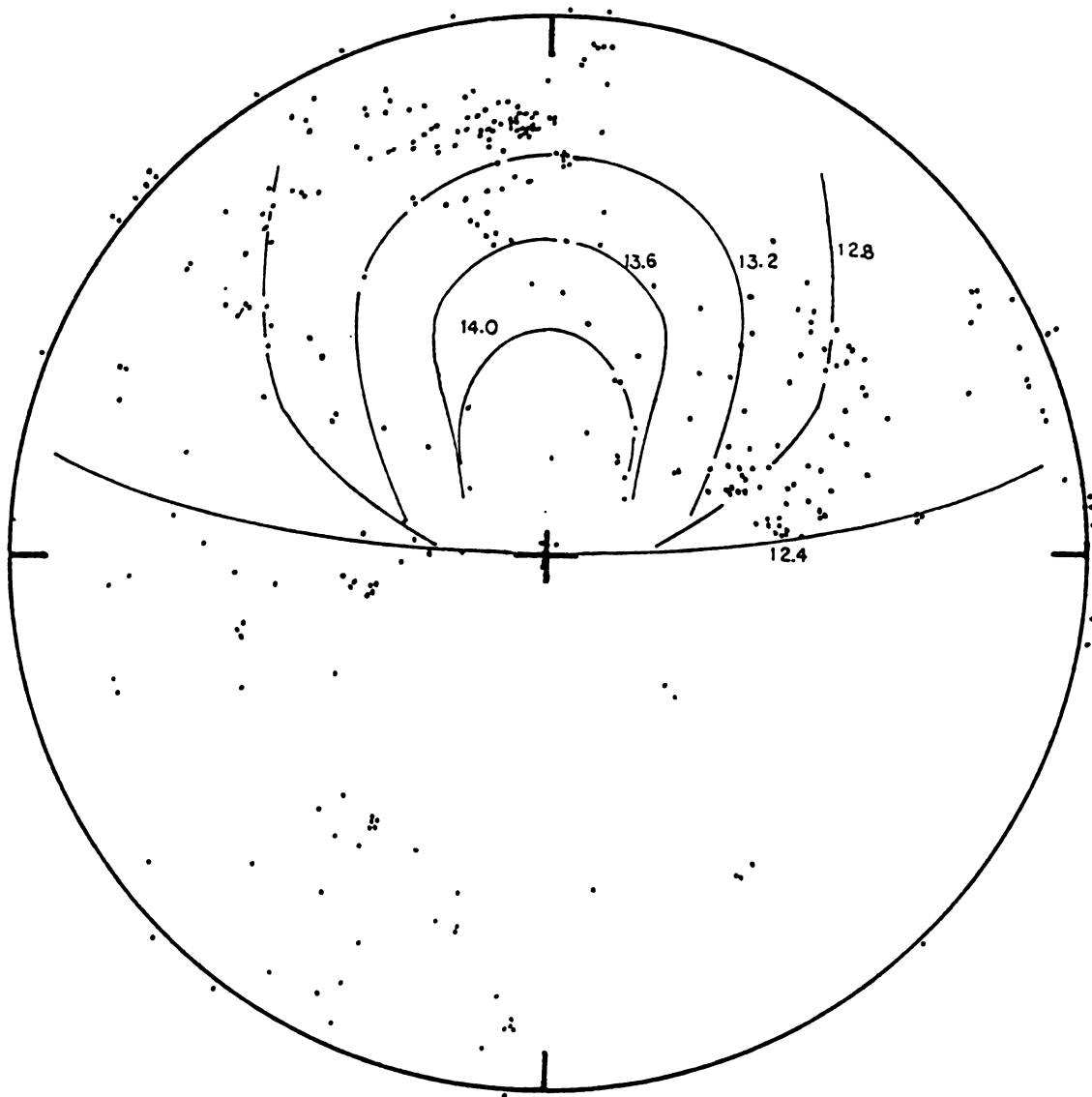
FIGURE 12

2.5 Effects on Focal Mechanism Plotting

Another theoretical effect of the subducting slab was noticed. This is not an effect on seismic signals but on seismic practice. As previously mentioned, at $\delta = 12.4^\circ$ rays leaving the source at a take-off angle of 33° can emerge at epicentral distances of between 34° and 85° from the source over about a 90° range in azimuth. According to standard angle of incidence tables (e.g. Pho and Behe, 1972) a ray arriving at a station 85° from the source should leave that source at a take-off angle of around 17.6° . If a focal mechanism is plotted using standard practice, the assumption will be that the 17.6° take-off angle is the correct one, when in fact the ray left the source with a take-off angle of 33° . This can lead to more or less serious errors in focal mechanism plots, the degree of error depending largely on the distance between the earthquake and the slab. It is not clear whether the theoretical ray paths for this study are sufficiently accurate to allow correction of focal mechanisms for this effect. In any case, some focal mechanisms were plotted both with and without this theoretical ray path correction, and it is observed that the "corrected" mechanisms seem to show less intermixing of compressional and dilatational arrivals compared to uncorrected ones (Figure 12).

2.6 The Practical Limits of Slab Mislocation Effects in the Aleutians

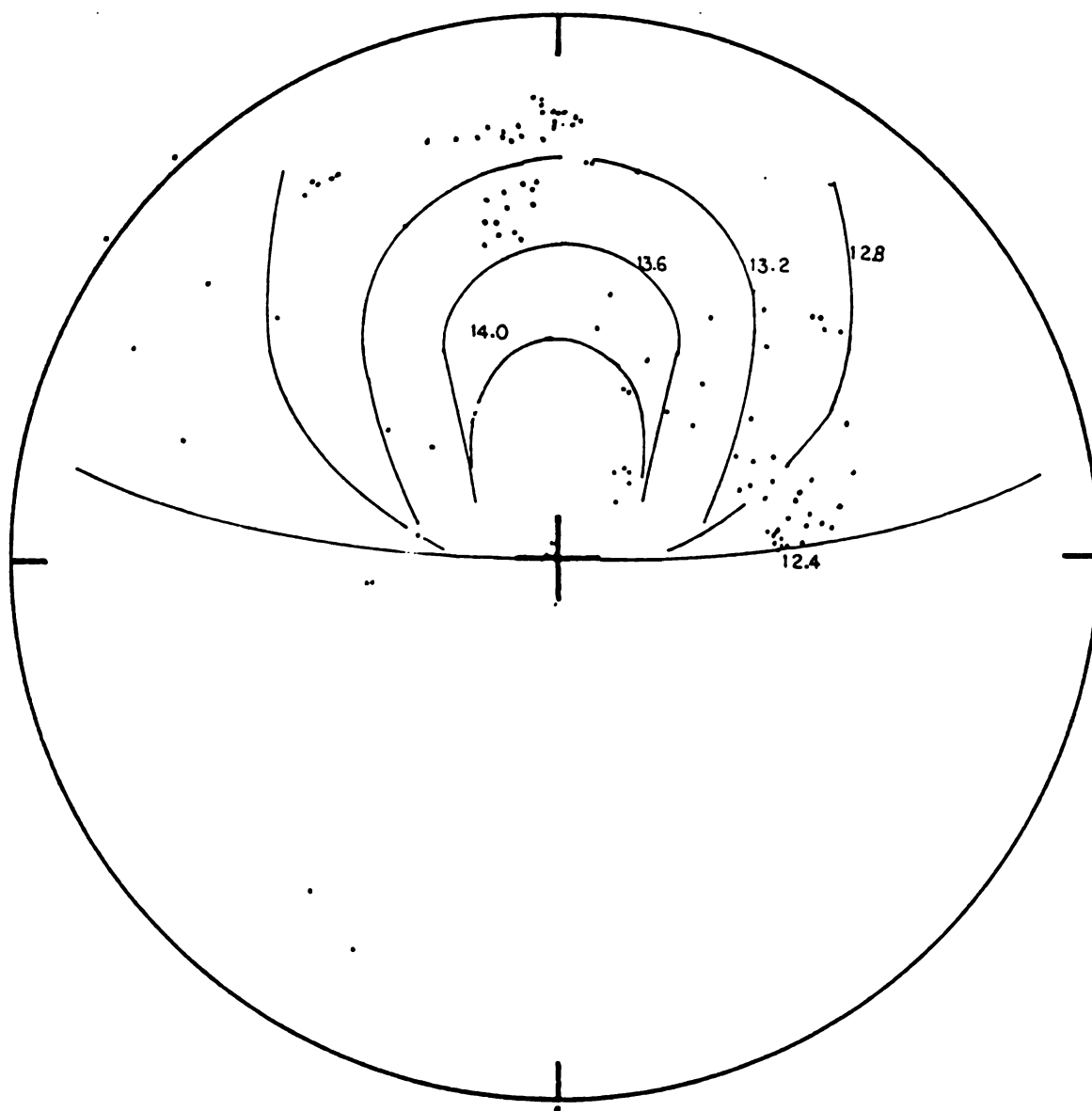
The problem remains that, although theoretically present, slab effects have not been detected for forearc and outer rise earthquakes. Examination of arc normal slab effects diagrams (Figure 6) shows that earthquakes across most of the study area should show noticeable slab effects. However, these slab effects will not be generally noticed unless a statistically significant percentage of seismological stations



February 27, 1970 Mb 6.0, 327 observations

FIGURE 13

STATIONS DETECTING THE EARTHQUAKE OF FEB. 27, 1970, SHOWING WHICH
ONES WOULD HAVE SHOWN SLAB EFFECTS FOR DIFFERENT VALUES OF δ .



May 30, 1967 Mb 5.0, 107 observations

FIGURE 14

STATIONS DETECTING THE EARTHQUAKE OF MAY 30, 1967, SHOWING WHICH ONES WOULD HAVE SHOWN SLAB EFFECTS FOR DIFFERENT VALUES OF δ .

are affected by them for a given earthquake. Using the arc normal slab effects diagrams, it is possible to investigate this question.

Figures 13 and 14 show the location of all ISC seismological stations which reported receiving signals from two of the earthquakes studied in this thesis: that of February 27, 1970, and that of May 30, 1967 respectively. On both plots the earthquake epicenter is at the origin. It can be seen that the question of statistical significance of slab effects is complicated by uneven distribution of seismometers. Large empty areas exist north of the epicenters, due to the Arctic Ocean and Bering Sea; an even larger empty area is the Pacific Ocean, south of the epicenters. From the distribution of seismological stations shown on these figures, it appears that for Aleutian earthquakes slab effects will be detected at a statistically significant number of stations if the area of slab effects extends into North America or Europe.

Also shown on Figures 13 and 14 are lines marking the limits of slab effects for different values of δ . These lines are the lines of zero travel time anomalies; they mark the absolute limit of possible slab effects. Under actual operating conditions the areas in which travel time effects would be noticed would be smaller, as arrival times can be determined only to within about 0.3 seconds and any deviation smaller than this could not be detected.

At $\delta = 12.4$ most of the reporting seismological stations for both earthquakes could theoretically be affected by slab effects. The -0.3 second travel time residual contour line extends well into northern Europe. Stations farther north, in Scandinavia and Greenland, should show even greater travel time effects. As regards amplitude anomalies,

most stations in northern Europe or farther north fall into a relatively pronounced "shadow zone" (Sleep, 1973) and so should show noticeable amplitude loss as well.

The trench axis in the Aleutians falls around $\delta = 13.0^\circ$. Moving beyond this to $\delta = 13.2^\circ$, the travel time residual at the distance of Stuttgart has been reduced essentially to zero, and that near Copenhagen and Eskdalemuir has fallen to about 0.3 seconds, about the limit of readability and just a tenth of what it was at $\delta = 12.4^\circ$. At this level it is doubtful that the residual would be noticed. Travel time effects and amplitude effects should still be noticed in the Scandinavian and Greenland areas, although at this point it becomes doubtful whether the number of stations affected is still statistically significant. Moving out onto the outer rise, at $\delta = 13.4^\circ$ the shadow zone has retreated so that no slab effects should be detected south of northern Finland and Greenland. At this point slab effects would probably go unnoticed simply because no teleseismic stations would be in a position to record them. Beyond this point the slab effects, although still seen on the arc normal slab effects diagrams, rapidly decline to insignificance.

Figure 15 shows the maximum possible percentages of stations detecting slab effects as a function of δ . It can be seen that the statistical significance of the number of stations affected drops rapidly with increasing δ . Slab effects cause errors in teleseismically determined hypocentral locations, but as the number of affected stations decreases the probable mislocation decreases as well. It would seem that for earthquakes much seaward of the trench the teleseismic hypocentral location would be fairly accurate. There are

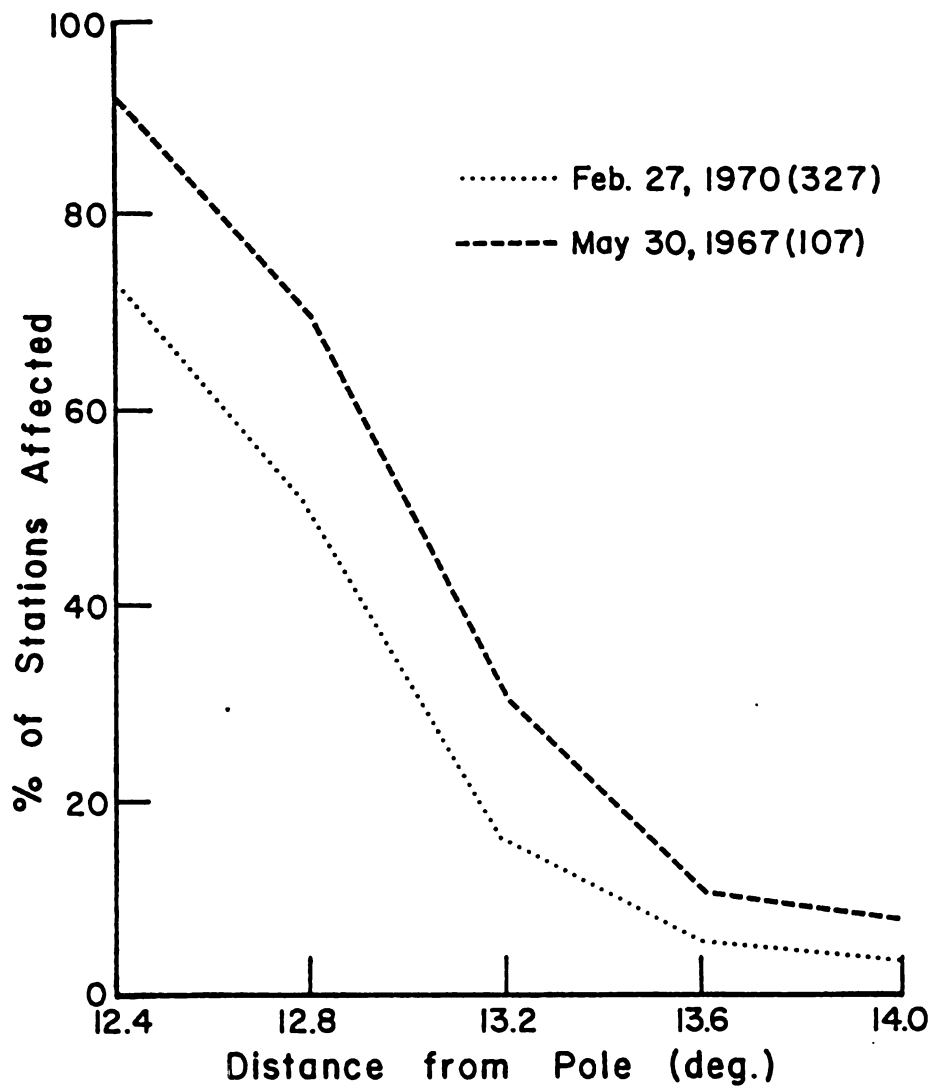


FIGURE 15

PERCENTAGES OF STATIONS AFFECTED FOR DIFFERENT VALUES OF δ .

two problems with this, however. First, as shown in Figure 15, earthquakes of smaller magnitude show a higher percentage of seismological stations in areas which should show slab effects. This is because smaller earthquakes tend to register only at relatively close stations, which then are more often in slab effect areas than distant stations are. Second, earthquakes are far more common in and around the trench (aside from the shallow thrust zone) than elsewhere (Forsyth, 1980) which puts them on a statistical borderline as far as teleseismic mislocations are concerned.

In conclusion, it seems that in the Aleutians larger earthquakes (Mb 6) at $\delta = 13.0^\circ$ or more should be relatively well located by teleseismic means without slab corrections. Inside this line, i.e. inside the trench axis, slab corrections will become increasingly important. Smaller earthquakes, however, tend to be mislocated more easily than large ones and may require slab mislocation corrections well out onto the outer rise. It should be noticed that this statistical conclusion agrees with the conclusion drawn from the observed amplitude data.

CONCLUSIONS

[1] Slab effects in the forearc and outer rise include amplitude effects, travel time anomalies of up to -4 seconds, and incidentally, distortion of ray paths sufficient to obscure focal mechanisms somewhat. All effects are less pronounced and occur over a smaller area the farther the seismic source is from the slab. This makes these effects less distinct and harder to detect as distance from the slab increases.

[2] Theoretical ray tracing indicates that slab effects should be seen for some earthquakes on the forearc and outer rise, being detected mainly at stations in Europe and the western United States due to the geography and geometry involved. Observed amplitude effects seem to correlate well with theoretical ones. The correlation is somewhat faulty closer to the slab, probably due to slab-induced mislocation of the earthquakes. Correlation also worsens with increasing distance beyond about $\delta = 13.2^\circ$, probably due to the fact that slab effects should weaken and become less distinct as the seismic source is moved further from the slab.

[3] Statistical studies of the number of stations detecting slab effects for earthquakes of different magnitudes and at different distances from the slab indicate that for $M_b = 6$ or so, slab effect mislocation corrections can probably be dispensed with beyond the trench axis in the Aleutians, but for smaller events the slab corrections may need to be carried out onto the outer rise. The rapid decline in the number of stations affected with increasing distance from the slab, along with the relatively small magnitude of slab effects at this distance, probably explain why these effects have not been previously observed.

BIBLIOGRAPHY

BIBLIOGRAPHY

- Aki, K., and Richards, P.G., 1980. Quantitative Seismology: Theory and Methods. W.H. Freeman, San Francisco. 932 p.
- Baer, A.J., 1981. Geotherms, evolution of the lithosphere, and plate tectonics: *Tectonophysics*, v. 72, p. 203 - 227.
- Barazangi, M., and Isacks, B.L., 1979. A comparison of the spatial distribution of mantle earthquakes determined from data provided by local and by teleseismic networks for the Japan and Aleutian arcs: *Bull. Seismol. Soc. Am.*, v. 69, p. 1763 - 1770.
- Beaumont, C., 1979. On rheological zonation of the lithosphere during flexure; *Tectonophysics*, v. 59, p. 347 - 365.
- Biswas, N. N., 1973. P-wave travel time anomalies: Aleutian - Alaska region: *Tectonophysics*, v. 19, p. 361 - 367.
- Bodine, J.H., Steckler, M.S., and Watts, A.B., 1981. Observations of flexure and the rheology of the oceanic lithosphere: *J. Geophys. Res.* v. 86, p. 3695 - 3707.
- Caldwell, J.G., Haxby, W.F., Karig, D.E., and Turcotte, D.L., 1976. On the applicability of a universal elastic trench profile: *Earth Planet. Sci. Lett.*, v. 31, p. 239 - 246.
- Caldwell, J.G., Turcotte, D.L., Haxby, W.F., and Karig, D.E., 1977. Thin elastic plate analysis of outer rises (abstract): In Talwani, M., and Pitman, W.C. III (eds.), Island Arcs, Deep Sea Trenches and Back-Arc Basins. Am. Geophys. Union, Washington, D.C. p. 467.
- Chapple, W.M., and Forsyth, D.W., 1979. Earthquakes and bending of plates at trenches: *J. Geophys. Res.*, v. 84, p. 6729 - 6749.
- Chen, A.T., Frolich, C., and Latham, G.V., 1981. The seismicity of the forearc marginal wedge (accretionary prism): submitted to *J. Geophys. Res.*
- Cleary, J., 1967. Azimuthal variation of the Longshot source term: *Earth Planet. Sci. Lett.*, v. 3, p. 29 - 37.
- Davies, D., and McKenzie, D.P., 1969. Seismic travel-time residuals and plates: *Geophys. J. R. astr. Soc.*, v. 18, p. 51 - 63.

- Engdahl, E.R., 1973. Relocation of intermediate depth earthquakes in the central Aleutians by seismic ray tracing: *Nature Phys. Sci.*, v.245, p 23 - 25.
- Engdahl, E.R., 1977. Seismicity and plate structure in the central Aleutians. In Talwani, M., and Pitman, W.C. III (eds.), *Island Arcs, deep Sea Trenches and Back-Arc Basins*. Am. Geophys. Union, Washington, D.C. p. 259 - 271.
- Engdahl, E.R., Sleep, N.H., and Lin, M.-T., 1977. Plate effects in North Pacific subduction zones: *Tectonophysics*, v. 37, p. 95-116.
- Forsyth, D.W., 1980. Comparison of mechanical models of the oceanic lithosphere: *J. Geophys. Res.*, v. 85, p. 6364 - 6368.
- Fujita, K., 1979. Tectonics of divergent and convergent plate margins: Ph.D. thesis, Northwestern University, 300 p.
- Fujita, K., Engdahl, E.R., and Sleep, N.H., 1981. Subduction zone calibration and teleseismic relocation of thrust zone events in the central Aleutian Islands: *Bull. Seismol. Soc. Am.*, v. 71, p. 1805 - 1828.
- Fujita, K., and Kanamori, H., 1981. Double seismic zones and stresses of intermediate depth earthquakes. *Geophys. J. R. astr. Soc* v.66, p.131-156.
- Fujita, K., Rogers, W.J. Jr., and Sleep, N.H., 1980. Enhanced arrivals due to subducting slabs (abstract): *Eos (Trans. Am. Geophys. Union)* v. 61, p. 1045.
- Hanks, T.C., 1979. Deviatoric stresses and earthquake occurrence at the outer rise: *J. Geophys. Res.* v. 84, p. 2343 - 2347.
- Herrin, E., and Taggart, J., 1968. Source bias in epicenter determinations: *Bull. Seismol. Soc. Am.*, v. 58, p. 1791 - 1796.
- Hong, T.-L., and Fujita, K., 1981. Modelling of depth phases and source processes of some central Aleutian earthquakes: *Earth Planet. Sci. Lett.*, v. 53, p. 333 - 342.
- Isacks, B.L., and Barazangi, M., 1977. Geometry of Benioff zones: lateral segmentation and downwards bending of the subducted lithosphere. In Talwani, M., and Pitman, W.C. III (eds.), *Island Arcs, Deep Sea Trenches and Back-Arc Basins*. Am. Geophys. Union, Washington, D.C., p. 99 - 114.
- Isacks, B., Oliver, J., and Sykes, L.R., 1968. Seismology and the new global tectonics: *J. Geophys Res.*, v. 73, p. 5855 - 5899.
- Jacob, K.H., 1970. Three-dimensional seismic ray tracing in a laterally heterogeneous spherical earth: *J. Geophys. Res.*, v. 75, p. 6675 - 6689.

- Jacob, K.H., 1972. Global tectonic implications of anomalous seismic P-travel times from the nuclear explosion Longshot: J. Geophys. Res., v. 77, p. 2556 - 2573.
- Jin, D.J., and Herrin, E., 1980. Surface wave studies of the Bering Sea and Alaska area: Bull. Seismol. Soc. Am., v. 70, p. 2117 - 2144.
- Johnson, A., 1970. Physical Processes in Geology. Freeman, Cooper, and Co., San Francisco. 577p.
- Jordan, T.H., 1977. Lithospheric slab penetration into the lower mantle beneath the Sea of Okhotsk: J. Geophys., v. 43, p. 473 - 496.
- Julian, B.R., 1970. Ray tracing in arbitrarily heterogeneous media: Lincoln Lab. Tech. Note 1970-45.
- Julian, B.R., and Gubbins, D., 1975. Two-point seismic ray tracing: a comparison of methods (abstract): Eos (Trans Am. Geophys. Union) v. 56, p. 1027.
- Kirby, S.H., 1970. Tectonic stress in the lithosphere: constraints provided by the experimental deformation of rocks: J. Geophys. Res., v. 85, p. 6353 - 6363.
- Lambeck, K., 1980. Estimates of stress differences in the crust from isostatic considerations: J. Geophys. Res., v. 85, p. 6367 - 6402.
- Liu, H.-P., 1980. The structure of the Kurile Trench - Hokkaido Rise system computed by an elastic time-dependent plastic plate model incorporating rock deformation data: J. Geophys. Res., v. 85, p. 901 - 912.
- McAdoo, D.C., Caldwell, J.G., and Turcotte, D.L., 1978. On the elastic-perfectly plastic bending of the lithosphere under generalized loading with application to the Kuril Trench: Geophys. J. R. astr. Soc., v. 54, p. 11 - 26.
- Murdock, J.N., 1969. Short-term seismic activity in the central Aleutian region: Bull. Seismol. Soc. Am., v. 59, p. 789 - 797.
- Pho, H.-T., and Behe, L., 1972. Extended distances and angles of incidence of P waves: Bull. Seismol. Soc. Am., v. 62, p. 885 - 902.
- Pitman, W.C. III, Larson, R.L., and Herron, E.M., 1974. The age of the ocean basins: Geol. Soc. Am. map.
- Richardson, R.M., and Solomon, S.C., 1977. Apparent stress and stress drop for intraplate earthquakes and tectonic stress in the plates: Pure Appl. Geophys., v. 115, p. 317 - 331.

- Richardson, R.M., Solomon, S.C., and Sleep, N.H., 1976. Intraplate stress as an indicator of plate tectonic driving forces: J. Geophys. Res. , v. 81, p. 1847 - 1856.
- Richardson, R.M., Solomon, S.C., and Sleep, N.H., 1977. Tectonic stress in the plates: Rev. Geophys. Space Phys., v. 17, p. 981 - 1019.
- Segawa, J., and Tomoda, Y., 1976. Gravity measurements near Japan and study of the upper mantle beneath the oceanic trench-marginal sea transition zones. In Sutton, G.H., Manghnani, M.H., and Moberly, R., editors: The Geophysics of the Pacific Ocean Basin and its Margin (A.G.U. Monograph # 19), American Geophysical Union, Washington, D.C., p. 35-52.
- Sleep, N.H., 1973. Teleseismic P-wave transmission through slabs: Bull. Seismol. Soc. Am., v. 63, p. 1349 - 1373.
- Solomon, S.C., Richardson, R.M., and Bergman, E.A., 1980. Tectonic stress: models and magnitudes: J. Geophys. Res., v. 85, p. 6086 - 6092.
- Sorrells, G.G., Crowley, J.G., and Veith, K.F., 1971. Methods for computing ray paths in complex geological structures. Bull. Seismol. Soc. Am., v. 61, p. 27 - 53.
- Spencer, C.P., and Engdahl, E.R., 1981. Inversion for hypocenters and structure beneath the central Aleutian island arc (abstract): Eos (Trans. Am. Geophys. Union) v. 62, p. 335.
- Stauder, W., 1968a. Mechanism of the Rat Island earthquake sequence of February 4, 1965, with relation to island arcs and sea floor spreading: J. Geophys. Res. v. 73, p. 3847 - 3858.
- Stauder, W., 1968b. Tensional character of earthquake foci beneath the Aleutian trench with relation to sea-floor spreading: J. Geophys. Res., v. 73, p. 7693 - 7701.
- Stein, S., 1978. An earthquake swarm on the Chagos-Laccadive ridge and its tectonic implications: Geophys. J. R. astr. Soc., v.55, p. 577 - 588.
- Stein, S., 1979. Intraplate seismicity on bathymetric features - the 1968 Emperor Trough earthquake: Jour. Geophys. Res., v. 84, p. 4763 - 4768.
- Suyehiro, K., and Sacks, I.S., 1979. P- and S-wave velocity anomalies associated with the subducting lithosphere determined from travel-time residuals in the Japan region: Bull. Seismol. Soc. Am., v. 69, p. 97 - 114.
- Sykes, L.R., 1966. The seismicity and deep structure of island arcs: J. Geophys. Res. v. 71, p. 2981 - 3006.

- Toksöz, M.N., Sleep, N.H., and Smith, A.T., 1973. Evolution of the downgoing lithosphere and the mechanism of deep focus earthquakes: Geophys. J. R. astr. Soc., v. 35, p. 285 - 310.
- Umino, N., and Hasegawa, A., 1975. On the two-layered structure of deep seismic plane in northeastern Japan arc (in Japanese): Zisin (ii), v. 27, p. 129 - 135.
- Watts, A.B., Bodine, J.B., and Streckler, M.S., 1980. Observations of flexure and the state of stress in the oceanic lithosphere: J. Geophys. Res., v. 85, p. 6369 - 6376.
- Yoshii, T., Kono, Y., and Ito, K., 1976. Thickness of the oceanic lithosphere. In Sutton, G.N., Manghanani, M.H., Moberly, R., and McAfee, E.V. (eds.), The Geophysics of the Pacific Ocean Basin and its Margins (Geophys. Monograph 19). Am. Geophys. Union, Washington, D.C. p. 423 - 430.

APPENDICES

APPENDIX I

PROGRAM "RAYTRAK"

```

      PROGRAM RAYTRAK(INPUT,OUTPUT,TAPE4=INPUT,TAPES=OUTPUT,
+TAPES,TAPE7,TAPE8)
C
C....ROUTINE TO TRACE RAYS THROUGH UPPER MANTLE VELOCITY STRUCTURE
C....BY JULIAN AND SLEEP (1973). MODIFIED FOR INTERACTIVE USE
C....ON CDC 6600 BY FUJITA (1978). VERSION 4.1 31 OCTOBER, 1978
C....FREEFORM INPUT/OUTPUT,MODIFIED FOR BACKUP LOAD IN EVENT OF DUMP.
C....PROGRAM MODIFIED FOR PLOTTING OF RAY EMERGENCE POINTS USING
C....TEKTRONIX PLOTTING ROUTINES AND THE TEKTRONIX MODEL 4010-1
C....GRAPHICS TERMINAL BY W.J.ROGERS JR.,(1981).
      DIMENSION PLOTAZ (400)
      DIMENSION PLOTAD (400)
      DIMENSION TIME(100),Z4(100),Z5(100),PHIR(100),TOAR(100),AZR(1
+00), THETAR(100), M(3), DELAY(100), TIM(100), AZR7(100), D(100)
      DIMENSION KTYPE(5), KTYPE1(2), ICOUNTS(2), RAYDAT(5), FMT(10)
      REAL IDENT,LAT1,LAT2
      DIMENSION Z(5)
      COMMON /CMMDL/ RO,DR,NR,LAT1,DLAT,LAT2,NLAT,RADIUS,DRSQ,DLSQ,DRDL,
+LON1,LON2,H,DM2,NUMP,F
      COMMON /COMID/ ITHMAX
      COMMON /CMRAY/ RFOC,THFOC,RMIN,DT,EPS,IRAY,IRAYPL,IWVF,TMAX
      COMMON /CMAMP/ I15,ISLOFF,NPCP,I16,IPRAY
      DATA KTYPE1/2,2/,KTYPE/1,1,1,1,1/
      DATA ICOUNTS/1,1/,RAYDAT/12.0,0.1,0.1,1.,20./
      CALL INITT(30)
      CALL ANMODE
      PI = 3.1415926
      IRAYPL = 0
      PRINT 9250
9250  FORMAT(* TRACK RAYS>*)
      READ(4,*) IPRAY
      F = 57.29578
C
C.... READ IN MODEL
C
      10 CONTINUE
      REWIND 8
      REWIND 5
      NNN=0
      READ (5,9030) KTABLE,NUMP,NIERM,NRAD,ITHMAX,IRAY,KREAD,IPUNCH,IDL
      1TO,NOERR,NPCP,I16
      WRITE (6,9030) KTABLE,NUMP,NIERM,NRAD,ITHMAX,IRAY,KREAD,IPUNCH,ID
      1LTO,NOERR,NPCP,I16

```

```

      WRITE (7,9030) KTABLE,NUMP,NIERMX,NRAD,ITHMAX,IRAY,KREAD,IPUNCH,ID
      ILTO,NOERR,NPCP,IIG
      IDLTMX = IDLTO+KTABLE-1
      READ (5,9020) EPS,DTEST,POLON,TMAX,DT,FLAT,TOAEPS
      WRITE (6,9010) EPS,DTEST,POLON,TMAX,DT,FLAT,TOAEPS
      WRITE (7,9010) EPS,DTEST,POLON,TMAX,DT,FLAT,TOAEPS
C
C.... INPUT OCCURS IN MODL5
C
      CALL MODL5
      IF (NRAD.EQ.1) GO TO 20
C
C.... CONVERT TO RADIANS
C
      TOAEPS = TOAEPS/F
20  CONTINUE
      READ (5,9080) IRAD,JREAD,KSKIP
      READ (5,9090) DMAX,DFOC,BOT
      WRITE (6,9040) DFOC
C
C.... MAIN LOOP
C.... GET DELAY TABLE FOR ORDINARY RAY
C
      IF (KSKIP.NE.0) GO TO 50
      IF (KREAD.EQ.0) GO TO 30
      READ (5,9050) FMT
      READ (5,FMT) (TIM(K),K=1,KTABLE)
      GO TO 40
30  CONTINUE
40  CONTINUE
C
C.... A NEW EPICENTER AND SET OF RAYS IS CALCULATED ON EACH CYCLE OF LOO
C
50  CONTINUE
C
C.... READ IN EPICENTER PARAMETERS
C
      WRITE(6,9240)
9240  FORMAT(* ANG.FOCAL DX. FROM ARC CURVATURE CENTER FOR THIS SET?*/)
      READ(4,*) SMDEL
60  CONTINUE
70  WRITE (6,9060)
      READ(4,*) ITOA,IPHI
      IGRAB = ITOA*IPHI
      IF (IGRAB.LE.10) GO TO 80
      WRITE (6,9070) IGRAB
      READ (4,9210) SET
      IF (SET.NE.3HYES) GO TO 70
80  WRITE (7,9080) IRAD,JREAD,KSKIP
      WRITE (7,9010) DMAX,DFOC,BOT
      WRITE (6,9100)
      READ(4,*) DELTOA,DELPHI,TOASTR,AZRATS
      TOASTR = TOASTR/F
      AZRATS = AZRATS/F

```

```

      THFOCD = SMDEL
      THFOC = SMDEL/F
      DELTOA = DELTOA/F
      DELPHI = DELPHI/F
      BOT = BOT/F
      RMIN = RADIUS-DMAX
      IF (DMAX.EQ.0.) RMIN = 0.
      RFOC = RADIUS-DFOC
      ISLOFF = 0
C
C.... BEGIN TO MAKE TABLE OF CALCULATED RAYS
C
      N = JREAD+1
C
C.... ITOA*IPHI+JREAD.LE.N74
C
      IF (IPHI*ITOA.EQ.0) GO TO 130
C
C.... LOOP TO CALCULATE RAY PARAMETERS
C.... INITIALIZE TAKE-OFF AZIMUTH
C
      AZR(N) = AZRATS
      IQ = 0
      90 IQ = IQ+1
C
C.... INITIALIZE TAKE-OFF ANGLE
C
      TOAR(N) = TOASTR
      IT = 0
      100 IT = IT+1
      GO TO 140
      110 CONTINUE
      N = N+1
      IF (NIER.GT.1) GO TO 120
      TOAR(N) = TOAR(N-1)-DELTOA
      AZR(N) = AZR(N-1)
      IF (IT.LT.ITOA) GO TO 100
      120 CONTINUE
      AZR(N) = AZR(N-1)+DELPHI
      IF (IQ.LT.IPHI) GO TO 90
      N = N-1
      130 CONTINUE
      GO TO 210
      140 CONTINUE
C
C.... NOW READY TO CALCULATE A RAY
C
      NIER = 0
      150 CALL RAYS (TOAR(N),AZR(N),TIME(N),Z,IER)
C
C.... CHECK IF ERROR OCCURRED DURING CALCULATION
C

```

```

      IF (IER.EQ.0.OR.NOERR.NE.0) GO TO 160
      NIER = NIER+1
      IF (NIER.GT.NIERMX) GO TO 190
C
C.... RAY WAS TRAPPED IN LOW VELOCITY ZONE AND DID NOT EMERGE
C
      TOAR(N) = TOAR(N)+EPS
C
C.... VARY RAY TO GET IT UNTRAPPED
C
      GO TO 150
160 CONTINUE
      Z(1) = RADIUS-Z(1)
C
C.... CHECK IF RAY ENDED AT CORE BOUNDARY
C
      IF (Z(1).GT.FLAT) GO TO 180
C
C.... CHECK IF RAY ENDED AT SURFACE PROPERLY
C
      IF (ABS(Z(1)).LT.POLON) GO TO 170
C
C.... RAY DID NOT EMERGE CORRECTLY
C
      WRITE (6,9110) N,Z(1)
      WRITE (7,9110) N,Z(1)
170 CONTINUE
C
C.... SAVE RAY PARAMETERS FOR LATER OUTPUT
C
      THETAR(N) = Z(2)
      PHIR(N) = Z(3)
      Z4(N) = Z(4)
      Z5(N) = Z(5)
      GO TO 110
180 NIER = NIER+1
C
C.... RAY HAS HIT CORE
C
      IF (NIER.GT.NIERMX) GO TO 200
C
C.... VARY RAY TO AVOID CORE
C
      TOAR(N) = TOAR(N)+BOT
      GO TO 150
190 CONTINUE
      WRITE (6,9120)
      WRITE (7,9120)
C
C.... LOOP STEP ABANDONED ALL RAYS WERE TRAPPED
C
      GO TO 210
200 CONTINUE

```

```

C.... LOOP STEP ABANDONED RAYS HIT THE
WRITE (6,9130)
WRITE (7,9130)
C
C.... LOOP STEP RAY CALCULATION FINISHED
C.... PREPARE TO OUTPUT RAY TABLE
C
210 CONTINUE
C
C.... INITIALIZE THE DISTANCE ROUTINE
C
D(1) = DIST1(0.,THFOC,PHIR(1),THETAR(1))*F
C
C.... CALCULATE DISTANCE AND AZIMUTH OF EACH RAY RELATIVE TO EVENT
C
DO 240 IQ = 1,N
D(IQ) = DIST(PHIR(IQ),THETAR(IQ))
AZR7(IQ) = ASIN(SIN(PHIR(IQ))/SIN(D(IQ))*SIN(THETAR(IQ)))
ZETA = DIST(AZR7(IQ),D(IQ))
C
C.... GET CORRECT BRANCH OF AZIMUTH
C
IF (ABS(ZETA-THETAR(IQ)).GT.DTEST) AZR7(IQ) = PI-AZR7(IQ)
C
C.... CONVERT TO DEGREES
C
AZR7(IQ) = AZR7(IQ)*F
D(IQ) = D(IQ)*F
C
C.... CALCULATE TRAVEL TIME DELAY RELATIVE TO TRAVEL TIME TABLE
C
IDLT = D(IQ)
IF (IDLT.LE.IDLTO.OR.IDLT.GE.IDLTMX) GO TO 220
AF = D(IQ)-IDLTO
IDLT = IDLT-IDLTO+1
DELAY(IQ) = TIME(IQ)-(TIM(IDLT)*(1.-AF)+TIM(IDLT+1)*AF)
GO TO 230
C
C.... SET DELAY TO 0.0 IF DELTA IS NOT PART OF TRAVEL TIME TABLE
C
220 DELAY(IQ) = 0.0
230 CONTINUE
C
C.... CONVERT TO DEGREES
C
TOAR(IQ) = TOAR(IQ)*F
AZR(IQ) = AZR(IQ)*F
THETAR(IQ) = THETAR(IQ)*F
PHIR(IQ) = PHIR(IQ)*F
Z4(IQ) = Z4(IQ)*F
Z5(IQ) = Z5(IQ)*F
240 CONTINUE
C

```

C.... OUTPUT RAY PARAMETER TABLE

C

```

WRITE (7,9140) DFOC,THFOCD
WRITE (7,9150) N
WRITE (7,9170)
WRITE (6,9160)
DO 250 K = 1,N
    WRITE (7,9180) (K,TOAR(K),AZR(K),THETAR(K),PHIR(K),TIME(K),Z4(K)
1    ,Z5(K),D(K),AZR7(K),DELAY(K))
    WRITE (6,9190) (K,TOAR(K),AZR(K),D(K),AZR7(K),DELAY(K))
250  CONTINUE
    LLL=NNN+1
    NNN=NNN+N
    DO 270 K=LLL,NNN
        MMM=(K-LLL)+1
        PLOTAZ(K)=AZR7(MMM)
        PLOTRAD(K)=D(MMM)
270  CONTINUE
    WRITE (6,550)
550  FORMAT (* DO YOU WANT TO PLOT NOW? ENTER N FOR NO.*)
    READ (4,551) PLOTNO
551  FORMAT (A1)
    IF(PLOTNO.EQ.1HN) GO TO 561
555  WRITE (6,556)
556  FORMAT(* YOU ARE GOING INTO A PLOTTING ROUTINE. TO*)
    WRITE (6,557)
557  FORMAT(* CHANGE THE PAGE AND PROCEED WITH THE PROGRAM YOU *)
    WRITE (6,5571)
5571 FORMAT(* MUST ENTER THE LETTER "Y". THERE IS NO PROMPT*)
    WRITE (6,5572)
5572 FORMAT(* FOR THIS.WHEN YOU HAVE UNDERSTOOD THIS ENTER "Y"*)
    READ (4,558) FOOL
558  FORMAT(A1)
    IF (FOOL.EQ.1HY) GO TO 559
    GO TO 555
559  CONTINUE
    CALL PLOTZ (PLOTAZ,PLOTRAD,SMDEL,NNN,LLL)
    WRITE (6,560)
560  FORMAT (* VERY GOOD! CONGRATULATIONS! WE PROCEED.*)
    BOT = BOT*F
561  WRITE (6,9200)
    READ (4,9210) SET
    IF (SET.EQ.3HNO ) GO TO 260
    GO TO 60
260  CONTINUE
    WRITE (6,9220)
    READ (4,9230) SET2
    IF (SET2.EQ.3HYES) GO TO 10
    WRITE (6,444)
444  FORMAT (* CATALOG TAPE 7 BEFORE LOGGING OUT OR IT WILL BE LOST*)
    WRITE (6,445)
445  FORMAT (* AND YOU WILL LOSE MOST OF YOUR INFORMATION WITH IT.*)

```

```

      CALL FINITT(150.,90.)
C
C.... END OF MAIN LOOP
C
9010 FORMAT (6E10.2)
9020 FORMAT (8E10.2)
9030 FORMAT (5X,15I5)
9040 FORMAT (10H DEPTH = ,F6.2,3H KM)
9050 FORMAT (10A4)
9060 FORMAT (* #TAKEDOFF ANGLES, # AZIMUTHS (SEPARATE BY COMMAS)*)
9070 FORMAT (21H YOU ARE CALCULATING ,I5,20H RAYS, ARE YOU SURE?)
9080 FORMAT (15X,I5,5X,2I5)
9090 FORMAT (2E10.2,50X,E10.2)
9100 FORMAT (49H DELTOA,DELPHI,TOASTR,AZRATZ (SEPARATE BY COMMAS)
1,/)
9110 FORMAT (1H0,I5,18H BAD RAY DEPTH IS,F12.3)
9120 FORMAT (42H ROUTINE DOES NOT CONVERGE DUE TO TRAPPING)
9130 FORMAT (31H ERROR RAYS KEEP HITTING BOTTOM)
9140 FORMAT (16H0 DEPTH OF FOCUS,F12.5,10H KM THFOC,F12.5,4H DEG)
9150 FORMAT (1H ,I5,21H RAYS WERE CALCULATED,/)
9160 FORMAT (4H NO.,4X,3HTOA,4X,3HAZR,2X,5HDELTA,3X,4HAZIM,3X,5HRESID)
9170 FORMAT (4H NO.,4X,3HTOA,4X,15HAZR THETA PHI,4X,4HTIME,5X,7HI AZ
1AR,2X,20HDELTA AZIM RESID)
9180 FORMAT (I4,2(1X,F6.2),2(1X,F5.1),1X,F7.2,2(1X,F5.1),2(1X,F6.2),1X,
1F7.3)
9190 FORMAT (I4,2(1X,F6.2),2(1X,F6.2),1X,F7.3)
9200 FORMAT (49H DO YOU WANT ANOTHER SET OF ANGLES IN THIS MODEL?)
9210 FORMAT (A3)
9220 FORMAT (32H DO YOU WANT TO TRY A NEW MODEL?)
9230 FORMAT (A3)
      END
      SUBROUTINE VDER (R,LAT,LON,V,DVDR,DVDTH,DVDPH,DVDRDR,DVDRDT,DVDTDT
1)
      COMMON /BLYTHE/ VEL(54,41),V1(294)
C
C.... CALCULATES VELOCITY AND ITS SPATIAL DERIVATIVES AS FUNCTIONS OF
C.... POSITION IN Laterally Heterogeneous Earth Model
C
      REAL LAT,LAT1,LAT2,LON,LON1,LON2
      DIMENSION VV(4)
      DIMENSION AV(4), AD(4), AD2(4)
      COMMON /CMMDL/ R0,DR,NR,LAT1,DLAT,LAT2,NLAT,RADIUS,DRSQ,DLSQ,DRDL,
1LON1,LON2,H,DM2
      COMMON /CMAMP/ I15,ISLOFF
C
C.... Laterally Varying Part of Model
C
      COMMON /CMDL1/ DR1,R1,NR1,DR1SQ
      Y = (R-R0)/DR
      IR = Y
      IF (ISLOFF.EQ.1) GO TO 20
      IF (IR.LE.0.OR.IR.GT.NR) GO TO 30
      Y = Y-FLOAT(IR)
      X = (LAT-LAT1)/DLAT

```

```

      ILAT = X
      IF (ILAT.LE.0.OR.ILAT.GT.NLAT-3) GO TO 30
      X = X-FLOAT(ILAT)
      JL = ILAT-1
      DO 10 K = 1,4
        J = JL+K
10    CALL SPLN3 (VEL(IR,J),Y,AV(K),AD(K),AD2(K))
      CALL SPLN3 (AV,X,V,DVDTH,DVDTDT)
      DVDTH = -DVDTH/DLAT
      CALL SPLN3 (AD,X,DVDR,DVDRDT,DMY)
      DVDR = DVDR/DR
      DVDPH = 0.
      GO TO 40
20  CONTINUE
30  V = 0.
      DVDR = 0.
      DVDTH = 0.
      DVDPH = 0.
      DVDRDR = 0.
      DVDTDT = 0.
      DVDRDT = 0.
      GO TO 90

C
C.... HAS LONGITUDE EXCEEDED THE END OF THE ISLAND ARC
C
40  IF (LON.GT.LON1) GO TO 50
      Z = ((LON-LON1)/H)**2
      GO TO 60
50  IF (LON.LT.LON2) GO TO 90
      Z = ((LON-LON2)/H)**2
60  IF (Z.GT.40.) GO TO 70
      F = EXP(-Z)
      GO TO 80
70  F = 0.
80  CONTINUE
      FP = -DM2*Z*F
      DVDPH = V*FP
      V = V*F
      DVDR = DVDR*F
      DVDTH = DVDTH*F

C
C.... SPHERICALLY SYMMETRIC PART OF MODEL
C
90  DM1 = (R-R1)/DR1
      I = DM1
      X = DM1-FLOAT(I)
      I = MIN0(I,NR1)
      VV(1) = V1(I)
      VV(2) = V1(I+1)
      VV(3) = V1(I+2)
      VV(4) = V1(I+3)
      IF (I.LE.0) VV(1) = V1(1)
      IF (I.LE.-1) VV(2) = V1(1)
      IF (I.LE.-2) VV(3) = V1(1)

```

```

      IF (I.LE.-3) VV(4) = V1(1)
      CALL SPLN3 (VV,X,V2,DVDR1,DVDR2)
      V = V+V2
      DVDR = DVDR+DVDR1/DR1
      RETURN
      END
      SUBROUTINE SPLN3 (A,X,F,DER,DER2)
      DIMENSION A(4)
      XM1 = X-1.
      XP1 = X+1.
      DM1 = A(1)-A(4)+3.*(A(3)-A(2))
      DM2 = A(1)-2.*A(2)+A(3)
      F = 0.5*X*XM1*(A(1)-X*DM1)-XM1*XP1*A(2)+0.5*X*XP1*A(3)
      DER = X*(DM2-(1.5*X-1.)*DM1)+0.5*(A(3)-A(1))
      DER2 = DM2-(3.*X-1.)*DM1
      RETURN
      END
      SUBROUTINE MODL5
C
C.... INITIALIZE ARRAYS
C
      DIMENSION KYPE(2)
      REAL LAT1,LAT2,LON1,LON2,LADV(2)
      COMMON /BLYTHE/ V(54,41),V1(294)
      DIMENSION T(100), BOT(10), TP(100,10), N(10), NN(10), DVDPH(10)
      DIMENSION FMT(10)
      COMMON /CMMDL/ RO,DR,NR,LAT1,DLAT,LAT2,NLAT,RADIUS,DRSQ,DLSQ,DRDL,
1LON1,LON2,H,DM2,NUMP,F
      COMMON /COMID/ I25G
      COMMON /CMDL1/ DR1,R1,NR1,DR1SQ
      DATA KYPE/1,1/,LADV/75.54,-.0009/,NR/51/
      IFIX = 252
C
C.... CREATE VELOCITY OR DENSITY DISTRIBUTION TO BE USED IN MAIN PROGRAM
C
C.... SKIP IF THIS PART READ IN PREVIOUSLY
C
      IF (I25G.NE.0) GO TO 30
C
C.... SET UP SPHERICALLY SYMMETRIC PART OF MODEL
C
      READ (5,9040) RADIUS,DR1,NR1,NRAD,ITMP,IBACK,IGRAV
      WRITE (6,9040) RADIUS,DR1,NR1,NRAD,ITMP,IBACK,IGRAV
      WRITE (7,9040) RADIUS,DR1,NR1,NRAD,ITMP,IBACK,IGRAV
      DR1SQ = DR1**2
      R1 = RADIUS-FLOAT(NR1-1)*DR1
C
C.... READ IN SPHERICAL BASIC VELOCITY OR DENSITY DISTRIBUTION
C
      READ (5,9030) FMT
      READ (5,FMT) (V1(I),I=1,NR1)
      WRITE (6,9070) RADIUS,R1,DR1
      WRITE (7,9070) RADIUS,R1,DR1
      WRITE (6,9050)
      READ (4,9060) SET3

```

```

      IF (SET3.NE.3HYES) GO TO 10
      WRITE (7,9080) (I,V1(I),I=1,NR1)
10  CONTINUE
C
C.... SET DUMMY POINTS ABOVE SURFACE NEEDED BY NUMERICAL RAY CALCULATION
C
      DO 20 I = 1,3
20   V1(NR1+I) = V1(NR1)
C
C.... SET UP Laterally Varying Part of Model.
C.... LATITUDE IS RELATIVE TO POLE OF ISLAND ARC
C.... LONGITUDE IS RELATIVE TO POLE OF ARC AND EVENT
C
      READ (5,9100) DR,DLAT,NLAT,LON1,LON2,H
      WRITE (6,9100) DR,DLAT,NLAT,LON1,LON2,H
      WRITE (7,9100) DR,DLAT,NLAT,LON1,LON2,H
      WRITE (6,9090)
      READ(4,*) NR
      WRITE (6,9110)
      READ(4,*) LAT1,DVDT
      DM2 = 2./H
      DRSQ = DR**2
      RO = RADIUS-FLOAT(NR-1)*DR
      LAT2 = LAT1+FLOAT(NLAT-1)*DLAT
      WRITE (6,9120) RO,DR,LAT1,DLAT,LAT2,DVDT
      WRITE (7,9120) RO,DR,LAT1,DLAT,LAT2,DVDT
30  CONTINUE
C
C.... END OF SKIPPED REGION
C.... READ IN Laterally Varying Part of Density or Velocity
C
      READ (5,9030) FMT
      IF (ITMP.EQ.1) GO TO 50
C
C.... VELOCITY OR DENSITY IS READ IN DIRECTLY
C
      DO 40 II = 1,NR
        I = NR-II+1
        READ (5,FMT) (V(I,J),J=1,NLAT)
40   CONTINUE
C
C.... END OF MODL5 INPUT FOR THIS BRANCH
C
      GO TO 170
50  CONTINUE
C
C.... READ IN TEMPERATURE MODEL AND COMPUTE VELOCITY OR DENSITY
C
      READ (5,FMT) ((V(I,K),K=1,NLAT),I=1,NR)
C
C.... SKIPPED IF ALREADY READ IN
C
      IF (I25G.NE.0) GO TO 70
C

```

```

C.... READ IN PARAMETERS FOR P-T DEPENDENT PHASE CHANGES
C
      IF (NUMP.EQ.0) GO TO 70
C
C.... EXECUTE LOOP FOR EACH PHASE
C
      DO 60 NP = 1,NUMP
C
C....   READ PHASE PARAMETERS
C
          READ (5,9130) N(NP),NN(NP),BOT(NP),DVDPH(NP)
          WRITE (6,9130) N(NP),NN(NP),BOT(NP),DVDPH(NP)
          WRITE (7,9130) N(NP),NN(NP),BOT(NP),DVDPH(NP)
C
C....   READ CLAPEYRON CURVE
C
          READ (5,9030) FMT
          READ (5,FMT) (TP(J,NP),J=1,NR)
          WRITE (6,FMT) (TP(J,NP),J=1,NR)
          WRITE (7,FMT) (TP(J,NP),J=1,NR)
C
C....   END OF LOOP TO READ PHASE PARAMETERS
C
      60   CONTINUE
C
C.... END OF SKIPPED REGION
C.... END OF MODLS INPUT
C
      70   CONTINUE
C
C.... CONVERT MINEAR TEMPERATURE INTO SEISMIC VELOCITY OR DENSITY
C
      DO 160 I = 1,NR
          B4 = V(I,1)
          DO 80 K = 1,NLAT
              J = K
C
C....   REVERSE HORIZONTAL INDEX IN ARRAY
C
              IF (IBACK.GE.1) J = NLAT+1-K
C
C....   TEMPORARILY SAVE TEMPERATURE
C
              T(J) = V(I,K)
          80   CONTINUE
          DO 90 K = 1,NLAT
C
C....   COMPUTE ANOMALY WITH RESPECT TO END POINT
C
              V(I,K) = (T(K)-B4)*DVDT
              IF (IGRAV.EQ.0) GO TO 90
C
C....   CALCULATE DENSITY = T*RHO*ALPHA
C

```

```

      V(I,K) = V(I,K)+V1(I+IFIX)
90    CONTINUE
      IF (NUMP.EQ.0) GO TO 150
C
C.... COMPUTE ANOMALIES DUE TO PHASE CHANGES
C
      DO 140 L = 1,NUMP
C
C.... ONLY CHECK OF PHASE CHANGES WHERE NECESSARY
C
      IF (I.LT.N(L).OR.I.GT.NN(L)) GO TO 140
      DO 120 K = 1,NLAT
C
C.... FIND DIFFERENCE BETWEEN TEMPERATURE AT POINT AND P-T CURVE
C
      ATOP = T(K)-TP(I,L)
C
C.... FIND WHICH PHASES ARE PRESENT
C
      IF (ATOP.GE.0) GO TO 100
      IF (ATOP+BOT(L).LE.0.) GO TO 110
C
C.... MIXED PHASE REGION
C
      RI = -ATOP/BOT(L)
      GO TO 120
C
C.... ONLY HIGH TEMPERATURE PHASE PRESENT
C
100   RI = 0.0
      GO TO 120
C
C.... ONLY LOW TEMPERATURE PHASE PRESENT
C
110   RI = 1.0
C
C.... SAVE AMOUNT OF LOW PRESSURE PHASE
C
120   T(K) = RI
C
C.... COMPUTE ANOMALOUS AMOUNT OF PHASE PRESENT RELATIVE TO END POIN
C
      B = T(1)
      DO 130 K = 1,NLAT
C
C.... ADD PHASE EFFECT TO VELOCITY OR DENSITY
C
130   V(I,K) = V(I,K)+DVDPH(L)*(T(K)-B)
140   CONTINUE
C
C.... END OF PHASE CHANGE CALCULATIONS
C

```

```

150  CONTINUE
160  CONTINUE
C
C.... END OF VELOCITY CONVERSION
C
170  CONTINUE
C
C.... SET DUMMY POINTS ABOVE SURFACE NEEDED BY NUMERICAL RAY CALCULATION
C
      DO 180 I = 1,3
        DO 180 J = 1,NLAT
180    V(NR+I,J) = 0.
        IF (NRAD.EQ.1) GO TO 190
C
C.... CONVERT TO RADIANS
C
      LAT1 = LAT1/F
      LAT2 = LAT2/F
      LON1 = LON1/F
      LON2 = LON2/F
      DLAT = DLAT/F
190    DLSQ = DLAT**2
      DRDL = DR*DLAT
      WRITE (8,9140)
      READ (4,9150) SET4
      IF (SET4.EQ.3HNO ) GO TO 210
      DO 200 I=1,54
        WRITE (7,9160) (V(I,J),J=4,22)
200    CONTINUE
      DO 721 I=1,54
        WRITE(7,9160) (V(I,J),J=23,40)
721    CONTINUE
210    CONTINUE
      RETURN
C
9030  FORMAT(20A4)
9040  FORMAT (2F10.2,6I10)
9050  FORMAT (34H DO YOU WANT VELOCITY PRINTED OUT?)
9060  FORMAT (A3)
9070  FORMAT (9HORADIUS =,F8.1,5X,5HR1 =,F8.1,5X,5HDR1 =,F8.1/)
9080  FORMAT (1H ,5(I4,F8.3))
9090  FORMAT (28H NUMBER VERTICAL GRID POINTS/35H 51 FOR LONG SLAB 41 FO
1R SHORT SLAB,/)
9100  FORMAT (F10.5,15X,F10.5,I5,10X,3F10.5)
9110  FORMAT (11H LAT1,DV/DT,/)
9120  FORMAT (5H2R0 =,F8.1,5X,4HDR =,F6.1,5X,6HLAT1 =,F7.2,5X,6HDLAT =,F
16.2,7H LAT2 =,F7.2,5X,7HDV/DT =,E15.6)
9130  FORMAT (2I5,2E10.2)
9140  FORMAT (44H DO YOU WANT VELOCITY STRUCTURE PRINTED OUT?)
9150  FORMAT (A3)
9160  FORMAT (1X,19F4.2)
      END
      REAL FUNCTION DERPAP (Y,X,A,M)

```

```

C
C.... CALCULATES DY/DX AT CONSTANT A
C
  DIMENSION A(300), X(300), Y(300), M(3)
  I = M(1)
  K = M(2)
  J = M(3)
  S = A(I)*Y(J)-A(I)*Y(K)-A(K)*Y(J)-A(J)*Y(I)+A(J)*Y(K)+A(K)*Y(I)
  P = A(I)*X(J)-A(I)*X(K)-A(K)*X(J)-A(J)*X(I)+A(J)*X(K)+A(K)*X(I)
  DERPAP = S/P
  RETURN
  END
  SUBROUTINE RAYFIX (SPHI,STHETA,PHI,THETA)

C
C.... THIS IS MADE NECESSARY BY THE INANE WAY THE AMOD WORKS
C
  PHI = PHI-SPHI
  PHI = AMOD(PHI,PIX2)
  IF (PHI.LT.-PI) PHI = PHI+PIX2
  IF (PHI.GT.PI) PHI = PHI-PIX2
  DPHI = PHI
  PHI = PHI+SPHI
  IF (DPHI.GT.PIHF) GO TO 10
  IF (DPHI.LT.-PIHF) GO TO 20
  GO TO 40
10 PHI = PHI+PIHF
  GO TO 30
20 CONTINUE
  PHI = PHI-PIHF
30 THETA = -THETA
40 CONTINUE
  DTHETA = STHETA-THETA
  THETA = AMOD(DTHETA,PI)
  IF (THETA.LT.-PIHF) THETA = THETA+PI
  IF (THETA.GT.PIHF) THETA = THETA-PI
  THETA = STHETA-THETA
  RETURN
  ENTRY RFSET
  PI = 3.1415926
  PIHF = PI*.5
  PIX2 = PI*2.
  RETURN
  END
  SUBROUTINE DERIV (T,Z,DZDT)

C
=C.... DEFINES DIFFERENTIAL EQUATIONS FOR RAY TRACING THROUGH
C.... THREE DIMENSIONAL STRUCTURE
C
  DIMENSION Z(5), DZDT(5)
  CALL VDER (Z(1),1.570796-Z(2),Z(3),V,DVDR,DVDTHT,DVDPH,DVDR2,DVDRDT
1,DVDT2)
  ETA = Z(1)/V
  ETAI = 1./ETA

```

```

SINTH = SIN(Z(2))
COSTH = COS(Z(2))
COTTH = COSTH/SINTH
SINIR = SIN(Z(4))
COSIR = COS(Z(4))
SINZT = SIN(Z(5))
COSZT = COS(Z(5))
DZDT(1) = V*COSIR
DRDT = DZDT(1)
DM1 = SINIR/ETA
DM3 = SINZT/SINTH
DZDT(2) = DM1*COSZT
DZDT(3) = DM1*DM3
DZDT(4) = SINIR*(DVDR-ETA1)-COSIR/Z(1)*(COSZT*DVDTH+DM3*DVDPH)
DZDT(5) = ((DVDTH/SINIR-V*SINIR*COTTH)*SINZT-DVDPH*COSZT/SINIR/SIN
1TH)/Z(1)
RETURN
END

```

```

C
C.... CALCULATES DISTANCE ON SPHERE
C.... DISTANCE IS BETWEEN PHI1,THETA1 AND PHI5,THETA5
C.... PHI1,THETA1 ARE SAVED FOR FUTURE CALLS TO DIST
C

```

```

REAL FUNCTION DIST1 (PHI1,THETA1,PHI5,THETA5)
COMMON /HARVEY/ STORE,CT,ST
THETA2 = THETA5
PHI2 = PHI5
CT = COS(THETA1)
ST = SIN(THETA1)
STORE = PHI1
B = PHI1-PHI2
D = COS(THETA2)*CT+ST*SIN(THETA2)*COS(B)
DIST1 = ACOS(D)
RETURN
END
REAL FUNCTION DIST (PHI3,THETA3)

```

```

C
C.... CALCULATES DISTANCE ON SPHERE
C.... DISTANCE IS BETWEEN PHI1,THETA1 AND PHI3,THETA3
C

```

```

COMMON /HARVEY/ STORE,CT,ST
PHI2 = PHI3
THETA2 = THETA3
B = STORE-PHI2
D = COS(THETA2)*CT+ST*SIN(THETA2)*COS(B)
DIST = ACOS(D)
RETURN
END
SUBROUTINE DIFSYS (F,N,H,X,Y,EPS,S,NEWH)

```

```

C
C.... F IS THE NAME OF A SUBROUTINE CALLED BY *CALL F(X,Z,DZ)* WHICH
C.... STORES IN THE VECTOR DZ THE N COMPONENTS OF THE DERIVATIVE
C.... DZ/DX ACCORDING TO THE DIFFERENTIAL EQUATION WHICH IS BEING

```

C.... SOLVED, $DZ/DX=F(X,Z)$
 C.... X,Z, AND DZ MUST BE OF REAL TYPE
 C.... N IS THE ORDER OF THE SYSTEM OF DIFFERENTIAL EQUATIONS.
 C.... N MUST BE NO GREATER THAN MAXORD WHICH IS SET BELOW
 C.... ITEST HAS TO BE SET EQUAL TO ONE IN THE CALLING PROGRAM IN ORDER T
 C.... TEST THE ERROR RETURN OPTION
 C.... ERROR IS SET TO 1 IF THE FUNCTION DOES NOT CONVERGH
 C.... H IS THE BASIC STEP SIZE
 C.... X AND Y (VECTOR) ARE THE INITIAL VALUES
 C.... EPS AND S(VECTOR) ARE THE ERROR BOUNDS.
 C.... ABS(EPS) SHOULD BE NO SMALLER THAN 1.0E-06
 C.... NEWH IS A FLAG WHICH IS SET EQUAL TO .TRUE. IF THE STEP SIZE USED
 C.... BY DIFSYS IS DIFFERENT FROM THE STEP SIZE H GIVEN IN THE
 C.... PARAMETER LIST. NEWH IS SET EQUAL TO .FALSE. OTHERWISE.
 C

```

      INTEGER ERROR
      LOGICAL NEWH
      LOGICAL EPSERR
      LOGICAL KONV,BO,BH
      INTEGER R,SR
      DIMENSION Y(5), S(5)
      DIMENSION D(7)
      DIMENSION YA(5), YL(5), YM(5), DY(5), DZ(5), DT(5,7)
      DIMENSION YG(8,5), YH(8,5)
      COMMON /STUPID/ NEWRAY
      COMMON /DIF/ ITEST,ERROR
      DATA EPSERR/.FALSE./
      DATA MAXORD/15/
      ICNT = 0
      ERROR = 0
      IF (NEWRAY.EQ.0) GO TO 20
      DO 10 IZ = 1,5
        DO 10 JZ = 1,7
          DT(IZ,JZ) = 0.0
10    CONTINUE
      NEWRAY = 0
20    CONTINUE
      XMAG = X+H
      IF (N.GT.0.AND.N.LE.MAXORD) GO TO 30
      WRITE (6,9010)
      STOP
30    E = ABS(EPS)
      IF (E.GE.1.0E-06) GO TO 50
      IF (EPSERR) GO TO 40
      EPSERR = .TRUE.
      WRITE (6,9020)
40    E = 1.0E-06
  
```

C
 C.... EACH CALL OF DIFSYS PERFORMS ONE INTEGRATION STEP OF THE
 C.... EQUATION $DY/DX=F(X,Y)$ ACCORDING TO THE METHOD OF R. BULIRSCH AND
 C.... J. STÖR (NUMERISCHE MATHEMATIK, IN PRESS). THE STEP SIZE WILL
 C.... BE LESS THAN OR EQUAL TO H. THE PROGRAM TAKES THE FIRST OF THE
 C.... NUMBERS H,H/2,H/4,..., AS STEP SIZE FOR WHICH NO MORE THAN 9

C.... EXTRAPOLATION STEPS ARE NEEDED TO OBTAIN A SUFFICIENTLY ACCURATE
 C.... RESULT. IF THE STEP SIZE USED IS DIFFERENT THAN THE STEP SIZE
 C.... GIVEN IN THE PARAMETER LIST, THEN THE LOGICAL FLAG NEWH WILL BE
 C.... SET EQUAL TO .TRUE., OTHERWISE IT WILL BE SET EQUAL TO .FALSE..
 C.... X AND Y ARE THE INITIAL VALUES FOR THE STEP TO BE COMPUTED. AFTER
 C.... LEAVING THE SUBROUTINE, THE ORIGINAL VALUES OF THE PARAMETERS X
 C.... AND Y WILL HAVE BEEN REPLACED BY $X+H^*$ AND $Y(X+H^*)$, RESPECTIVELY,
 C.... WHERE H^* IS THE STEP SIZE ACTUALLY USED. IN ADDITION THE STEP SIZ
 C.... WILL HAVE BEEN CHANGED AUTOMATICALLY TO AN ESTIMATED OPTIMAL
 C.... STEP SIZE FOR THE NEXT INTEGRATION STEP. THE ARRAY S AND THE
 C.... CONSTANT EPS ARE USED TO CONTROL THE ACCURACY OF THE COMPUTED
 C.... VALUES. THE SUBROUTINE IS LEFT, IF ALL $I=1, 2, \dots, N$ TWO
 C.... SUCCESSIVE VALUES FOR $Y(I)$ DIFFER AT MOST BY AN AMOUNT $EPS*S(I)$
 C.... EPS SHOULD NOT BE SMALLER THAN $1.0E-06$. FOR THE FIRST INTEGRATION
 C.... STEP IT IS ADVISABLE TO SET $S(I)=0.0$. BEFORE RETURN TO THE
 C.... CALLING PROGRAM, THE ARRAY S WILL HAVE HAD ITS CONTENTS MODIFIED
 C.... SO THAT $S(I)=\max(S(I), \text{ABS}(Y(I,X)))$, WHERE THE MAXIMUM IS TAKEN OVER
 C.... THE INTEGRATION INTERVAL $(X, X+H^*)$.

C

```

50 CALL F (X,Y,DZ)
   BH = .FALSE.
   NEWH = .FALSE.
   DO 60 I = 1,N
60   YA(I) = Y(I)
70   A = X+H
   ICNT = ICNT+1
   IF (ICNT.GT.10) GO TO 230
   FC = 1.5
   BO = .FALSE.
   M = 1
   R = 2
   SR = 3
   JJ = -1
   DO 210 J1 = 1,10
     J = J1-1
     D(2) = 2.25
     IF (BO) D(2) = 4.0/D(2)
     D(4) = 4.0*D(2)
     D(6) = 4.0*D(4)
     KONV = J.GT.2
     IF (J.LE.6) GO TO 80
     L = 6
     D(7) = 64.
     FC = 0.6*FC
     GO TO 90
80   L = J
     D(L+1) = M*M
90   M = 2*M
     G = H/LOAT(M)
     B = 2.0*G
     IF (BH.AND.J.LT.8) GO TO 140
     KK = (M-2)/2
     M = M-1
     DO 100 I = 1,N

```

```

      YL(I) = YA(I)
100    YM(I) = YA(I)+G*DZ(I)
      IF (M.LE.0) GO TO 160
      DO 130 K = 1,M
        CALL F (X+G*FLOAT(K),YM,DY)
        DO 110 I = 1,N
          U = YL(I)+B*DY(I)
          YL(I) = YM(I)
          YM(I) = U
          U = ABS(U)
110      S(I) = AMAX1(U,S(I))
          IF (K.NE.KK.OR.K.EQ.2) GO TO 130
          JJ = JJ+1
          DO 120 I = 1,N
            YH(JJ+1,I) = YM(I)
120          YG(JJ+1,I) = YL(I)
130      CONTINUE
      GO TO 160
140    DO 150 I = 1,N
      YM(I) = YH(J+1,I)
150    YL(I) = YG(J+1,I)
160    CALL F (A,YM,DY)
      DO 200 I = 1,N
        V = DT(I,1)
        DT(I,1) = 0.5*(YM(I)+YL(I)+G*DY(I))
        C = DT(I,1)
        TA = C
        IF (L.LE.0) GO TO 190
        DO 180 K = 1,L
          B1 = D(K+1)*V
          B = B1-C
          U = V
          IF (B.EQ.0.0) GO TO 170
          B = (C-V)/B
          U = C*B
          C = B1*B
170        V = DT(I,K+1)
          DT(I,K+1) = U
180        TA = U+TA
190      IF (ABS(Y(I)-TA).GT.E*ABS(S(I))) KONV = .FALSE.
200      Y(I) = TA
      IF (KONV) GO TO 220
      D(3) = 4.0
      D(5) = 16.0
      BO = .NOT.BO
      M = R
      R = SR
210    SR = 2*M
      BH = .NOT.BH
      NEWH = .TRUE.
      H = 0.5*H

```

```

C.... THE FOLLOWING TEST IS TO PREVENT INFINITE LOOPONG
C.... THE NUMBER 1.E-7 COULD BE CHANGED IF SO DESIRED
C
      IF (ABS(H/XMAG).LT.1.0E-7) GO TO 230
      GO TO 70
220 H = FC*H
      X = A
      GO TO 250
230 IF (ITEST.NE.1) GO TO 240
      ERROR = 1
      WRITE (6,9030)
      GO TO 250
240 WRITE (6,9030)
      WRITE (6,9040)
      STOP
250 RETURN
C
9010 FORMAT (28HORDER TOO LARGE FOR DIFSYS.)
9020 FORMAT (51HERROR LIMIT TOO SMALL FOR DIFSYS. WE USE 1.0E-06.)
9030 FORMAT (1H0,46HMESSAGE FROM DIFSYS,FUNCTION DOES NOT CONVERGE)
9040 FORMAT (1H0,25HPROGRAM IS FORCED TO STOP)
      END
      SUBROUTINE RAYS (TOA,AZ,TS,ZS,IER)
C
C.... TRACES RAY THROUGH TWO-DIMENSIONAL VELOCITY STRUCTURE
C.... Z(1)=R      Z(2)=THETA      Z(3)=PHI      Z(4)=I
C.... Z(5)=ZETA      Z(6)=DR/DIO      Z(7)=DTHETA/DIO      Z(8)=DPHI/DIO
C
      REAL IDENT,LAT1,LAT2
      LOGICAL NEWH
      EXTERNAL DERIV
C
C.... A NEW STEP TO OUTPUT RAY PATHS TO CARDS FOR LATER PLOTTING HAS BEE
C
      DIMENSION Z(5), DZDT(5), ZS(5), S(5)
      DIMENSION IUVV(100), JUVV(100)
      DIMENSION CS(12), SN(12)
      COMMON /CMMDL/ RO,DR,NR,LAT1,DLAT,LAT2,NLAT,RADIUS,DRSQ,DLSQ,DRDL,
1LON1,LON2,HH,DM2
      COMMON /CMRAY/ RFOC,THFOC,RMIN,DT,EPS,IRAY,IRAYPL,IWVF,TMAX
      COMMON /CMAMP/ I15,ISLOFF,NPCP,I16,IPRAY
      COMMON /STUPID/ NEWRAY
      DATA CS,SN/.866,.5,0.,-.5,-.866,-1.,-.866,-.5,0.,.5,.866,1.,.5,.86
16,1.,.866,.5,0.,-.5,-.866,-1.,-.866,-.5,0./
C
C.... INITIALIZE PARAMETERS
C
      NEWRAY = 1
      M = 0
      JLAT = (NLAT-1)*10
      WLAT = 3.141593/2.-LAT1
      IER = 0
      N = 5

```

```

      ITER = 0
      T = 0.
      H = DT
      Z(1) = RFOC
      Z(2) = THFOC
      Z(3) = 0.
      Z(4) = 3.141593-TOA
      Z(5) = 3.141593-AZ
      IF (IRAY.EQ.0) GO TO 10
      CALL DERIV (T,Z,DZDT)
      WRITE (6,9020) T,(Z(I),I=1,N),(DZDT(I),I=1,N)
10  CONTINUE
      DO 20 I = 1,N
20   S(I) = AMAX1(ABS(Z(I)),1.0)
30  DO 40 I = 1,N
40   ZS(I) = Z(I)
      TS = T
      GO TO 60

C
C.... REUSE ORIGINAL TIME WHEN PLOTTING
C
50  H = H2
      IF (H.LE.0.01) H = DT
60  ERP = EPS
      OH = H

C
C.... INTEGRATE ONE STEP
C
      CALL DIFSYS (DERIV,N,H,TS,ZS,ERP,S,NEWH)
      H2 = T+OH-TS
      IF (ITER.NE.0) GO TO 130

C
C.... CHECK FOR RAYS HITTING CORE
C
      IF (ZS(1).LT.RMIN) GO TO 110

C
C.... CHECK IF RAY HAS RETURNED TO SURFACE
C
      IF (ZS(1).GT.RADIUS) GO TO 100

C
C.... CHECK IF EXCESS TRAVEL TIME HAS OCCURRED WITHOUT RAY EMERGING
C
      IF (TS.LT.TMAX) GO TO 70

C
C.... SET ERROR FLAG
C
      IER = 1
      RETURN
70  DO 80 I = 1,N
80   Z(I) = ZS(I)
      T = TS
      IF (IRAY.EQ.0) GO TO 90
      CALL DERIV (T,Z,DZDT)
      WRITE (6,9020) T,(Z(I),I=1,N),(DZDT(I),I=1,N)
90  CONTINUE

```

```

      IF (I16.EQ.0) GO TO 60
C
C.... SAVE RAY PATH FOR LATER PUNCH OUT
C
      IGG = (RADIUS-Z(1))/DR*10.
      LGG = (WLAT-Z(2))/DLAT*10.
      IF (I16.LT.0) LGG = (JLAT-LGG)
      M = M+1
      IWWW(M) = LGG+1
      JWWW(M) = IGG+1
C
C.... IS BUFFER FULL
C
      IF (M.GE.100) GO TO 140
      GO TO 50
C
C.... RAY ENDS AT SURFACE
C
      100 RF = RADIUS
      GO TO 120
C
C.... RAY ENDS AT BOTTOM OF MODEL
C
      110 RF = RMIN
C
C.... DO NOT WASTE TIME WITH RAYS WHICH HIT CORE
C
      IF (NPCP.EQ.0) GO TO 140
C
C.... ITERATE TO FIND END OF RAY
C
      120 ITER = 1
      CALL DERIV (T,Z,DZDT)
      H = (RF-Z(1))/DZDT(1)
      GO TO 30
      130 D = RF-ZS(1)
      IF (ABS(D).LT.EPS*S(1)) GO TO 140
      IF (ITER.GT.4) GO TO 140
      ITER = ITER+1
      CALL DERIV (TS,ZS,DZDT)
      H = OH+D/DZDT(1)
      GO TO 30
140  CONTINUE
      IF(IPRAY.EQ.1) PRINT 9025, M
9025  FORMAT(1X,I5)
      IF(IPRAY.EQ.1) PRINT 9030, ((IWWW(I),JWWW(I)),I=1,M)
9030  FORMAT(1X,16I5)
      RETURN
C
9010  FORMAT (1H1,20A4//3X,4HTIME,7X,1HR,5X,5HTHETA,4X,3HPHI,6X,4HZETA,5
1X,1HI,8X,5HDR/DT,8X,9HDTHETA/DT,4X,7HDPHI/DT,6X,8HDZETA/DT,5X,5HDI
2/DT/)
9020  FORMAT (1P9E12.4)
      END

```

SUBROUTINE PLOTZ (PLOTAZ,PLOTRAD,SMDEL,NNN,LLL)

C
C THIS SUBROUTINE PLOTS THE DATA ON A TEKTRONIX TERMINAL. IT USES
C ALMOST EXCLUSIVELY CANNED TEKTRONIX ROUTINES AND SO YOU SHOULD
C REFER TO AN APPROPRIATE MANUAL IF YOU WANT TO UNDERSTAND ANY
C OF THIS STUFF.

C

```

    DIMENSION PLOTAZ (400)
    DIMENSION PLOTRAD (400)
    CALL ERASE
    CALL DWINDO (0.,100.,0.,180.)
    CALL SWINDO (10,1013,10,1013)
    CALL POLTRN (0.,180.,0.)
    CALL MOVEA (100.,0.)
    CALL DRAWA (100.,180.)
    CALL MOVEA (0.,0.)
    CALL DRAWA (5.,90.)
    CALL MOVEA (100.,0.)
    CALL DRAWSA (100.,180.,14)
    CALL MOVEA (80.,0.)
    CALL DASHSA (80.,180.,14)
    CALL MOVEA (60.,0.)
    CALL DASHSA (60.,180.,14)
    CALL MOVEA (40.,0.)
    CALL DASHSA (40.,180.,14)
    CALL MOVEA (20.,0.)
    CALL DASHSA (20.,180.,14)
    CALL MOVEA (0.,0.)
    CALL DASHA (100.,30.,14)
    CALL MOVEA (0.,0.)
    CALL DASHA (100.,60.,14)
    CALL MOVEA (0.,0.)
    CALL DASHA (100.,90.,14)
    CALL MOVEA (0.,0.)
    CALL DASHA (100.,120.,14)
    CALL MOVEA (0.,0.)
    CALL DASHA (100.,150.,14)
    L=LLL-1
    IF(L.EQ.0) GO TO 110
    DO 101 I=1,L
    IF(PLOTAZ(I).GE.180.00) PLOTAZ(I)=0.
    CALL POINTA (PLOTRAD(I),PLOTAZ(I))
    CALL MOVREL (-4,0)
    CALL DRWREL (8,0)
    CALL MOVREL (-4,-4)
    CALL DRWREL (0,8)
101  CONTINUE
110  CONTINUE
    DO 111 I=LLL,NNN
    IF(PLOTAZ(I).GE.180.00) PLOTAZ(I)=0.
    CALL POINTA (PLOTRAD(I),PLOTAZ(I))
    CALL MOVREL (-8,0)
    CALL DRWREL (16,0)

```

```
      CALL MOVREL (-8,-8)
      CALL DRWREL (0,10)
111  CONTINUE
      CALL MOVEA (0.,0.)
      CALL MOVREL (0,740)
      CALL ANMODE
      WRITE (6,222) SMDEL
222  FORMAT (* ANG. DIST. IS*, 1F6.2)
      WRITE (6,223) NNN
223  FORMAT (I5,* RAYS.*)
224  READ (4,225) FLAG
225  FORMAT (A1)
      IF(FLAG.EQ.1HY) GO TO 333
      GO TO 224
333  RETURN
      END
```

APPENDIX II

USING "RAYTRAK"

APPENDIX II

USING "RAYTRAK"

As mentioned in the text, Raytrak is a computer ray tracing program using the ray tracing method developed by Julian (1970). It is based on Fermat's principle of stationary time; that is, a ray travels from one point to another via the path that takes the minimum time (or the maximum, but that does not concern us here). The program was first written by Julian and Sleep in 1973. It was modified for interactive use by Fujita in 1978. In 1981 it was modified by the present author to plot ray emergence points on a Tektronix 4010-1 graphics terminal. These modifications make the program much faster and easier to operate than it would be otherwise.

First, a few warnings are in order.

1. The program calculates ray emergence points and stores their locations for plotting. Since it plots all calculated points each time (not just the ones most recently calculated) these points can be numerous. The arrays for plot radius and plot azimuth are set up for four hundred points, so you should never calculate more points than this before ending the run and either considering another distance from the slab, or stopping completely. You will probably never calculate anything near this number of points on a single plot, but you should know about this limitation.

2. As set up, the program calculates all the rays first and prints out the results afterward. This means that should the time limit be reached before the end of the program, all your results will be lost. If you are going to run a lot of points it would be better to reset the time limit before you start in order to avoid this problem.

3. The plot produced by the Tektronix is useful, but not detailed. All of the detailed results are on a local file called Tape 7. This should be cataloged at least temporarily before you sign off, or it will be lost forever. Log on again on some hard-copy terminal and list the file to get your permanent copy.

When you run RAYTRAK, it sends you messages and prompts. You should respond to these as follows.

TRACK RAYS>

If you respond to this message with the number 1, the computer will print out the coordinates of the ray as it moves through the velocity model. Its path can then be plotted. If you respond with the number 0 these coordinates will not be printed out.

DO YOU WANT VELOCITY PRINTED OUT?

The usual answer for this is No, as the printout is extensive otherwise.

NUMBER VERTICAL GRID POINTS

51 FOR LONG SLAB 41 FOR SHORT SLAB

This is more or less self explanatory. The long slab is 350 km deep at the maximum, and this is the model used for this thesis. To get this model, answer with the number 51.

DO YOU WANT VELOCITY STRUCTURE PRINTED OUT?

If you answer "yes", you will get extensive printout showing the velocity model you are using. You don't usually need this, so your usual answer should be "no".

ANGULAR FOCAL DX. FROM ARC CURVATURE CENTER FOR THIS SET?

This is a distance measured in geocentric angular distance, as in the text of this thesis. Put in whatever distance you are interested in, out to 14.0. The trench falls at about 12.4, the outer rise at 13.0 and the volcanic front at 11.4 in the Aleutians.

TAKEOFF ANGLES, #AZUMUTHS

(SEPARATE BY COMMAS)

These are the number of takeoff angles and azimuths for which rays will be calculated. The machine takes a given azimuth and keeping that fixed calculates the results for however many takeoff angles you order, then goes on to the next azimuth. Takeoff angle becomes smaller for each iteration (which makes the rays generally emerge farther from the source). Azimuth moves away from the direct downdip direction with each iteration. How far they move each time is decided by your response to a later question.

YOU ARE CALCULATING ____ RAYS, ARE YOU SURE?

This message only appears when you order more than 10 rays. It serves as a safeguard. If you respond with "yes" you get the rays calculated for you. If you answer "no" you go back to the previous question and have to choose the number of take-off angles and azimuths again.

DELTOA, DELPHI, TOASTR, AZRATZ
(SEPARATE BY COMMAS)

Respond with four floating point numbers separated from each other by commas. Deltoa is the step in take-off angle between adjacent rays, delphi is the step in azimuth between them, toastr is starting take-off angle, and azratz is starting azimuth. Given, say, the response

2., 5., 32., 0.

the computer will send the first ray off at a take-off angle of 32° and an azimuth with respect to the downdip direction of the slab of 0° (or in other words, directly down the slab). If you chose to order more than one take-off angle earlier, the second ray calculated will be of the same azimuth (0.) but will have a take-off angle 2° SMALLER than the first one. The computer will calculate rays in this manner until it has done as many take-off angles as you ordered. Then, if you ordered more than one azimuth, it will switch to an azimuth 5° greater than the first one and start over with the original take-off angle of 32° .

If you should want to send a single ray, respond to the question #TAKEOFF ANGLES, # AZIMUTHS with 1,1. Then when the computer asks for DELTOA, DELPHI, TOASTR, AZRATZ you can put in anything you wish for deltoa and delphi. In this case they are meaningless. Put in the takeoff angle and azimuth you want for toastr and azratz.

Hopefully you will start to get results at this point. You will probably first get a lot of messages like

19 BAD RAY DEPTH IS 12.9

which means, in the example above, that ray number 19 did not converge

to the surface as it was supposed to. Instead it converged to a depth of 12.9 km. You have to correct your travel times for this error by hand. Nevertheless, this is not a fatal problem and if the "bad ray depth" is small the corrected solution is still fairly accurate. Large "bad ray depths" cause serious errors in travel time calculations and ray emergence point location as well.

If you get

ROUTINE DOES NOT CONVERGE DUE TO TRAPPING

or

ERROR RAYS KEEP HITTING BOTTOM

you're in trouble. Either the rays are trapped in some layer and never reach the surface or they are hitting the Earth's core. In either case the set is useless to you, especially since the computer abandons the calculation at this point and shuts your program down. This forces you to start at the beginning again.

Assuming you avoid this problem, you get a list of output. You will lose much of this on the Tektronix screen due to over-writing and when you "change pages" to clear the screen. Don't worry about this. The printout on your screen is just to tell you that the program is working properly. There is a copy in the local file Tape 7 .

Your next message is

DO YOU WANT TO PLOT NOW? ENTER N FOR NO

The no message is specified because if you respond with anything else the computer goes ahead and plots your data. Therefore enter "N" for no, and anything else for yes. A "no" answer skips you over the plotting routines. A "yes" answer results in your getting the following message.

YOU ARE GOING INTO A PLOTTING ROUTINE. TO CHANGE THE PAGE AND PROCEED WITH THE PROGRAM YOU MUST ENTER THE LETTER "Y". THERE IS NO PROMPT FOR THIS. WHEN YOU HAVE UNDERSTOOD THIS ENTER "Y".

This refers to the end of the plotting routine itself, after the plot is finished. To avoid writing messages all over your plot, the program is set up to just sit there and do nothing until it gets that "y" it is waiting for. That is the only way to get out of the plotting routine, and you can punch anything else you can think of with no effect. This is very frustrating if you happen to forget that you're still in the plotting routine.

So, having read the message above, enter "y". The computer will plot a pretty picture on the screen of your terminal. When it has finished, and when you have made a hard copy of the plot if you wish (and if you can), enter "y" again to exit the plot routine. The computer responds with

VERY GOOD! CONGRATULATIONS! WE PROCEED.

DO YOU WANT ANOTHER SET OF ANGLES IN THIS MODEL?

If you answer "yes", you return to the point of entering the number of take-off angles and azimuths desired. The distance from the slab and the slab model itself remain unchanged.

If you answer "no", you get

DO YOU WANT TO TRY A NEW MODEL?

If you answer "yes" you go back to the point of setting slab length and so on. You proceed from there as before.

If you answer "no" you get

CATALOG TAPE 7 BEFORE LOGGING OUT OR IT WILL BE LOST AND YOU
WILL LOSE MOST OF YOUR INFORMATION WITH IT.

This means what it says and I suggest you take heed of it.

The program ends immediately after this, automatically. Make
a hard copy of tape 7 if you wish. If you want, you can use this to
make a plot of your ray emergence points by hand; you can do a
slightly better job than the Tektronix can. Other than that, you're
through.

MICHIGAN STATE UNIV. LIBRARIES



31293104372234